

*“An Experimental Study of Bulk Foam Properties  
with Commercial Surfactants in Saline  
Environments”*

*By*

***Mohammad Alhaji***

*Master thesis*

*Petroleum Technology-Reservoir Chemistry*



Department of Chemistry

Faculty of Mathematics and Natural Science

University of Bergen

June 2019

# Acknowledgments

At last, after a long journey, this thesis is completed. It is certainly the most trying period of my life so far, but also the one with the richest experiences, both professionally and personally. I could not have hoped to conclude this work without the constant encouragement and support of my colleagues, friends, and my family. I do not believe that words can show how grateful I am to them, but I hope to be able to express at least a glimpse of my gratitude below.

This thesis is submitted in June 2019, for a master's degree in petroleum chemistry at the University of Bergen.

First of all, I would like to express my gratitude to my supervisor, Prof. Kristine Spildo, for her unlimited support and advice throughout the academic process of this thesis and for being understanding.

I am extremely grateful to my Co-supervisor Dr. Jonas Solbakken. I cannot thank him enough for everything he has done for making this work possible. For kindly answering my questions, for all help and guidance, both during experimental work at the laboratory, and during the process for writing this thesis, and for training me on how to use instruments, which are used in this thesis.

Very special thanks to Dr. Morten Aarra for sharing his knowledge, ideas and his valuable comments and feedback.

I also would like to express my gratitude to my friends Abdul Majid Murad, Emilie Ryen Jomark, Anders Dalva, Adam Nour and Nina Nilsen for their friendship, support and for the wonderful times we shared.

Words cannot express the feelings I have for my mom (Khadija), sisters and my brothers for their constant unconditional support in both my study and my career. Above all, I thank God Almighty for my father (Zakarya), for letting me through this journey of life. I feel your guidance day by day and in every step of the way.

Sincerely

Mohammad Zakarya Alhaji

## Abstract

Foam is a fascinating two-phase phenomenon with a wide range of different industrial applications; contaminated-aquifer remediation, separation of wastewaters, enhanced oil recovery, gas leakage prevention and matrix-acidizing treatments to name a few. The success of these applications relies heavily on the choice of the foam-stabilizing agent (e.g., surfactant). The surfactant should provide a set of specific and desirable foam properties under the intended conditions. Since many variables affect surfactants and foam, it is important to understand how and under what conditions various factors contribute to foam properties.

The aim of this study is to evaluate salt effects on bulk foam properties with commercial surfactants. Salt tolerance to surfactants and the effect of salinity on foam properties are important first-hand knowledge in all surfactant selection processes. Such knowledge will usually eliminate many surfactant candidates for different saline environments.

In this thesis, effect of salt type, concentration, and ionic strength are evaluated in a standard bulk mixer test at ambient conditions with respect to foamability and foam stability. Foamability refers to the “ability” of the surfactant to generate foams under given conditions, while foam stability is understood as a parameter describing changes in the foam with time, immediately after the foam is generated. Two commercial anionic surfactants (i.e., AOS and SDS) and one cationic surfactant (MTAB) are used. Salt effects on bulk foam properties are also evaluated with different complex non-polar phases present (i.e., crude oils from different oil fields).

Based on the results obtained, cationic MTAB surfactant shows significantly higher salt tolerances compared to anionic AOS and SDS surfactants. The anionic surfactants are sensitive to relatively low concentrations of  $\text{CaCl}_2$ . Nevertheless, interestingly high tolerances to  $\text{MgCl}_2$  ( $> 9 \text{ mol/L}$ ) are observed with all surfactants.

Tests with  $\text{NaCl}$  and  $\text{MgCl}_2$  salt solutions adjusted to the same ionic strengths show that foamability with AOS surfactant is more dependent on ionic strength than salt type. The opposite trend is observed with MTAB surfactant, showing a reduction in foamability with increasing salt concentration and ionic strength. Foamability is in general better with anionic surfactants (AOS and SDS) compared with cationic surfactant (MTAB).

In the presence of oil, foamability is in general reduced in the presence of oil compared to without oil. Increasing surfactant concentration increases foamability for the two surfactants, nonetheless. We couldn't observe a clear trend of changes in ionic strength and salt solutions on the foamability when crude oil is added. In addition, the results indicate that there might be a different influence of salinity and ionic strength on bulk foam stability with and without oil present.

# Contents

<b>Acknowledgments</b> .....	I
<b>Abstract</b> .....	II
<b>Nomenclature</b> .....	IX
<b>Chapter 1: Introduction and Theory</b> .....	1
<b>1. Introduction</b> .....	2
1.1 Thesis Objectives.....	3
<b>2. Fundamentals</b> .....	4
2.1 Foam.....	4
2.1.1 Definition of foam.....	4
2.1.2 Foam applications.....	5
2.1.3 Enhanced Oil Recovery .....	5
2.1.4 Foam for enhanced oil recovery .....	7
2.1.5 Foam in Porous Media .....	8
2.2 Surfactant .....	10
2.2.1 Surfactants used .....	12
2.2.2 Effects of electrolytes on the solubility and aggregation of surfactant in the liquid.....	13
2.2.3 Krafft Point.....	14
2.2.4 Surface/Interfacial tension and CMC Determination.....	15
2.3 Importance of Salinity .....	18
2.3.1 The Electrical Double Layer (EDL) .....	19
<b>3. Foam Stability</b> .....	20
3.1 Gravity drainage .....	21
3.2 Surface elasticity.....	22
3.3 Laplace Capillary pressure .....	23
3.4 Disjoining pressure .....	23
3.5 Foams stabilized by ions.....	25
3.6 Surfactant concentration .....	27
3.7 Effect of oil on foam stability .....	27
<b>Chapter 2: Experimental procedures</b> .....	32
<b>4. Experiments descriptions</b> .....	33
4.1 Materials and methods .....	33
4.2 Preparations of Brines.....	34
4.3 Preparation of surfactant solutions .....	35
4.4 Crude oils.....	35

4.5	Measuring of surface tension (ST) and CMC .....	36
4.6	Bulk Foam test.....	37
4.7	Spinning Drop method .....	38
<b>Chapter 3: Results and Discussion .....</b>		<b>41</b>
<b>5.</b>	<b>Results .....</b>	<b>42</b>
5.1	Solubility tests .....	42
5.2	Surface tension and CMC .....	44
5.3	Effect of surfactant concertation on bulk foamability and stability.....	45
5.3.1	Effect of surfactant concentration on bulk foamability .....	45
5.3.2	Effect of surfactant concertation on bulk foam stability.....	46
5.4	Effect of salinity on bulk foamability and stability .....	49
5.4.1	Effect of salinity on bulk foamability.....	49
5.4.2	Effect of salinity on bulk foam stability .....	50
5.5	Effect of surfactant type on Foamability and stability of foam.....	53
5.6	Foam-oil interactions analyzed by static foam tests .....	54
5.6.1	Effect of oil on AOS foamability and stability .....	55
5.6.2	Effect of salinity on oil-foam .....	56
5.6.3	Effect of surfactant concentration on foam-oil interaction .....	57
5.6.4	Spreading, entering and Bridging, and lamella number .....	59
5.7	Visual observations during and after the experiment: .....	62
5.7.1	Visual observations of foam stability in the absence of Oil.....	62
5.7.2	Visual observations of foam stability in the presence of oil.....	63
<b>Chapter 4: Summary and Further Work.....</b>		<b>64</b>
<b>6.</b>	<b>Summary .....</b>	<b>65</b>
<b>7.</b>	<b>Further Work.....</b>	<b>68</b>
<b>Reference .....</b>		<b>69</b>
<b>Appendix.....</b>		<b>73</b>
A.	Experimental preparations and observations.....	73
B.	Results .....	78

## List of figures

Figure 1: Foam structure and foam components (Vikingstad et al., 2005).....	3
Figure 2: A schematic illustration of a foam system. Lamella and Plateau details in the bulk foam are enlarged on the left-hand side. A container with bulk foam is an illustration on the right-hand side (Schramm, 2006). .....	4
Figure 3: Simplified view of EOR methods (Mandal, 2015).....	6
Figure 4: Recovery efficiency from gas injections may be low due to (a) poor microscopic sweep efficiency, $ED$ ; (b) poor volumetric (areal/vertical) sweep, $EV$ ; (c) viscous fingering problems; (d) gas override; or (e) gas channeling through highly permeable intervals ( thief Zones).modified from (Solbakken, 2015). .....	6
Figure 5: Field applications of foam for EOR: (a) Injection well treatments; support gas injections with mobility control to combat viscous fingering problems, gas overrides, or excessive flow of gas through high-permeable “thief zones” in the reservoir (i.e., conformance control, selective blocking, gas diversion, gas sweep improvements). (b) Production well treatments; prevent unwanted fluids from coning, channeling into the wells (i.e., Gas-Oil-Ratio/Water-Oil-Ratio control). The figure modified from (Solbakken, 2015).....	8
Figure 6: Typical morphology of foam in a porous medium (Skauge, 2012). .....	8
Figure 7: Schematic of snap-off mechanism showing (A) gas penetrates to a constriction and a new bubble is formed (B) (Ransohoff and Radke, 1988) .....	9
Figure 8: Schematic of the lamella division mechanism showing a lamella is approaching the branch point from (A) and divided gas bubbles formed (B) (Ransohoff and Radke, 1988) .....	9
Figure 9: Schematic of leave-behind mechanism showing gas invasion (A) and forming lens (B) (Ransohoff and Radke, 1988). .....	10
Figure 10: Schematic representation of small amphiphilic surfactant molecules (Roland.chem, 2006) .....	11
Figure 11: Surfactant monomer concentration curve and illustration of a typical surfactant monomer. modified from (Lake, 1984) .....	12
Figure 12: Molecular structure of an Alpha-Olefin Sulfonate (AOS) (Negin et al., 2017) .....	13
Figure 13: Molecular structure of MTAB (Sigma).....	13
Figure 14: A schematic phase diagram of a surfactant close to the Krafft point (Abbott). .....	15
Figure 15: From force vs. time curves different stages of the experiment. Modified from Kjem319 (UIB, 2016). .....	16
Figure 16: Effect of counter ions on molecular packing of AOS at the air/ water interface. Area per molecule ( $A_m$ ): $AmNa + > AmMg2 +$ . This picture modified from (Pandey et al., 2003) .....	18
Figure 17: Schematic of an electric double layer. Modified from (Kontogeorgis and Kiil, 2016). .....	19
Figure 18: Illustration of a thin film stabilized by surfactant molecules (Solbakken, 2015). .....	21
Figure 19: A sketch demonstrating the Gibbs-Marangoni effect. the locally lowered surfactant concentration causes contraction of the surface modified from (Schramm, 1994).....	22
Figure 20: Illustration of a foam film between two Plateau borders. Modified from (Bent, 2014). ....	23

Figure 21: Schematic representation of the disjoining pressure curve (resultant from the attractive and repulsive forces), Modified from (Kornev et al., 1999).....	24
Figure 22: Disjoining pressure as a function of lamella thickness (Rossen, 1996).....	26
Figure 23: Effect of counter-ion size on the electrostatic repulsion between two negatively charged surfactant films, modified from(Schelero and von Klitzing, 2015). The dotted lines represent the hydration shell of the inorganic ions.....	26
Figure 24: Illustration of the different entering and spreading scenarios of an oil phase in contact with a lamella .....	28
Figure 25: A schematic representation of the meaning of the bridging coefficient (Bent, 2014). .....	29
Figure 26: Illustration of type A, B and C foams, modified from (Schramm and Novosad, 1990). .....	30
Figure 27: Illustration of Tensiometer instrument.....	36
Figure 28: Example of CMC measurement for AOS in 1 wt.% NaCl at 23 °C.....	37
Figure 29: On the left a schematic of foam stability test modified from (Schramm, 2006, and on the right example of foam preparation.....	38
Figure 30: Setup for measurements of IFT with the Spinning Drop Tensiometer SITE100.....	39
Figure 31: Spinning drop Method, modified from (Viades-Trejo and Gracia-Fadrique, 2007).....	40
Figure 32: Comparison of AOS and MTAB solubility limits ( $22\pm 1^\circ\text{C}$ ), Black lines represent maximum salt ionic strength used .....	44
Figure 33: Foamability of AOS and MTAB at different concentrations with a constant concentration of NaCl (5 wt.%) at 0 min after mixing.....	46
Figure 34: Foam half-life and free water at a function of AOS concentration (5 wt. % NaCl and $22\pm 1^\circ\text{C}$ ) .....	47
Figure 35: Foam half-life and free water at a function of MTAB concentration (5 wt.% NaCl and $22\pm 1^\circ\text{C}$ ).....	47
Figure 36: AOS foam height as a function of time .....	48
Figure 37: MTAB foam height as a function of time .....	49
Figure 38: Initial foam height in the presence of salt at different concentration.....	50
Figure 39: Foam half-life as a function of different salt type and concentration (0.5 wt.% AOS and $22\pm 1^\circ\text{C}$ ).....	50
Figure 40: Foam half-life as a function of different salt type and concentration (0.5 wt.% MTAB and $22\pm 1^\circ\text{C}$ ).....	51
Figure 41: Foam Height vs. Different type of Surfactant at different concentration of $\text{MgCl}_2$ to find the optimum salinity.....	52
Figure 42: Foam height against time for the same ionic strength of different salts.....	53
Figure 43: Variation of foam height with time for different surfactants (0.5 wt.% surfactant, 1 wt.% NaCl and $22\pm 1^\circ\text{C}$ ).....	54
Figure 44: Foam column height as a function of time for the different crude oils and free oils using 0.5 wt.% oil and 0.5wt.% AOS in distilled water .....	55

Figure 45: Explanation of the effect of salinity on foamability with different crude oils present. ....	56
Figure 46: Half-life of foam at different concentration of salts with different oils. The concentration of the oil and AOS are constant 0.5 wt. %.....	57
Figure 47: Foamability in the presences of 0.5 wt.% Oil 3 with 5 wt.% NaCl.....	58
Figure 48: Foam stability in the presence of Oil 3, foam generating from the solution containing 5 wt.% NaCl and different concentration of AOS / MTAB.....	58
Figure 49: Gap between the foam and the liquid surface for MgCl <sub>2</sub> , 1. AOS with MgCl <sub>2</sub> , 2. MTAB with MgCl <sub>2</sub> and 3. AOS with NaCl .....	62
Figure 50 : Foamability of 5 wt.% AOS + 5 wt.% NaCl + 0,5 wt. % Oil 3 .....	63
Figure 51: picture shows the solubility limit of AOS fir NaCl solution which is 7 wt. % .....	73
Figure 52: picture shows 2% of the surfactant in different concentrations of CaCl <sub>2</sub> . It notes that AOS completely dissolved at 0.2% CaCl <sub>2</sub> , while precipitated at 0.5 wt. % and 1 wt. % respectively.....	74
Figure 53: Illustration of the recording of foam height and free water (liquid). ....	74
Figure 54: Illustration of cloudy formation in low concentration of AOS+ 0. 2% CaCl <sub>2</sub> . ....	75
Figure 55: Foam Height for different concentration of AOS with (5.wt. % NaCl). ....	76
Figure 56: Foam Height for different concentration of MTAB with (5.wt. % NaCl). ....	76
Figure 57: Variation of foam height as a function of time for different solutions with 0.5 wt. % MTAB in the absence of oil. ....	78
Figure 58: Variation of foam height as a function of time for different solutions with 0, 5 wt. % AOS in the absence of oil. ....	79
Figure 59: Comparing the foamability between AOS and MTAB at different solutions. ....	79
Figure 60: Foam Height Vs, different oils with distilled water in 0.5 w.% AOS.....	80
Figure 61: Foam Height Vs, different oils with 1 wt. % NaCl in 0.5 w.% AOS.....	80
Figure 62: Foam Height Vs, different oils with 5 wt. % NaCl in 0.5 w.% AOS.....	80
Figure 63: Foam Height Vs, different oils with 5 wt. % MgCl <sub>2</sub> in 0.5 w.% AOS. ....	81
Figure 64: Change in foam height with respect to time for 0.5 wt.% AOS foam in the presence of MgCl <sub>2</sub> at different concertation.....	81
Figure 65: Change in foam height with respect to time for 0.5 wt.% MTAB foam in the presence of MgCl <sub>2</sub> at different concertation.....	82
Figure 66: Change in foam height with respect to time for 0.5 wt.% AOS foam in the presence of NaCl at different concertation.....	82
Figure 67: Change in foam height with respect to time for 0.5 wt.% MTAB foam in the presence of NaCl at different concertation. ....	82
Figure 68: Change in foam height with respect to time for 0.5 wt.% AOS and MTAB foam in the presence of two complex brines. ....	83



## List of Tables

Table 1: Foam stability prediction by the lamella number theory .....	30
Table 2: Criterion is used to evaluated and ranked surfactants in bulk tests based on their foamability and foam stability properties (Solbakken, 2015) .....	31
Table 3: Foam predication by the sign of E, S and B coefficients, modified by (Simjoo et al., 2013) ...	31
Table 4: Concentrations and ionic strength of brines .....	33
Table 5: Composition of synthetic Brines.....	34
Table 6: The details of the different surfactants with different active concentrations used in our experiments.....	34
Table 7: Crude oil properties (22±1 °C, atm).....	35
Table 8: Solubility limit of AOS and MTAB in different concentrations of NaCl solutions (22±1°C) .....	42
Table 9: Solubility limit of AOS and MTAB in different concentrations of MgCl <sub>2</sub> solutions (22±1°C) ...	43
Table 10: Solubility limit of AOS and MTAB in different concentrations of CaCl <sub>2</sub> solutions (22±1°C) ..	43
Table 11: Solubility of AOS and MTAB in typical complex brines (22±1°C).....	43
Table 12: CMC values for AOS and MTAB surfactants in different electrolyte solutions (22±1°C). .....	45
Table 13: Spreading coefficients, entering coefficients, lamella number and bridging coefficients at equilibrium for the AOS with 1 wt.% NaCl .....	59
Table 14: Spreading coefficients, entering coefficients, lamella number and bridging coefficients at equilibrium for the AOS with 5 wt.% NaCl. ....	59
Table 15: Spreading coefficients, entering coefficients, lamella number and bridging coefficients at equilibrium for the AOS with 5 wt.% MgCl <sub>2</sub> .....	60
Table 16: Comparison of AOS foam stability predictions for different salt concentrations based on different criteria (U: Unstable, M: Moderate, and S: Stable).....	61
Table 17: Comparing between AOS and MTAB Oil3 effect in 5 wt.% NaCl on foam .....	61
Table 18: composition of Brine 1 for 1 kg solution. ....	77
Table 19: composition of Brine 2 for 1 kg solution .....	77
Table 20: composition of Brine 3 for 1 kg solution .....	77
Table 21: Surface tension for different salt solutions and concentrations without surfactant (22°C, atm.) .....	78
Table 22: Spreading coefficients, entering coefficients, lamella number and bridging coefficients at equilibrium for the AOS with 1 wt.% NaCl .....	78

## Nomenclature

### Abbreviations

AOS	Alpha-olefin sulfonate
<i>MTAB</i>	Myristyltrimethylammonium bromide
EDL	Electrical double layer
<i>SDS</i>	Sodium dodecyl sulfate
<i>SDS<sub>n</sub></i>	Sodium dodecyl sulfonate
CMC	Critical micelle concentration
$E_D$	Microscopic displacement efficiency
$E_{VOL}$	Volumetric displacement efficiency
$E_V$	Vertical displacement efficiency
$E_A$	Areal displacement efficiency
EOR	Enhance oil recovery
$P_c$	Capillary pressure
$P_L$	Liquid pressure
$P_G$	Gas pressure
IFT	Interfacial tension
St	Surface tension
L	Lamella number
B	Bridging coefficient
S	Spreading coefficient
E	Entry coefficient
$E_R$	Recovery efficiency
$N_P$	Produced reserves
$N$	Total reserves

## Symbol

$\sigma_{o/w}$	Interfacial tension between oil and water
$\sigma_{o/g}$	Surface tension between oil and gas
$\sigma_{g/w}$	Surface tension between gas and water
$\Pi_{VW}$	Van der Waals forces disjoining pressure
$\Pi_E$	Electrostatic disjoining pressure
$\Pi_S$	Steric forces disjoining pressure
$\Pi$	Disjoining pressure
$\frac{dp}{dx}$	Pressure gradient.
$\Delta\rho$	Density difference between phases
$C_i$	Molarities of the ions in the solution
A	Cross-sectional area to flow
$\omega$	Velocity of rotation
$\sigma$	Surface Tension
R	Cylinder radius
$\theta$	Contact angle
$K^{-1}$	Debye length
I	Ionic strength
$Z_i$	Ion valance
WT.%	Weight percent
H	Foam height
$v$	Velocity
$\mu$	Viscosity
L	Length
$\rho$	Density

# Chapter 1: Introduction and Theory

## 1. Introduction

Foam is a mixture of gas, liquid and a foamer (Figure 1). The gas becomes the discontinues phase (dispersed) and liquid is the continuous phase (the dispersion medium). In bulk foam, gas bubbles are separated by thin liquid films called lamella. In recent decades, the fundamentals foam systems and their nature and behavior in different conditions were studied well and wide. In addition, many laboratory experiments have been performed in various areas of foam applications (Schramm, 1994, Schramm, 2006, HIRASAKI, 1989, Rubio et al., 2002).

Foaming properties of solutions of various surfactants are generally described in terms of their foamability and foam stability. The term foamability refers to the ability of the surfactant solution to form foam under given conditions. The term foam stability is variation/duration of the foam bubbles (mostly as changes of height or volume) with the time immediately after the foam is generated.

Foam is by definition a thermodynamically unstable system and cannot be treated as a new phase. Several parameters can influence the properties of foam, such as the surfactant type and concentration, gas composition, brine composition and salinity, interactions with oil, media, and temperature and pressure conditions and so on. A change in one or several of these parameters may affect the performance of foam and, consequently, the success potential for the intended foam application. A good understanding of the properties/tolerances/limits/performance to various foam-stabilizing agents is therefore important. It is also important to understand foam on a broad experimental scale.

In this thesis, the fundamentals of foam are presented, studied and discussed well. To understand more about the behavior of foam in different conditions and to improve knowledge and develop a new understanding of different stabilizing agents to foam, many experiments are performed including the effect of salinity and concentration, the type of surfactant, and oil-foam interaction by using different crude oils.

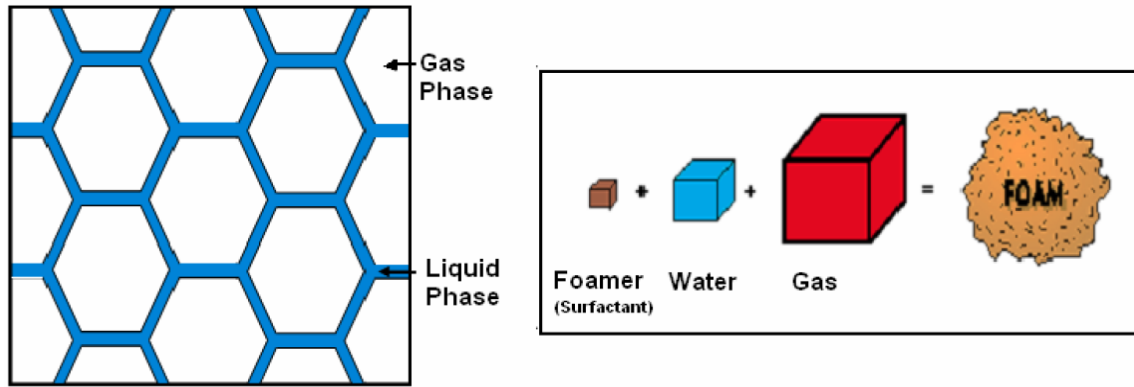


Figure 1: Foam structure and foam components (Vikingstad et al., 2005)

## 1.1 Thesis Objectives

The success rate of all foam applications relies heavily on the choice of the foam-stabilizing agent (e.g., surfactant). The surfactant should provide a set of specific and desirable foam properties under the intended conditions. Since many variables affect surfactants and foam, it is important to understand how and under what conditions various factors contribute to foam properties.

The following questions are addressed in this thesis:

- What is the difference between anionic and cationic surfactants in bulk foam properties?
- Is there an optimum salt type or ionic strength which provides the best foam properties?
- Is there an optimum surfactant concentration which provides the best foam properties?
- Can changes in salinity or surfactant concentration improve foam properties in the presence of oil?

A series of experiments are done to study:

1. Properties of surfactant-stabilized systems (surfactant solubility, salt tolerance, surface tension and CMC).
2. Bulk foam properties (foamability and stability):
  - Effect of salt type, concentration and ionic strength
  - Effect of surfactant type (cationic and anionic) and concentration
  - Effect of oil (low concentration, five different crude oils)
3. Study the different theories about foam stability in the presence and absence of oil. (i.e., determination and evaluations of Spreading and Entering coefficient, Lamella number and Bridging coefficient).

## 2. Fundamentals

This section pertains with the fundamentals of surfactant method of chemical oil recovery, which includes foam, surfactant and salinity effect.

### 2.1 Foam

One of the objectives of this section is to present the fundamentals of foams used in enhanced oil recovery. We also briefly discuss some basic scientific concepts that will help the readers to understand more about foam generation under different conditions.

#### 2.1.1 Definition of foam

Foam is defined as gas dispersed in a continuous liquid phase (Schramm, 2006). Foams can stabilize by using surfactants. The illustration of a foam system can be seen in Figure 2. Lamella and Plateau border details are specified within the enlarged area. The lamella is the thin film, between two plateau borders, where three lamellae meet at angles of  $120^\circ$  due to a polyhedral arrangement of bubbles in foam (Schramm, 2006). The width of this region (plateau border) is dependent on the capillary pressure. If the capillary pressure increases the lamellae thickness decrease until it reaches the critical thickness  $h^{cr}$ , which will make the lamellae collapse (Rossen, 1996). Generation of foam can take place by disturbing an aqueous solution with surfactant while in contact with gas (Sheng, 2013). The thin liquid films are stabilized by adsorption of surfactant molecules on both sides of the film (Farajzadeh et al., 2011). The properties of thin liquid films are important in the discussion of foam stability.

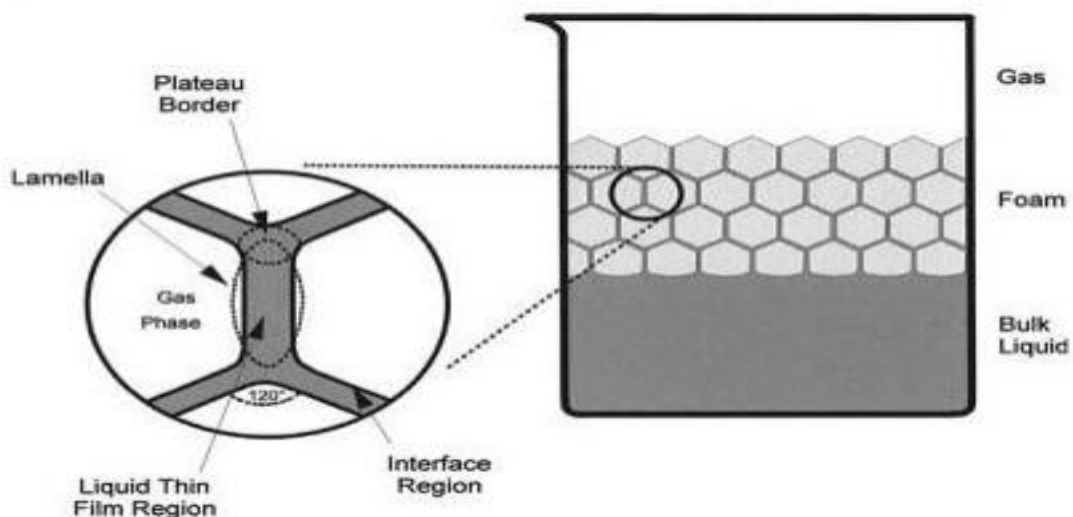


Figure 2: A schematic illustration of a foam system. Lamella and Plateau details in the bulk foam are enlarged on the left-hand side. A container with bulk foam is an illustration on the right-hand side (Schramm, 2006).

### 2.1.2 Foam applications

The oil industry has several applications with foam including enhanced oil recovery, well stimulation and drilling. There are also numerous other applications of foam, ranging from a variety of everyday uses (e.g., personal care/house products such as shaving cream, shampoo, bubble bath, and firefighting) to many chemical and industrial processes (e.g., food/beer industry, environmental remediation and mineral flotation). In the food industry, foams play an important part in both appearance and taste like bread. Froth flotation is a process for separating minerals from nonvaluable rock and dirt by using foam. Furthermore, foam can be applied for environmental purposes, like wastewater treatment systems. They use foam to remove fine solids from the water stream by absorbing the solids onto the foam (Rubio et al., 2002).

### 2.1.3 Enhanced Oil Recovery

More than half of oil discovered around the world remains unrecovered after using conventional production techniques, namely, primary and secondary recovery. Enhanced oil recovery, also called tertiary recovery, is a class of methods that aim to increase the recovery factor of a reservoir beyond the levels typically achievable with primary and secondary [Sheng, 2010], using thermal, chemical or other methods. The major shortcomings of these EOR methods are their poor volumetric sweep efficiency, especially gas injection due to poor gas contact with oil (Kuehne et al., 1990, Rossen and Van Duijn, 2004). In other words, the injected fluids are only able to contact and displace a rather small portion of the oil in the reservoir. Consequently, large volumes of oil remain uncontacted and unswept in parts of the reservoir. Under such conditions, the application of foam can be a technically feasible way to overcome this problem (Rossen, 1996, Schramm, 1994, Kovscek and Radke, 1994).

The main target for EOR applications is to improve both the volumetric and the microscopic displacement efficiency. Improving the volumetric displacement efficiency can be achieved with mobility control. By either increasing or decreasing the viscosity of one of the fluids, ideal mobility ratios can be obtained. Increasing the microscopic displacement efficiency targets the capillary trapped oil. By reducing the interfacial tension between the displacing and displaced fluid, the capillary trapped oil can be produced. EOR methods can be classified into four classes, according to Figure 3. Foam, as studied in this thesis, is partly classified as gas-based EOR methods and partly as chemical (surfactant)-based EOR-methods.



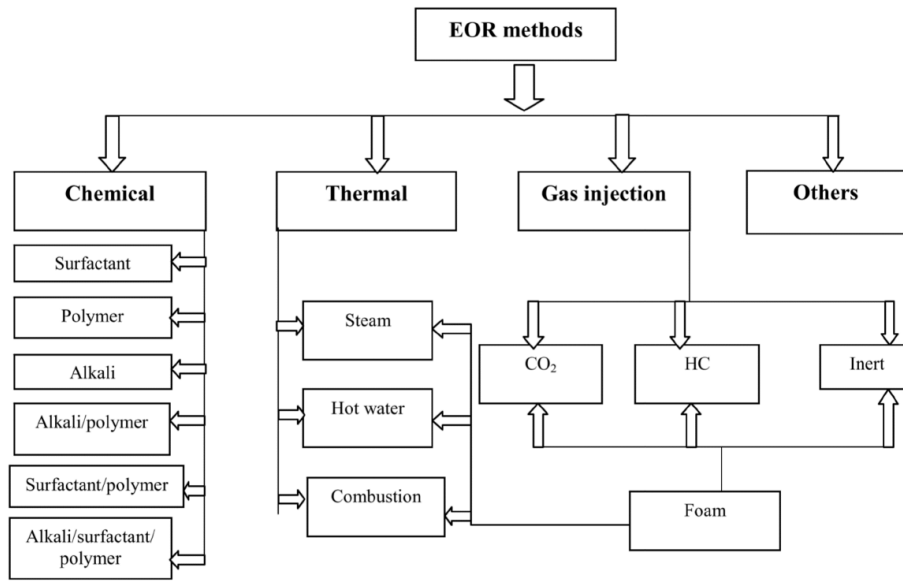


Figure 3: Simplified view of EOR methods (Mandal, 2015).

Based on the material balance the recovery factor,  $E_R$ , can be defined as (Skarestad and Skauge, 2009):

$$E_R = \frac{N_p}{N} = E_D \cdot E_{vol} = E_D \cdot E_V \cdot E_A \quad (1)$$

Where  $N_p$  is the produced reserves,  $N$  is the total reserves,  $E_D$ ,  $E_{vol}$ ,  $E_V$  and  $E_A$  are the microscopic volumetric, vertical and areal displacement efficiency, respectively. These concepts are illustrated in Figure 4.

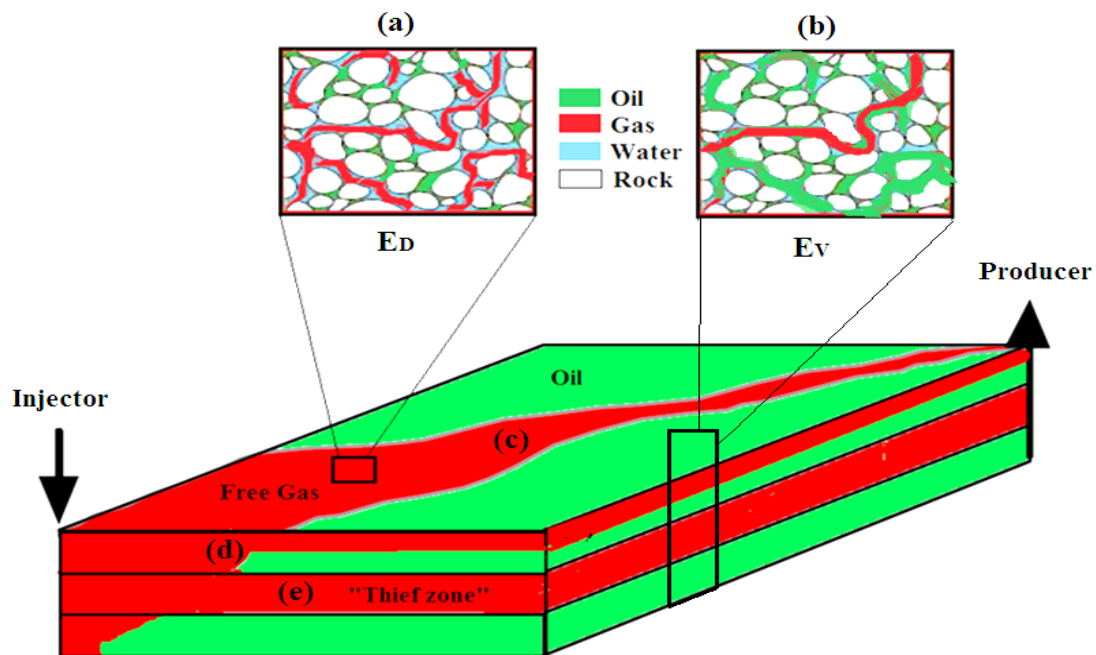


Figure 4: Recovery efficiency from gas injections may be low due to (a) poor microscopic sweep efficiency,  $E_D$ ; (b) poor volumetric (areal/vertical) sweep,  $E_V$ ; (c) viscous fingering problems; (d) gas override; or (e) gas channeling through highly permeable intervals ( thief Zones).modified from (Solbakken, 2015).

The microscopic displacement efficiency,  $E_D$ , and the volumetric displacement efficiency,  $E_{vol}$ , can further be defined as:

$$E_D = \frac{\text{volume oil displaced}}{\text{volume oil contacted}} \quad (2)$$

$$E_{vol} = \frac{\text{volume oil contacted}}{\text{volume oil in place}} \quad (3)$$

The aim of increasing the microscopic displacement efficiency,  $E_D$  is a production of oil that remains in the part of the reservoir already swept by the displacing fluid (decreasing residual oil saturation,  $S_{or}$ ), e.g. reducing capillary force by injection of surfactant.

The aim for increasing the volumetric displacement efficiency  $E_{vol}$  is to produce oil that remains in the reservoir not swept by the displacing fluid, e.g. trapping mechanism and increasing the displacing fluid viscosity using polymers.

#### 2.1.4 Foam for enhanced oil recovery

In EOR methods, foam has primarily been used to regulate the mobility ratio during gas injection (Figure 5 - a), or it has been used to shut off unwanted gas inflow in production well treatments (Figure 5 - b). In fact, the combination of water, gas and surfactant to generate foam in a reservoir can mitigate the problems associated with gas injections and improve gas sweep efficiency to recover more oil. The presence of a foaming agent in porous rocks can reduce the mobility of gas and water simultaneously, stabilize the gas injection front and prevent unwanted production of gas and water from the reservoir. These unique effects can assist the reservoir engineer with a “tool” in different optimization processes that can improve the ultimate recovery and economics in mature oil fields.

One of the major challenges to the success of foam in EOR is the adverse influence of oil on foam stability and characterization of the complex interaction between the foam and oil (Farajzadeh et al., 2012, Nikolov et al., 1986). Results from bulk foam experiments in the literature show an apparent contradiction of the effect of oil on foam stability. Some authors have argued that the presence of oil, especially lighter hydrocarbons, destroy or prevent the generation of foam (Minssieux, 1974, Denkov, 2004). Others, on the other hand, have shown that stable foams can be generated in the presence of oil if an appropriate foaming agent is selected (Nikolov et al., 1986, Mannhardt et al., 1998).

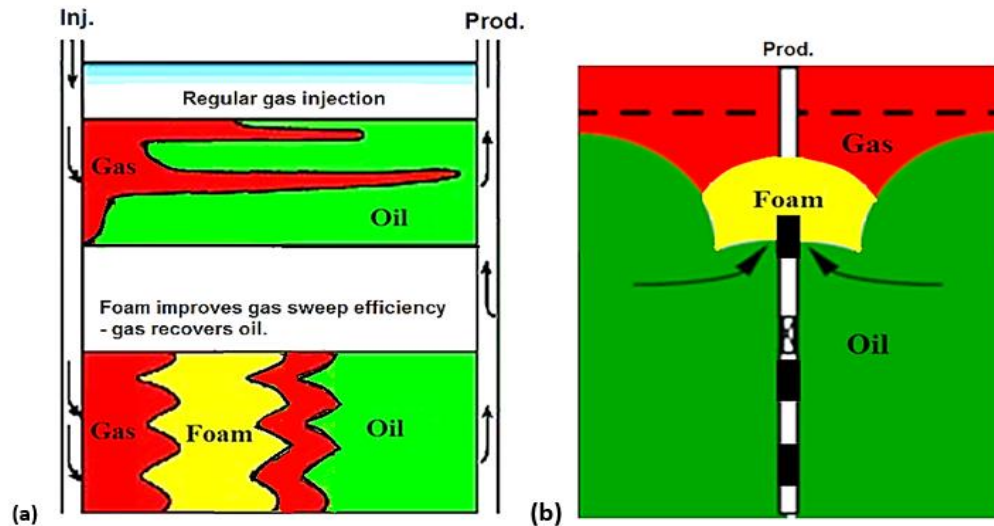


Figure 5: Field applications of foam for EOR: (a) Injection well treatments; support gas injections with mobility control to combat viscous fingering problems, gas overrides, or excessive flow of gas through high-permeable "thief zones" in the reservoir (i.e., conformance control, selective blocking, gas diversion, gas sweep improvements). (b) Production well treatments; prevent unwanted fluids from coning, channeling into the wells (i.e., Gas-Oil-Ratio/Water-Oil-Ratio control). The figure modified from (Solbakken, 2015).

### 2.1.5 Foam in Porous Media

Foam confined inside the pore network of a reservoir rock has a fundamentally different morphology from the structure of the bulk foam. The confined foam is made up of individual bubble of gas separated by liquid sheaths or lamellae as in Figure 6. Interaction between lamellae and pore walls dominates flow behavior.

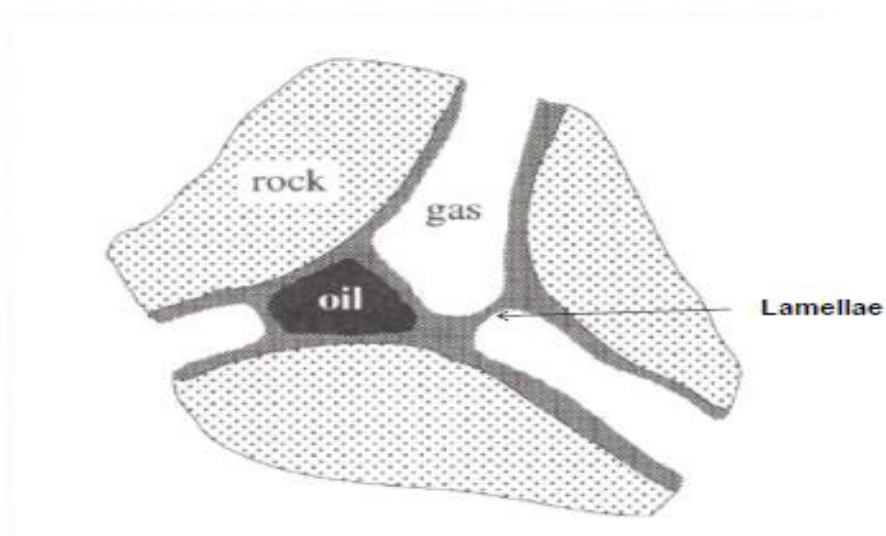


Figure 6: Typical morphology of foam in a porous medium (Skauge, 2012).

It is commonly accepted that lamella is created by following three mechanisms inside a realistic media (Ransohoff and Radke, 1988):

1. Snap off: is a mechanical process, liquid accumulates in the pore-throat and creates a new lamella. It is controlled by liquid saturation, pore geometry of the porous media and rock wettability. This kind of mechanism generates stable and so-called strong foams (Haugen et al., 2012) whose bubble size is of the order of the size of the bodies' of the pores. This mechanism puts some gas into discontinuous form.

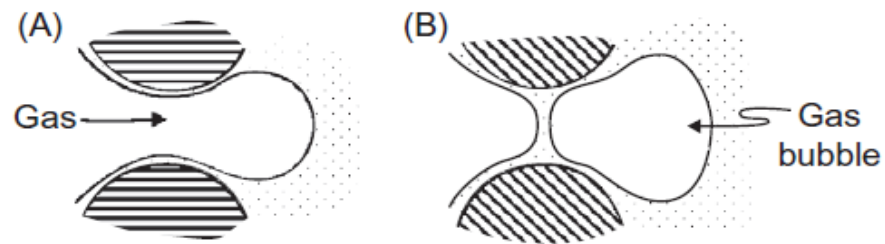


Figure 7: Schematic of snap-off mechanism showing (A) gas penetrates to a constriction and a new bubble is formed (B) (Ransohoff and Radke, 1988)

2. Lamellae division denotes the event when two or more lamella is created from one. The lamella approaches a branch point and branches into two lamellae. Lamella division primarily occurs when generated gas bubbles exceed the pore size (Skarestad and Skauge, 2009). This mechanism leads to increasing the number of lamellae of the foam and thus bubbles, in the porous medium. Snap-off and lamella division mechanisms are in effect at high flow velocities.

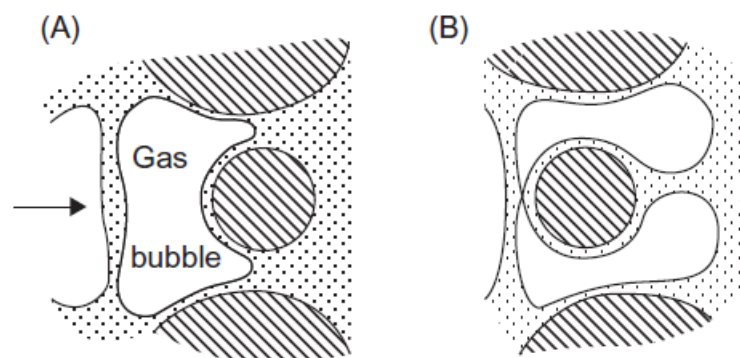


Figure 8: Schematic of the lamella division mechanism showing a lamella is approaching the branch point from (A) and divided gas bubbles formed (B) (Ransohoff and Radke, 1988)

3. Leave behind: is considered a local fingering of gas in adjacent pores initially filled with liquid. Leave-behind does not generate separate gas bubbles but establishes a continuous gas flow path. likewise, it happens when gas flowing from two different directions converges to the same pore, trapping liquid in a pore throat between the two fronts, thus creating a lamella. This mechanism is important at low velocities and generates relatively weak forms.

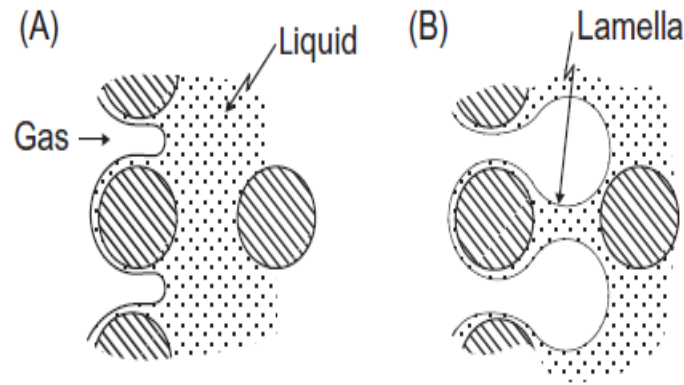


Figure 9: Schematic of leave-behind mechanism showing gas invasion (A) and forming lens (B) (Ransohoff and Radke, 1988).

## 2.2 Surfactant

Surfactants are needed to create foam. It is possible to stabilize foam using surfactant (Schramm, 1994). Surfactants are chemical compounds that have a greater influence on the surface and interface properties. The surfactant molecules are composed of two parts; a polar head (ionic-anionic-or cationic – or polar group) as shown in Figure 10 and a hydrophobic tail. The hydrophobic part is typically a hydrocarbon chain of varying length, which does not show affinity to water. Surfactants have an alkyl chain with 8-22 carbons. Adsorption of surfactant molecule at gas-liquid interfaces results in stabilizing foam film and reducing the interfacial tension. The reduction of tension in the water and oil interface is the main driving force that enables the use of chemical EOR (Gurgel et al., 2008).

Surfactants have plenty of industrial and domestic applications; they are present in detergents for cleaning of both soft and hard surface, as emulsifiers, foaming agents or stabilizers for colloidal dispersions; in various applications in biotechnology, e.g. separation of proteins in reversed micelles, and catalysis and as components in many complex products, e.g. paints and coatings.

Depending on their polar moieties, surfactants can be classified into four main groups:

- Anionic: These surfactants are the most used in oil recovery since they are soluble in the aqueous phase; efficiently reduce IFT, relatively resistant to retention, stable and not

expensive. If an anionic surfactant is dissolved in an aqueous phase, the surfactant starts to dissociate into a cation ( $Na^+$ ) and a monomer.

- Cationic: have little use due to the high adsorption by the anionic surface of interstitial clays.
- Non-Ionics: are mainly used as co-surfactants.
- Zwitterion: have not been used in oil recovery.

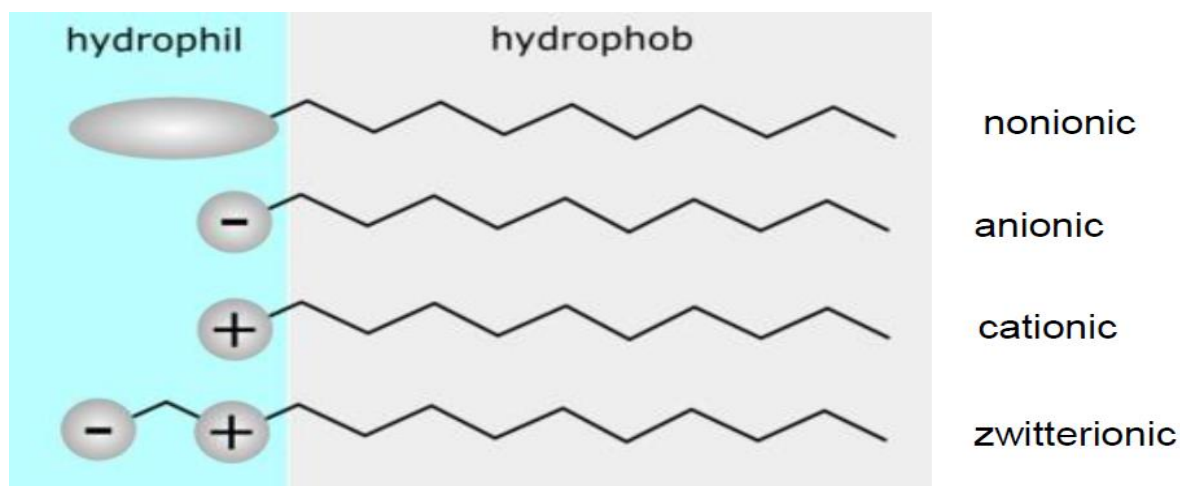


Figure 10: Schematic representation of small amphiphilic surfactant molecules (Roland.chem, 2006)

When surfactants are added to an aqueous phase, some molecules enter the solution but most of them stick on the water-air surface, which reduces the surface tension. When the entire surface is saturated with surfactant monomers, the surfactants will find alternative ways to minimize the energy of the system; by creating semi-spherical liquid-like aggregates, called micelles (Figure 11). Micelles are of enormous importance in surface science. Micellization is another mechanism, to the adsorption, for minimizing the system's energy. These aggregates are created when we have reached a certain concentration of surfactants that is called the critical micelle concentration (CMC). The CMC is the concentration of surfactants above which micelles form and all additional surfactants added to the system go to micelles. Any further addition of surfactants after reaching CMC will just increase the number of micelles. Consequently, before reaching the CMC, the surface tension decreases sharply with the concentration of the surfactant. However, after reaching the CMC, the surface tension stays approximately constant. Micellization occurs over a narrow concentration range for a given system. This concentration is small about  $10^{-5}$  to  $10^{-4}$  mol/L for surfactants typically used in EOR. Therefore, CMC is often in the range of a few ppm to tens of ppm.

The desired properties of a surfactant such as cleaning and stabilizing capabilities depend on both the surfactant characteristics like CMC, the Krafft point and its chemistry and on the solution properties (temperature, time, presence of salts and co-surfactants).

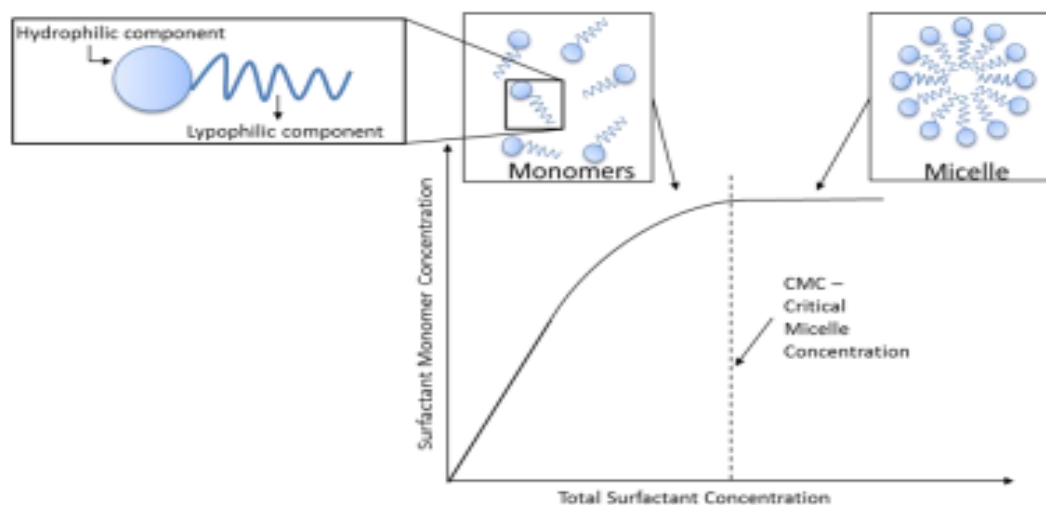


Figure 11: Surfactant monomer concentration curve and illustration of a typical surfactant monomer. modified from (Lake, 1984)

### 2.2.1 Surfactants used

In this study, four different surfactants are used: Alpha sulfonate surfactant (AOS), Myristyltrimethylammomium bromide surfactant (MTAB), sodium dodecyl Sulfate (SDS), sodium 1-decansulfonate (SDSs). However, we have further looked deeper into only two types of surfactants which are:

The AOS is a commercially available surfactant, acceptable with respect to health and environmental concerns, and can be produced in large volumes at a relatively low price. The most common formula from the AOS family of surfactants is the one with 14–16 carbons and it is commonly known as sodium C14-16 olefin sulfonate or AOS. Members of the AOS surfactant family are stable over the wide range of pH, and even in hard water. In numerous research work conducted to date, this surfactant has been used as an alternative foaming agent in reservoirs to achieve good gas mobility and increase oil recovery. AOS has been used in several successful field applications (Aarra et al., 1997, Aarra et al., 2002, Skauge et al., 2002).

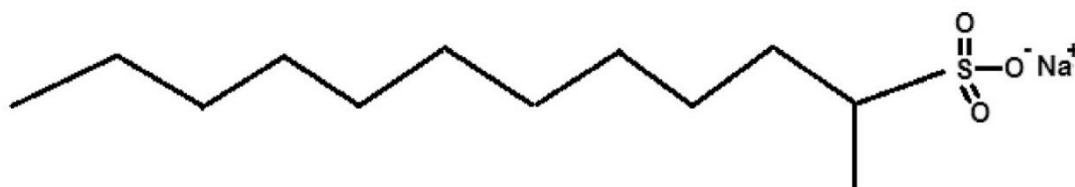


Figure 12: Molecular structure of an Alpha-Olefin Sulfonate (AOS) (Negin et al., 2017)

We used a cationic surfactant as well in this study, which is Myristyltrimethylammomium bromide (MTAB) to compare between anionic and cationic surfactants on surface tension, CMC and Bulk foam properties. Molecular structure of the surfactant (MTAB) is shown in Figure 13.

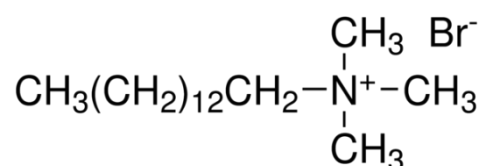


Figure 13: Molecular structure of MTAB (Sigma)

### 2.2.2 Effects of electrolytes on the solubility and aggregation of surfactant in the liquid.

Surfactant self-assembly is driven by many interactions, such as van der Waals, hydrogen-bonding, and electrostatic interactions, and they play important roles in determining how micellization occurs.

To understand deeply the physical mechanisms, which control self-assembly processes, requires detailed, microscopic level molecular information. Extracting this information experimentally is very challenging due to the characteristic length (20 nm) and time ( $1\mu\text{s}$ ) scales associated with surfactant micelles. Due to the hydrogen bonding between the polar groups of surfactants and water molecules, most surfactants have a good solubility in water. However, the solubility of surfactant is influenced by temperature and water salinity (Rico-Rico et al., 2009). CMC can also be influenced by the presence of electrolytes (Wennerstrom et al., 1991). The effects of the electrolytes on the solubility and aggregation behavior vary with the type of surfactant.

The existence of divalent cations, mainly  $\text{Ca}^{+2}$  and  $\text{Mg}^{+2}$ , are not desirable. They can significantly reduce the solubility of ionic surfactants (anionic and cationic) in solutions considering they can bind to the surfactant ions through electrostatic attraction (Yu et al., 2012). These cations have the potential of causing surfactant precipitation, which can result in blocking the pores, so they should be kept at low levels. Researchers who studied AOS showed that this family of surfactant performs particularly well in the presence of divalent ions (Negin et al., 2017).



Drawing on previous studies and calculations (Ghosh et al., 2001, Yan et al., 2010), the energy barrier between the head group and  $Mg^{+2}$  is the strongest, which means that it is the most difficult for  $Mg^{+2}$  to enter into the first water shell of head group to form ion-pair, while for  $Na^+$  it is the easiest. We can conclude that  $Ca^{+2}$  and  $Mg^{+2}$  can enter the hydration shell of the head group. Moreover, they can affect the orientation of water molecular surrounding the head group.

When the divalent ions are present, water molecules either can bind to the head group oxygen atoms directly or bridged by the ions; meanwhile, the cations, including  $Na^+$ , may form ion bridges between two head groups (Yan et al., 2010).

### 2.2.3 Krafft Point

Most physicochemical properties of ionic surfactants in aqueous solutions show a very complex dependence on the composition, ionic strength of the medium, and/or intensive variables. Another interesting property is the unusual temperature-dependence of surfactant solubility.

As for most solutes in water, increasing temperature produces an increase in surfactant solubility. Ionic surfactants are initially insoluble, however, there is often a temperature at which the solubility suddenly increases very dramatically. This is known as the Krafft point or Krafft temperature ( $T_k$ ) as shown in Figure 14 (Tsuji and Mino, 1978) and is defined as the intersection of the solubility and the CMC curves. In other words, the solubility of the monomeric surfactant is equivalent to its CMC at the same temperature at the temperature. The solubility of ionic surfactants increases very rapidly after the Krafft point. Knowledge of the Krafft point temperature is crucial in many applications since below it, the surfactant will clearly not perform efficiently; hence-typical characteristics such as maximum surface tension reduction and micelle formation cannot be achieved. This temperature is important in industrial preparations, especially where concentrated surfactant solutions are required.

The Krafft temperature increases with an increasing number of carbon atoms in the hydrophobic part. Extensive research work has been dedicated to the effect of chain length, head group size, and different additives on the  $T_k$  and the CMC of ionic surfactants (Chu and Feng, 2011, Davey et al., 1998). These studies have revealed that the CMC decreases while the  $T_k$  increases with increasing concentration of electrolytes. However, the Krafft point is typically much higher in the presence of divalent counter ions than monovalent counter ions.

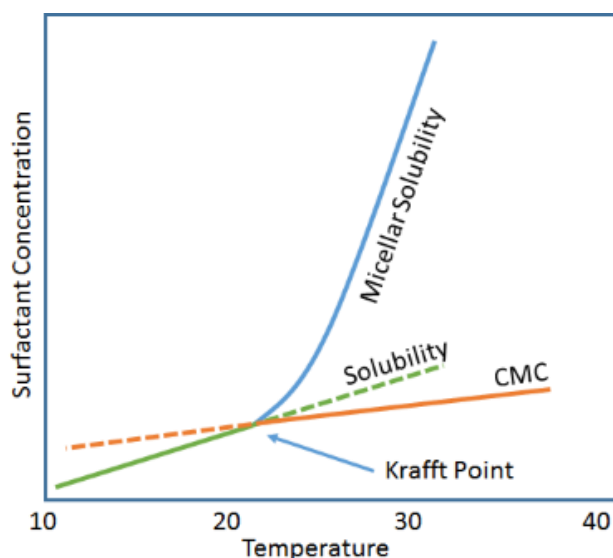


Figure 14: A schematic phase diagram of a surfactant close to the Krafft point (Abbott).

## 2.2.4 Surface/Interfacial tension and CMC Determination

### 2.2.4.1 Surface and interfacial tension

Surface tension is a measure of the force acting at a boundary between two phases. If this boundary is between a liquid or a solid and a gas (Weaire and Hutzler) the attractive forces are referred to as surface tension, but the attractive forces between two immiscible liquids, like oil and water, or between a liquid and a solid are referred to as interfacial tension. The common units for Surface/interfacial tension are dynes/cm or mN/m.

There are many ways to measure surface tension, such as; Wilhelmy plate technique, capillary rise technique, maximum-bubble-pressure method, drop-weight method and ring method. The surface tension of surfactant solutions depends on the number of surfactant molecules per unit area at the surface. For a given surfactant, the surface tension decreases with increasing surface concentration (Rosen and Tracy, 1998). In other words, the greater concentration of surfactant molecules at the surface results in the lower surface tension.

At constant pressure and temperature, the surface tension can be defined as the change in (G) Gibbs free energy per surface area (A), as seen in the equation below (4):

$$\gamma = \left( \frac{\partial G}{\partial A} \right)_{T,P} \quad (4)$$

One of the most famous equations when it comes to Interfacial tensions is the Laplace equation, which was derived in 1805. Any generally curved surface at any point can be identified in terms of two local radii of curvature ( $R_1$  and  $R_2$ ) orthogonal to each other at that point.

$$\Delta p = \gamma \cdot \left( \frac{1}{R_1} + \frac{1}{R_2} \right) \quad (5)$$

#### 2.2.4.2 Surface tension measurements - Ring Method

The Du Nöuy method utilizes a platinum ring (Fu et al., 2010), which is placed on a measurement hook connected to a high-sensitivity balance. The platinum ring is then submerged below the interface by moving the platform on which the liquid container is placed. When the ring is pulled to the liquid interface, there is a force that prevents the ring from leaving the liquid due to the intermolecular forces of the liquid. This force can be correlated to the surface tension. In other words, calculating surface tension is based on the measurement of the maximum force and the perimeter of the ring.

$$\gamma = \frac{F_{max} - F_v}{L \cdot \cos \theta} \quad (6)$$

$F_{max}$ : Maximum force measured

$F_v$ : Force of liquid volume =  $\rho \cdot v \cdot g$

L: Wetted length of the ring (circumference of the outer part of the ring + circumference of the inner part of the ring)

$\theta$ : Contact angle between liquid and ring (Usually zero, 0, when a platinum ring is used)

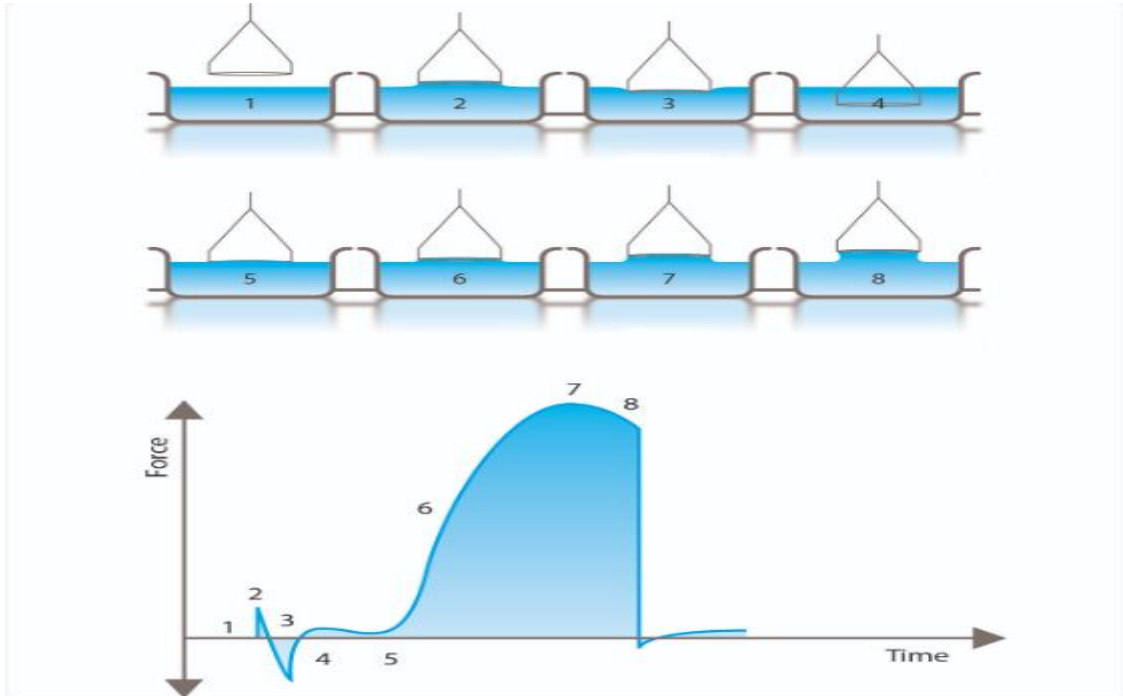


Figure 15: From force vs. time curves different stages of the experiment. Modified from Kjem319 (UIB, 2016).

Figure 15 can be explained as follows:

At the beginning (1), the ring has no contact with interface, and hence the force is zero. Then (2) the ring slightly touches the interface and due to adhesive force between the ring and surface, there is a small positive force. After that (3), the ring is forced through the interface leading to a small negative force. When the ring breaks through the interface and is fully submerged (4), a small positive force is measured due to the wires of the ring. As the ring is lifted through the interface (5 and 6), the measured force increases until it peaks (7), and then it reduces slightly until the lamella breaks (8).

#### 2.2.4.3 The critical micelle concentration, CMC

CMC is a key thermodynamic quantity of surfactant-water mixtures. Knowledge of this quantity is crucial for both scientific and practical understanding of how surfactants behave. The CMC is the concentration at which surfactants in solution change their initial molecular solvated state. To determine CMC, there are many ways such as light scattering and viscosity. Surface tension is one of the most common methods used to measure the CMC, because the method is easy to automate, and the equipment can be relatively inexpensive. The CMC is determined to be the point at which a change in slope occurs in a plot of surface tension versus surfactant concentration. We will go in more details about CMC determination in the next sections.

The CMC is influenced by a number of factors that are dependent on the nature of the surfactant and the aqueous environment. One of these factors is the ionic strength; The CMC in an aqueous solution is influenced by the degree of binding of the counter ions to the micelle. For aqueous systems, the increased binding of the counter ions to the surfactant causes a decrease in the CMC and an increase in the aggregation number (Mukerjee, 1967). The extent of binding of the counter ion increases with an increase in the polarizability and valence of counter ions and decreases with an increase in its hydrated radius. There are many researches showing the effect of monovalent and divalent ions on the micelle.

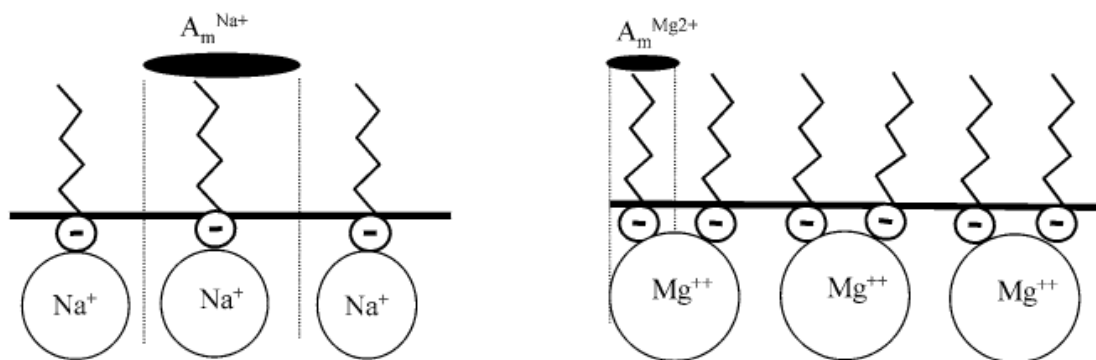


Figure 16: Effect of counter ions on molecular packing of AOS at the air/ water interface. Area per molecule ( $A_m$ ):  $A_m^{Na^+} > A_m^{Mg^{2+}}$ . This picture modified from (Pandey et al., 2003)

The phase behavior of anionic surfactant systems is much more sensitive to a change in divalent ions ( $Ca^{+2}$  and  $Mg^{+2}$ ) compared to monovalent ions ( $Na^+$ ), especially at low surfactant concentrations (Nelson, 1981).

Sammalkorpi and Karttunen have studied the effect of divalent ions on the surfactant aggregates. They found that the aggregate structures were markedly different in the cases of NaCl and  $CaCl_2$ . Especially, the aggregates appear much more compact in the case of  $CaCl_2$ . They observed also that the micelles in the presence of excess NaCl undergo rapid fluctuations in size and shape,  $CaCl_2$  reduces the magnitudes of fluctuations in both quantities (Sammalkorpi et al., 2009).

### 2.3 Importance of Salinity

At an interface of an aqueous solution containing anionic surfactant, there will be some repulsion between the surfactant head group as it carries the same charge. This in turn, makes the effective head-group area large due to its Electric Double Layer (EDL). Addition of electrolytes, however, will weaken the repulsive forces between the head groups and thus allows a higher concentration of surfactant at the interface/surface. An increase in surfactant/area ratio will decrease IFT/ST (Tichelkamp et al., 2014). Surfactant solution phase behavior is strongly affected by the salinity of the brine/salts.

The effect of increasing salinity not only has on pertains to adsorption of molecules at the interface, but it also alters the aqueous phase solubility. As the concentration of salt increases, the solubility of surfactant in the aqueous phase decreases.

### 2.3.1 The Electrical Double Layer (EDL)

A conceptual description of this topic will be helpful in understanding foams and other chemical enhanced oil recovery methods. A schematic description of an electric double layer is shown in Figure 17. When a charged particle is present in a solution containing an excess of ions, the ions will locate themselves around the particle to neutralize the surface charge. This accumulation of ions is named the electrical double layer (EDL). The double layer refers to two parallel layers of charge surrounding the particle surface. The first layer called the Stern layer which is formed by ions of opposite charge to the particle surface. These ions are named counter-ions and are adsorbed onto the particle surface. The counter-ions dominate close to the interface due to attractions with the surface. The second layer is a diffuse layer consisting of free ions that move under the influence of electrostatic attraction to the surface charge, and consists of both counter ions and co-ions - ions of the same charge as the surface (Berg, 2010, Hunter, 2013, Kontogeorgis and Kiil, 2016).

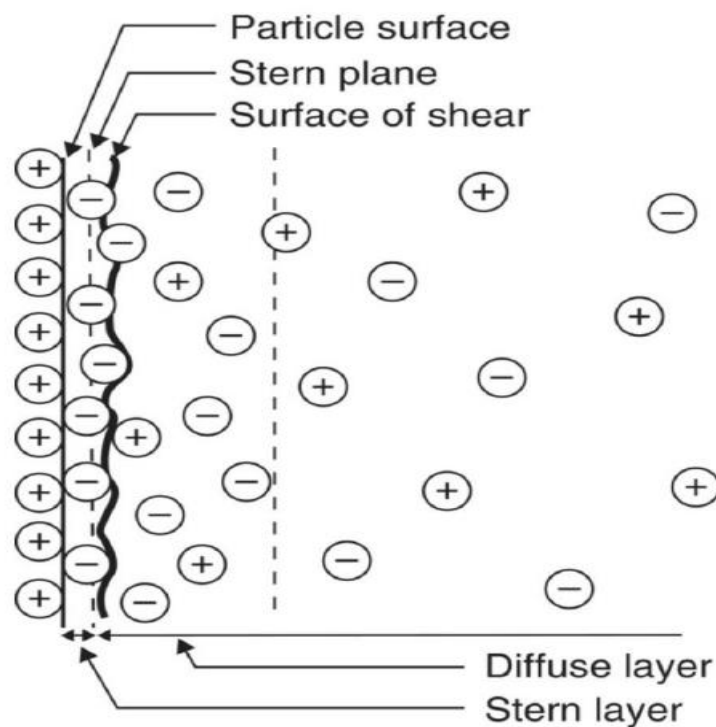


Figure 17: Schematic of an electric double layer. Modified from (Kontogeorgis and Kiil, 2016).

The thickness of the electrical double layer is called the Debye length,  $K^{-1}$  [nm]. The Debye length depends on salt concentration and valency of ions and can be expressed by the following equation for electrolyte solutions at 25<sup>0</sup> C (Berg, 2010, Hunter, 2013).

$$K^{-1} = \frac{0.304}{\sqrt{I}} \quad (7)$$

Where  $I$  is the ionic strength of the solution, which is a measure of the total concentration of ions in solution, given by:

$$I = \frac{1}{2} \sum z_i^2 C_i \quad (8)$$

Where  $z$  is the ion valency, and  $C$  is the molarities of the ions in the solution (Berg, 2010, Hunter, 2013). From this equation, the Debye length must decrease with increasing concentration and /or valance of ions in the solution, and vice versa. This is consistent with the intuitive idea that a higher concentration of ions neutralizes the surface charge within a shorter range, due to a more effective screening of the particle surface.

When two surfactant monomers with the same charge of the head group are present at an interface, their EDL will interact and repel each other. However, when salt is introduced into the system, positive and negative ions will interact with the double layer, decreasing the size of the EDL, and hence decreasing the repulsion between the two monomers (Brown et al., 2016). This is the reason why CMC, as well as ST /IFT, decrease in a surfactant-containing system when salt is introduced to the system.

### 3. Foam Stability

Foam are thermodynamically unstable systems, which eventually will collapse (Sheng, 2013). They evolve irreversibly over time because the interfacial area in the lamella diminishes in order to minimize the interfacial free energy of the system (Kornev et al., 1999).

Foam stability is the ability of foam to resist bubble collapse or coalescence (Romero-Zeron and Kantzas, 2007) and it is one of the most important aspects in foam characterization. However, foam stability is relatively difficult to control, since it is affected by many parameters, such as the amount and type of foaming agent and the method of foam preparation (Ghorbani et al., 2019). Foam stability can be quantified by measuring its half-life (Sheng, 2013), which can be monitored by the evolution of liquid content of foam as a function of time. There are three different mechanisms governing the half-life of foam: foam drainage (liquid drains out of the foam mainly through Plateau Borders and nodes under gravity), coarsening (enlargement of large bubbles by gas diffusion from smaller adjacent bubbles induced by the capillary differences) and bubble coalescence (merging of neighboring bubbles due to the rupture of the liquid films between them)(Cantat et al., 2013).

For foam in porous media, the principal mechanisms are the capillary suction coalescence, the capillary pressure, the interfacial elasticity, and the disjoining pressure. The attribute that distinguishes foam in porous media from the ordinary gas-liquid flow is the stability of the lamella. The stability of the lamella is also very dependent on the chemical properties of the surfactants. The foam films (lamella) are thin

free staying layers of aqueous solution surrounded by gas from both sides (Figure 18). Usually, surfactant molecules adsorb on both film sides and stabilize the film. The thickness of the films is usually only a few micrometers but could be even only a few nanometers while their area could be extended to a few square meters (Weaire and Hutzler, 2001).

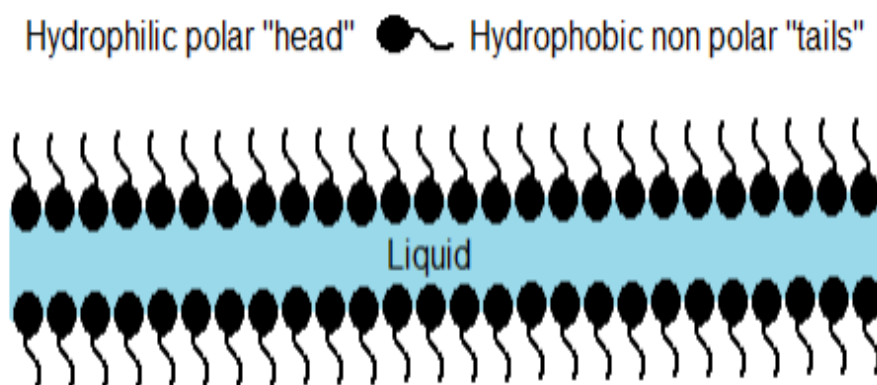


Figure 18: Illustration of a thin film stabilized by surfactant molecules (Solbakken, 2015).

Surfactants stabilize lamellae by reducing IFT, improving lamella elasticity, and increasing disjoining pressure. (Farajzadeh et al., 2012, Bureiko et al., 2015).

### 3.1 Gravity drainage

The most obvious force acting on foam is the gravitational force, causing drainage of the liquid between the air bubbles. The drainage can be improved by increasing the viscosity of the bulk liquid. As a definition, the drainage is the irreversible flow of liquid through a foam film membrane via plateau borders under the influence of both gravity and capillary forces. As water begins to drain under gravity, the top of the foam quickly becomes dry, with <1% liquid, whilst the bottom remains wet. The shape of the bubbles transforms under the influence of drainage, going from a somewhat spherical shape to polyhedral shapes. This drainage mechanism leads to foam gas bubbles becoming less stable, and increasingly susceptible to bursting (Heuser et al., 2008).

Bubble size is also important. In foam with small bubbles, the viscous dissipation is larger, and drainage will therefore be slower. Foam bubbles usually have diameters > 10  $\mu\text{m}$  and may be larger than 1000  $\mu\text{m}$ . Even though foam stability is not necessarily a function of drop size, there may be an optimum size for an individual foam type. Some foams that have a bubble size distribution that is heavily weighted toward the smaller sizes will represent the most stable foam (Schramm, 1994).



### 3.2 Surface elasticity

Surface elasticity sometimes referred to as the “self-healing” effect, is a direct consequence of surfactant adsorption at the interface. The mechanism behind this phenomenon is called the Gibbs-Marangoni effect and is illustrated in Figure 19. Foam films should have some elasticity in order to be able to withstand small deformations without rupturing. The Gibbs-Marangoni effect (Schramm, 1994) is responsible for this elasticity. The Marangoni effect is the fluid mass transfer along with an interface between two regions due to surface tension gradient. In a foam system, when a surfactant-stabilized liquid film undergoes an expansion, the local surfactant concentration is lowered owing to the increased surface area, and the film becomes thinner. The lower surfactant concentration results in a locally higher surface tension, which causes a contraction of the expanded surface to maintain low energy. This effect provides resistance against film thinning, which could eventually lead to film rupture. In other words, the Marangoni effect due to surface tension gradient helps to stabilize a foam system.

This condition of a surface elasticity must be valid in the time during which the lamellae is stretched and restored. Thus, it is a prerequisite for foaming that the diffusion of the surface-active component from the bulk solution to the newly created surface is sufficiently slow. If this is not the case, the adsorption at the surface will decrease the surface tension and the temporary stretch of the foam lamella will be made permanent with a weakening of the lamellae as the result. A film having high elasticity has more stability (Xu et al., 2003). The film elasticity decreases with increasing surfactant concentration (Rao et al., 1982), which leads to the rapid collapse of the foam.

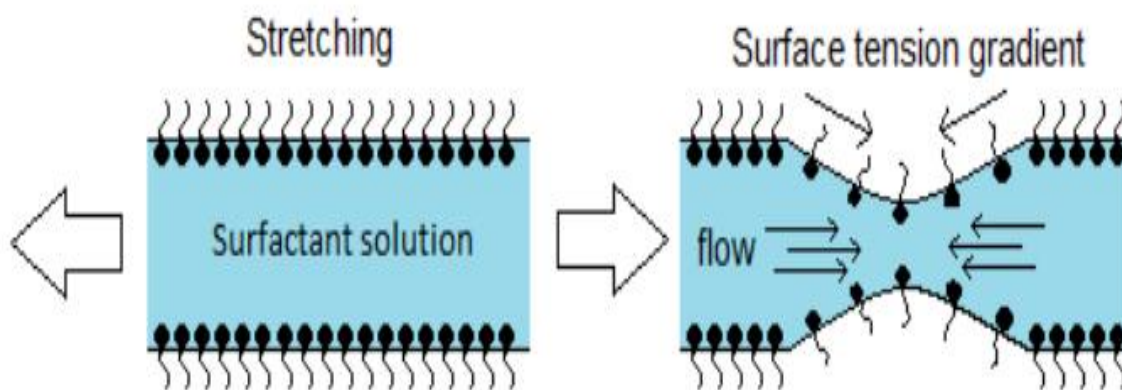


Figure 19: A sketch demonstrating the Gibbs-Marangoni effect. the locally lowered surfactant concentration causes contraction of the surface modified from (Schramm, 1994)

### 3.3 Laplace Capillary pressure

The pressure in the Plateau borders is lower than in the films. Due to the difference in the curvature of the liquid surface, the liquid will flow from the films to the plateau borders, which causes thinning of the films. The driving force that leads to liquid flow toward the borders is referred to as the capillary pressure suction. This thinning of the films can lead to rupture and foam collapse.

The Yong-Laplace equation describes how the pressure difference between the gas and liquid phase varies with the radius (R) of the curved surface.

$$\Delta P = P_G - P_L = \frac{2\gamma}{R} \quad (9)$$

Where  $P_G$  is gas pressure,  $P_L$  the liquid pressure and  $\gamma$  the surface tension. The quantity  $P_G - P_L$  is also known as the capillary pressure  $P_C$ . The radius of curvature at the surface of the Plateau border,  $R_2$  is smaller than the radius of curvature of the thin liquid film, but the gas pressure  $P_G$  in the bubble is equal.

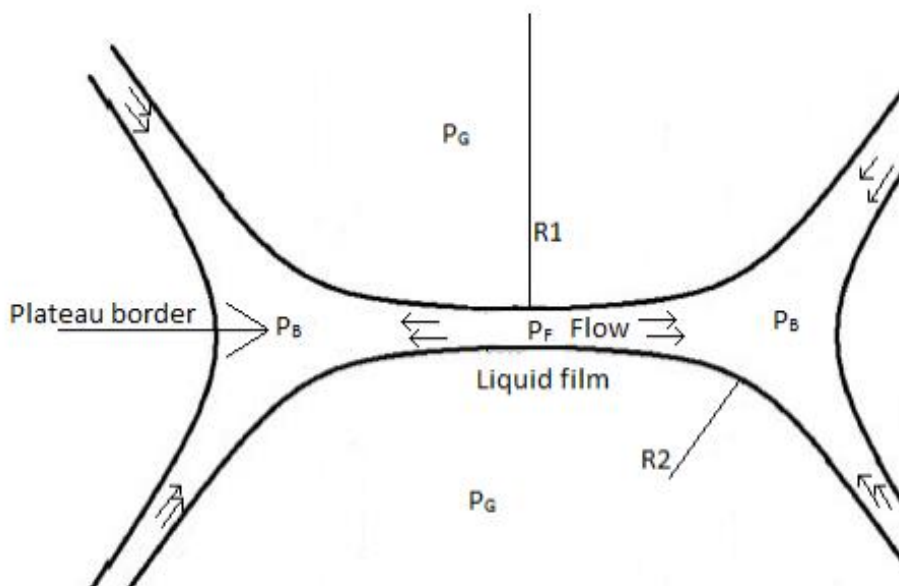


Figure 20: Illustration of a foam film between two Plateau borders. Modified from (Bent, 2014).

### 3.4 Disjoining pressure

Disjoining pressure can be defined as the total pressure difference between the liquid phase and the gas phase within a foam film and it is particularly dependent on the film thickness (Aronson et al., 1994).

The thin liquid film formed between bubbles initially thins under the influence of the capillary pressure. When the film thickness reduced to 300-200 nm, film drainage owing to the capillary pressure is slowed down and interactions between the film surfaces called the disjoining pressure start affecting the film drainage (Yaminsky et al., 2010).

This is only stopped when the surfactant molecules at the outer surfaces of the lamella begin to interact with each other. There are three different components that contribute to the disjoining pressure ( $\Pi$ ): van der Waals forces ( $\Pi_{VW}$ ), electrostatic forces ( $\Pi_E$ ) and steric forces ( $\Pi_S$ ).

$$\Pi = \Pi_{VW} + \Pi_E + \Pi_S \quad (9)$$

The attractive van der Waals forces have a negative contribution to the disjoining pressure. The electrostatic forces stabilize the foam film. When equally charged interfaces approach each other and their electric double layer overlap, repulsive forces will be created, which is a positive contribution to disjoining pressure. The steric forces arise from the fact that each atom within a molecule occupies a certain amount of space; they are repulsive and only observed a very short length scale. Molecule size can be important for steric interaction (Sedev and Exerowa, 1999). The disjoining pressure is thought only for thin films (i.e., < 100 nm). For thicker films, the disjoining pressure is not expected to be important (Schramm, 1994).

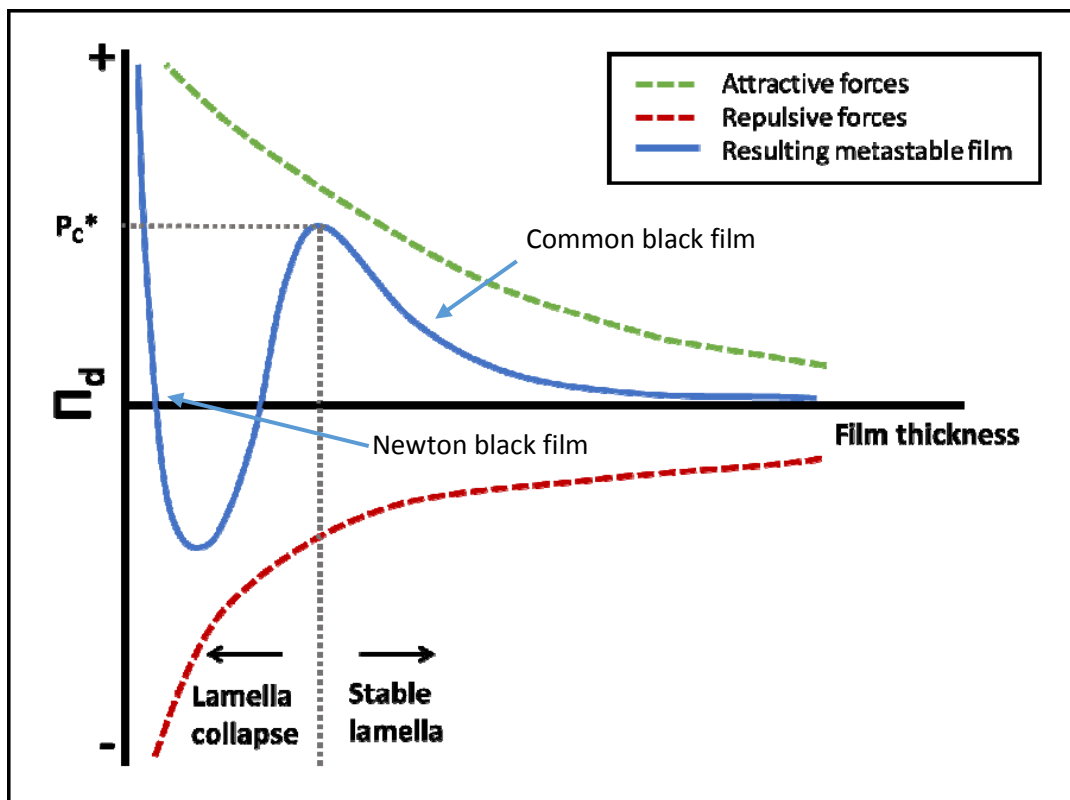


Figure 21: Schematic representation of the disjoining pressure curve (resultant from the attractive and repulsive forces), Modified from (Kornev et al., 1999)

The magnitude and the sign of the total disjoining pressure vary with the film thickness (Figure 21). When the film thickness is decreasing, a local maximum in disjoining pressure is encountered. The repulsive overlap of the electrostatic double layer is overpowering the van der Waals attraction. Films on this branch are called common black films. If the film thickness decreases further, van der Waals forces become more dominant. Stability is reached again when steric forces become significant; these films are called Newton black films.

### 3.5 Foams stabilized by ions

The addition of other chemicals (additives) to surfactant solution has been considered to enhance foam surface properties, which ultimately can strengthen the lamellae. Specific types of additive may produce the synergetic effect with the surfactant to increase foam stability by several ways, such as improving the elasticity of lamellae, decreasing the drainage of the liquid phase, and increasing the surface viscosity. There are several categories of additives that can be used to stabilize foam, such as polymers, particles and electrolytes.

Salts are either naturally present or added in many applications of foams. Salt influences the adsorption of surfactant molecules at the air-water interface and consequently alters the charge at the interface (Kralchevsky et al., 1999). Therefore, the adsorption and the stability of foam are strongly affected by the presence of salt. The ions of different valency affect the adsorption of surfactant to different extents due to their varied effect on the screening of electrostatic charge. The binding of counter ions can drastically reduce the forces at the air-water interface (Kralchevsky et al., 1999). Even salts having the same ions can lead to a significant difference in surfactant adsorption. This ion-specific effect has been attributed to the difference in the hydrated radius of the counterions (which leads to the difference in the area occupied by the ions in the Stern layer) and the effect of the counter ions on the structure of water (Kunz, 2010).

The properties of thin liquid films are important in the discussion of foam stability. The thickness of film depends on surfactant concentration in the solution. The film thickness decreases smoothly with increasing salt concentration. To verify this (Farajzadeh et al., 2008) had investigated two surfactant concentration (0.01 wt.% and 0.3 wt.%), and he found that the film of 0.01 wt.% surfactant concentration was thicker than the film which was prepared with 0.3 wt.% surfactant. This is because surfactant is an electrolyte itself and at low salt concentrations, its concentration determines the ionic strength of the solution.

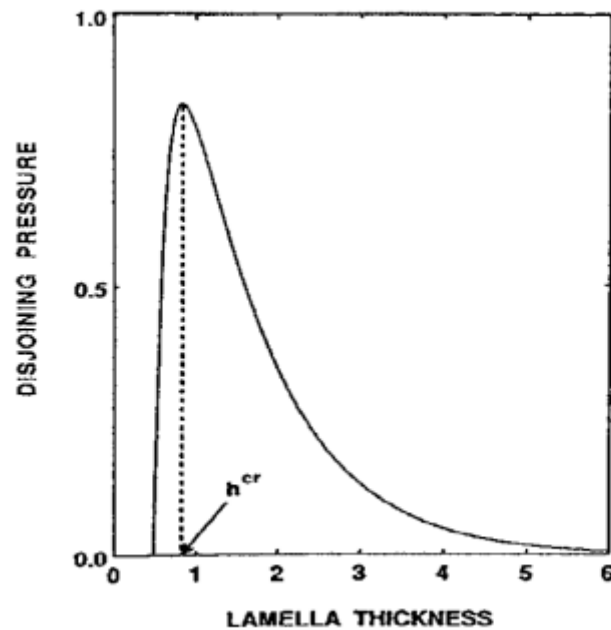


Figure 22: Disjoining pressure as a function of lamella thickness (Rossen, 1996)

In the presence of ionic surfactants, the electrostatic double-layer repulsion between the two opposing surfactant films also has a stabilizing effect. In that case, the presence of counter-ions can modify the foam stability by at least two mechanisms:

1. Screening of the electrostatic repulsion between the two charged film surfaces, allowing to thinner films, and thus possibly reducing the foam stability (Pugh, 1996). This effect is dependent on the ion charge and its size (Sett et al., 2015). Large ion penetrates more deeply in the surfactant film which leads to decreasing more effectively the electrostatic repulsion between the two opposing films see (Figure 23)

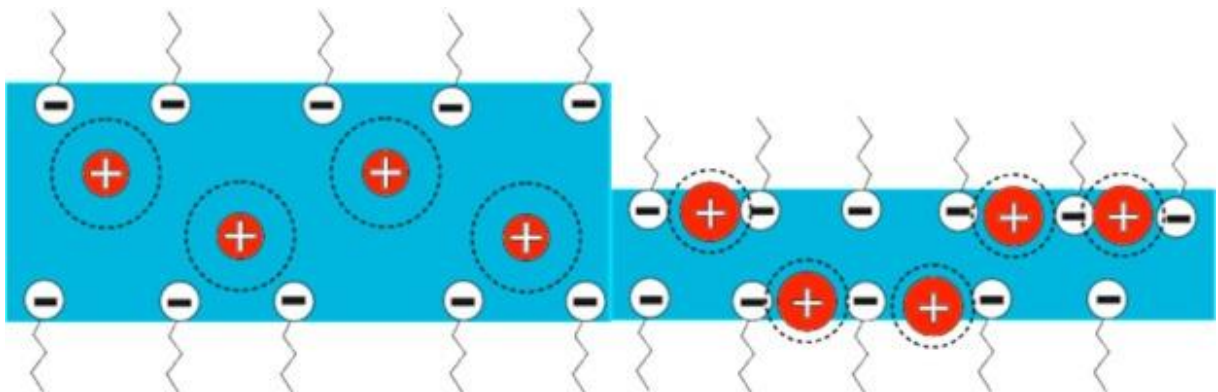


Figure 23: Effect of counter-ion size on the electrostatic repulsion between two negatively charged surfactant films, modified from (Schelero and von Klitzing, 2015). The dotted lines represent the hydration shell of the inorganic ions.

2. By screening of the repulsion between the charged surfactant head groups in the surfactant film. This leads to an increase in the amount of adsorbed surfactant at the air-water interface, therefore reducing the surface tension of the bubbles and increasing the film stability. This phenomenon is also dependent on the size as deeper penetration of the counter-ion in the surfactant film allows a more effective screening of the charged surfactant head group (Pandey et al., 2003, Sett et al., 2015, Schelero and von Klitzing, 2015).

The two previous mechanisms act in opposite directions: the former tend to destabilize the foam while the latter tends to stabilize it. Although the counter-ions appear to increase the lifetime of foams stabilized by ionic surfactant, (Sett et al., 2015) have shown that a rapid destabilization of the surfactant film occurs when a critical concentration of counter-ions is exceeded.

### 3.6 Surfactant concentration

Several studies show in their results the influence of surfactant concentration on foam generation, stability and bubble coalescence in presence and absence of salts are also reported in the literature (Farzaneh and Sohrabi, 2015, Rojas et al., 2001, Simjoo et al., 2013, Wang and Chen, 2013). Some of them reported that foam stability increases with increasing surfactant concentration while others reported increasing foam stability with the increasing surfactant concentration until a certain concentration is attained. Confirmed later that foam stability either decreases or remains the same from this surfactant concentration and beyond. The changes in surfactant concentration have a great influence on foam generation ability. In EOR foam application, surfactant concentrations are typically applied in the range of 0.1-1 wt.% (for economic reasons) (Mannhardt and Svorstøl, 2001).

### 3.7 Effect of oil on foam stability

Foam performance in the presence of oil plays an important role in foam applications in EOR. It is known that the addition of small traces of oil, hydrophobic particles, or a mixture of both strongly influences the foam stability. Since the foam is a closed system, the oil reaches only the outer surface of the foam. The defoaming activity of oil is usually explained in terms of the effects resulting from the surface activity of the oil or dewetting of the oil by the aqueous solution. This in turn depends on several physicochemical parameters.

There are many studies and laboratory experiments on the effect of oil on the stability of foam (Simjoo et al., 2012, Schramm and Novosad, 1990). Some researchers report that foam stability decreases in the presence of oil. others show that the composition of the oil phase has a great effect on the foam stability such that the existence of light component is detrimental to foam stability (Schramm et al.,

1993, Kuhlman, 1990). However, the parameters that determine foam – oil interactions the most are Entering (E), Spreading (S) and Bridging (B) coefficients and Lamella number (L).

To rupture a foam film, an oil droplet or a hydrophobic particle must firstly emerge from the aqueous phase into the gas-water interface during a process called entering. The entry coefficient is used to determine if it is thermodynamically favorable for the oil droplet to enter the solution gas surface:

$$E = \sigma_{wg} + \sigma_{wo} - \sigma_{og} \quad (10)$$

Where  $\sigma_{wg}$  is surface tension between gas and water,  $\sigma_{wo}$  is interfacial tension between oil and water, and  $\sigma_{og}$  is surface tension between oil and gas. The ability of oil drop to enter the gas-water interface is a necessary condition to rupture foam lamellae. A positive entering coefficient means the surface tension of the antifoam liquid ( $\sigma_{og}$ ) is lower than the sum of the surface tension of the foaming liquid ( $\sigma_{wg}$ ) and the interfacial tension (IFT) between the antifoam and the foaming liquid ( $\sigma_{wo}$ ).

If E is negative the oil droplet cannot enter the foam interface, and the surfactant solution completely wets the oil drop (Figure 24). After this entering, some oil from the droplet can spread on the solution-gas interface in a second step. When an oil drop spreads over the gas-water surface, a new gas-oil surface and water-oil interface are created, and the change is measured by a spreading coefficient, S:

$$S = \sigma_{wg} - \sigma_{og} - \sigma_{wo} \quad (11)$$

Spreading oils have a negative effect on foam stability. A positive value of the spreading coefficient indicates oil that will spread along with the gas solution interface. A high spreading rate will have a negative effect on foam stability. A negative spreading coefficient indicates that the oil not spread.

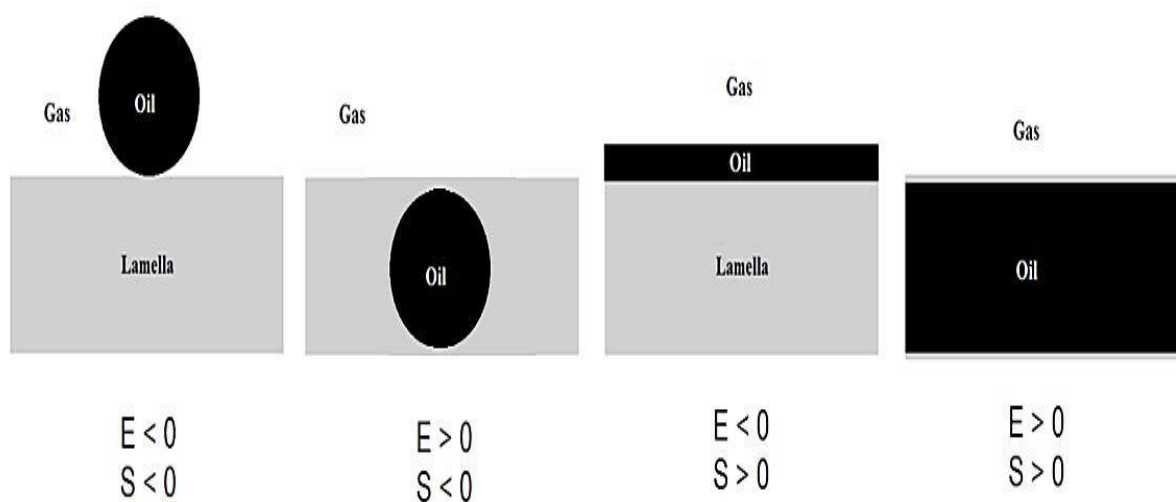


Figure 24: Illustration of the different entering and spreading scenarios of an oil phase in contact with a lamella

(Solbakken, 2015).

When an oil drop fully breaks through the thin liquid film an oil bridge is formed (Figure 25).

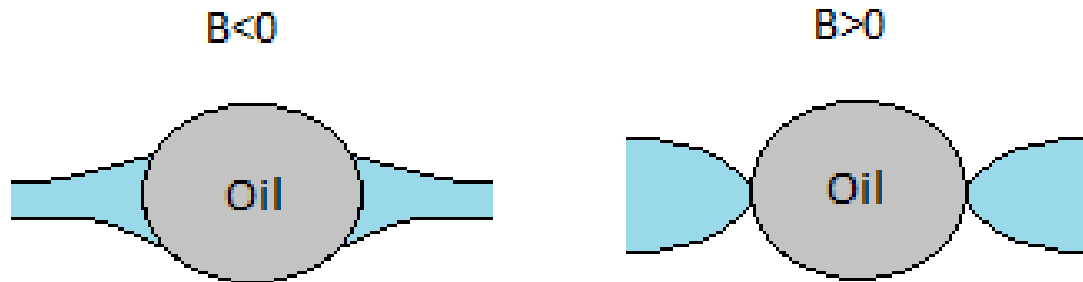


Figure 25: A schematic representation of the meaning of the bridging coefficient (Bent, 2014).

If  $B$  is negative, a stable bridge can be formed. Positive values of  $B$  corresponds to unstable bridges, which in turn leads to rupture the foam film. The bridge coefficient can be determined by the following equation:

$$B = \sigma_{wg}^2 - \sigma_{og}^2 + \sigma_{wo}^2 \quad (12)$$

Schramm and Novosad (Schramm and Novosad, 1990) proposed another mechanism for foam stability in terms of oil emulsification and imbibition in the foam structure. The main step of this mechanism is to form small oil droplets by emulsification, which allows oil droplets to move inside the foam structure. A dimensionless parameter, called Lamella number ( $L$ ), is proposed to describe foam stability. It is defined as a ratio of capillary pressure at Plateau borders to the pressure difference across the oil-water interface:

$$L \approx 0.15 \left( \frac{\sigma_{wg}}{\sigma_{wo}} \right) \quad (13)$$

Where 0.15 denotes the ratio between the radius of an oil droplet engulfed by water and the radius of the Plateau border contacting the oil surface.

They defined three types of foam depending on the value of the lamella number ( $L$ ): type (A) foam when  $L < 1$ , type B foam when  $1 < L < 7$ , and type C foam when  $L > 7$ . The lamella number theory is summarized in table 1, while Figure 26 illustrates if and how oil is imbibed in the lamella in flowing foam.



Table 1: Foam stability prediction by the lamella number theory

Type of foam	Foam stability to oil	E	S
A	stable	negative	negative
B	Moderately stable	positive	negative
C	unstable	positive	positive

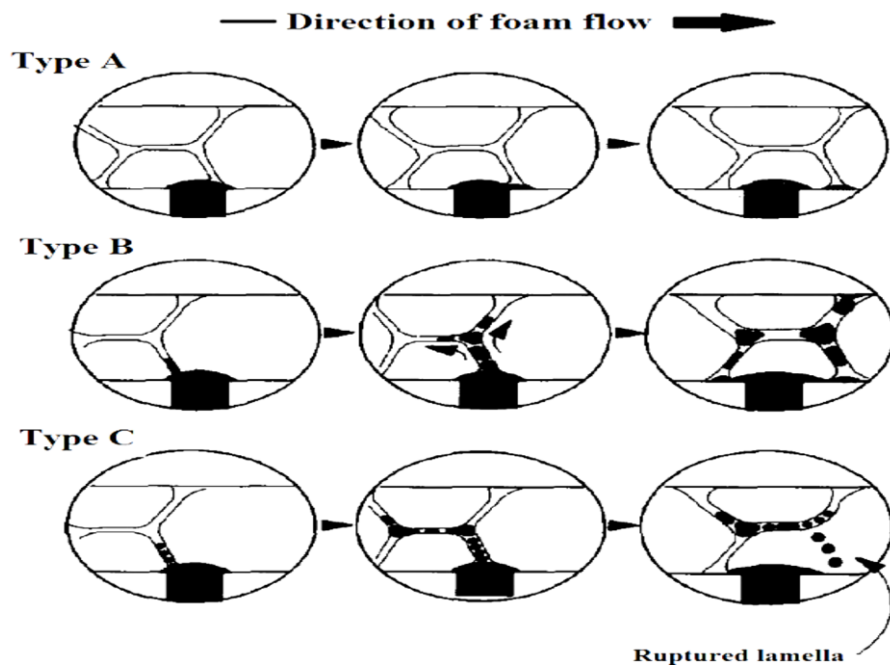


Figure 26: Illustration of type A, B and C foams, modified from (Schramm and Novosad, 1990).

There are two other criteria used to predict the stability of foam with and without oil. The following criterion is used to rank surfactants in the mixer method, modified from (Solbakken, 2015). The listed criteria were defined in this thesis based on earlier experiences and other surfactant screening studies using similar methods (Solbakken, 2015, Vikingstad et al., 2005, Arra et al., 1997, Arra et al., 2002):

Table 2: Criterion is used to evaluated and ranked surfactants in bulk tests based on their foamability and foam stability properties (Solbakken, 2015)

Good foamability:	Foam height, $h \geq 15$ cm after mixing.
Good stability:	Foam height, $h \geq 10$ cm for more than 24 hours.
Moderate foamability:	Foam height, $15 \text{ cm} > h \geq 10$ cm after mixing.
Moderate stability:	Foam height, $10 \text{ cm} > h > 5$ cm at 12-24 hours.
Poor foamability:	Foam height, $h < 10$ cm after mixing.
Poor stability:	Foam height, $h \leq 5$ cm at 0-12 hours.

The second most widely used Criteria depends on spreading and entering coefficients used to predict foam stability in the presence of oil:

Table 3: Foam predication by the sign of E, S and B coefficients, modified by (Simjoo et al., 2013)

<i>E</i>		-		+			
						<i>S</i>	
-		Stable foam		<i>B</i>			
						+	
-		Stable foam		Unstable foam			
						+	

## Chapter 2: Experimental procedures

## 4. Experiments descriptions

### 4.1 Materials and methods

This chapter provides an overview of the materials and methods used in this thesis. All measurements are done at ambient conditions (i.e.,  $22\pm 1^\circ\text{C}$  and atm).

Surfactants utilized in the experiments are four,  $C_{14} - C_{16}$  Alpha sulfonate surfactant (AOS) and Myristyltrimethylammomium bromide surfactant (MTAB) are used for the majority of the tests, while sodium dodecyl Sulfate (SDS) and sodium 1-decansulfonate (SDSs) are used in some supplementary tests. These surfactants are used as received without further purification. The surfactant solutions are prepared to single salt brines containing different concentrations of either NaCl,  $\text{MgCl}_2$  and  $\text{CaCl}_2$ , or in complex brines. The preparation of surfactant is greatly dependent on the activity of the surfactant feedstock and the desired weight percent of the stock solution. To know how complex brines or single salts and surfactant solutions are formed, as well as equations used to calculate the weight percent refer to Appendix A.

In this study, the main task consisted of surfactant aqueous solution preparation by mixing different concentration of surfactants with single salts and some complex brines. Distilled water is used as a solvent. The properties of salts/brines are shown in Table 4. Brine 1 is from the North Sea, the brine 2 is from the Mediterranean, and brine 3 is typical oil field formation water. The composition of these brines is shown in Table 5. A stock solution of 1 kg of each complex brine is prepared separately. The recipes for preparing these brines are shown in Appendix A, Tables 18, 19 and 20.

*Table 4: Concentrations and ionic strength of brines*

<b>Salts/ Brines</b>	<b>Concentration (wt. %)</b>	<b>Ionic strength mol/L</b>
NaCl	1 - 15	0.2 - 2.6
$\text{MgCl}_2$	1 - 40	0.3 - 12.6
$\text{CaCl}_2$	1 - 10	0.05 - 2.7
Brine 1	-	0.72
Brine 2	-	1.07
Brine 3	-	1.52

Table 5: Composition of synthetic Brines

Salt	Brine 1	Brine 2	Brine 3
Sodium	10843	12609	17868
Chloride	19569	28030	44219
Calcium	460	634	2811
Magnesium	1292	3256	3888
Bicarbonate	134	169	-
Sulfate	2668	3181	-
Potassium	347	453	387
<b>Total salinity (PPM)</b>	<b>35313</b>	<b>48333</b>	<b>69171</b>

The concentrations of surfactant of are: 0.01 wt.%, 0.05 wt.%, 0.1 wt.%, 0.1 wt.%, 0.5 wt.%, 1 wt.% and 2 wt.%. The chemical properties of these surfactants are summarized in Table 6.

Table 6: The details of the different surfactants with different active concentrations used in our experiments

	Surfactant	Formula	Purity (%)	Company
Anionic Surfactant	AOS (alpha olefin sulfonate)	$C_{14-16}$	39 %	Stepan
	SDS (Sodium dodecyl sulfate)	$C_{12}H_{25}NaO_4S$	92-100%	Stepan
	SDS (Sodium 1-decansulfonate)	$C_{10}H_{25}NaO_3S$	98≥%	Stepan
Cationic surfactant	MTAB (Myristyltrimethylammonium bromide)	$C_{17}H_{38}BrN$	99≥%	Stepan

#### 4.2 Preparations of Brines

Single salts solutions are prepared by weighing the amount of lab-grade (Sigma-Aldrich) NaCl, MgCl<sub>2</sub> and CaCl<sub>2</sub>, and adding them to the required volume of distilled water separately. Similarly, the complex brines are prepared by weighing the amount of salts and mixing them with distilled water then the solutions are left to stir for 1-2 hours until all the salts are dissolved. Then all brined are filtered using 150 mm filter paper. The brines are varied regarding to salinity and ionic strength.

### 4.3 Preparation of surfactant solutions

The surfactant solutions are prepared in standard 600 ml volumetric flasks. The surfactant is weighed and poured into the volumetric flask after which distilled water is added until the required final weight of the solution 300 g is obtained. To study the influence of electrolyte concentrations on surfactant and foaming characteristics, different surfactant solutions are prepared using NaCl, MgCl<sub>2</sub> and CaCl<sub>2</sub> single salts solutions and complex brines at different concentrations.

Equation 12 is used to measure the concentration of a salt solution or surfactant solution by weight percent (w/w):

$$\text{weight percent} = \frac{\text{weight of solute}}{\text{weight of solution}} \times 100 \quad (12)$$

The reason for using the percentage method in the calculation instead of volume is that we do not have the molecular weight of AOS, but we know its activity. Therefore, we use the same equation but multiply by the activity:

$$\text{weight percent} = \frac{\text{weight of solute}}{\text{weight of solution}} \times 100 \times \frac{100}{39.45} \quad (13)$$

### 4.4 Crude oils

In order to investigate the effect of crude oil on bulk foam properties, five different crude oil samples are used in this study. The crude oil samples are named 1-5. Physical properties of the oils at 22° C and atmospheric pressure are given in Table 7. Surface tensions of oils are measured using Sigma 700 Tensiometer. Densities and viscosities obtained from prior experiments (Vikingstad et al., 2005) (Solbakken, 2015).

Table 7: Crude oil properties (22±1 °C, atm)

Crude Oil ID	Density (± 0.01 g/cm <sup>3</sup> )	Viscosity (± 3% cp)	Surface tension to air (± 0.3 mN/m)
1	0.837	11.0	26.3
2	0.848	23.0	26.2
3	0.877	55.0	29.5
4	0.941	272	30.5
5	0.844	18.0	28.8

#### 4.5 Measuring of surface tension (ST) and CMC

Here the picture shows the Sigma 700 Tensiometer (KSV) used to measure the surface tension of the oils and some surfactant solutions and to determine CMC. The equipment uses the Du Nöuy which is explained in more detail in section 2.2.4.1.



Figure 27: Illustration of Tensiometer instrument.

To determine CMC experimentally, one plots surface tension against surfactant concentration and the slope changes when CMC is reached. Figure 28 is an example of an of CMC determination.

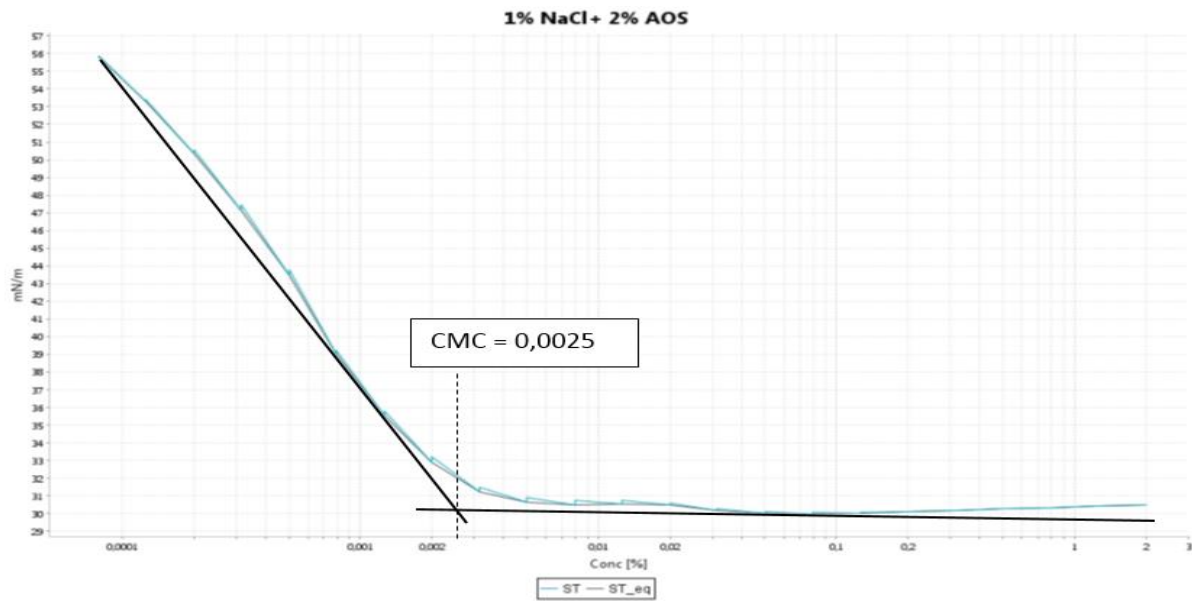


Figure 28: Example of CMC measurement for AOS in 1 wt.% NaCl at 23 °C

#### 4.6 Bulk Foam test

A schematic of the experimental set-up used for the bulk foam stability experiment is presented in Figure 29. The foam is generated by dispersing air into 300g test solution with a pedal connected to a mixer at a speed of 2000 rounds/min for 5 min for all the different cases. Solutions are mixed in 1000 ml glass cylinder, measuring 44 cm high and 6 cm in diameter. After mixing the glass cylinder is closed with a plastic seal. Immediately after the foam generation, the height of the foam column above the liquid phase is measured as a function of time (Appendix A Figure 53). The rate of the foam generation (foamability) is determined by the maximum height reached by the foam right after mixing. Foam stability is determined from the foam half-life, that is, the time is taken to reach half of the foam original height after generation and the rate of foam collapse is determined by monitoring foam height in 10 min intervals. Each test is repeated for at least two times. The uncertainty is measured for each test, but the values are around  $\pm 0.5$  cm. the mixing pedal is cleaned properly and dried before each foam preparation.



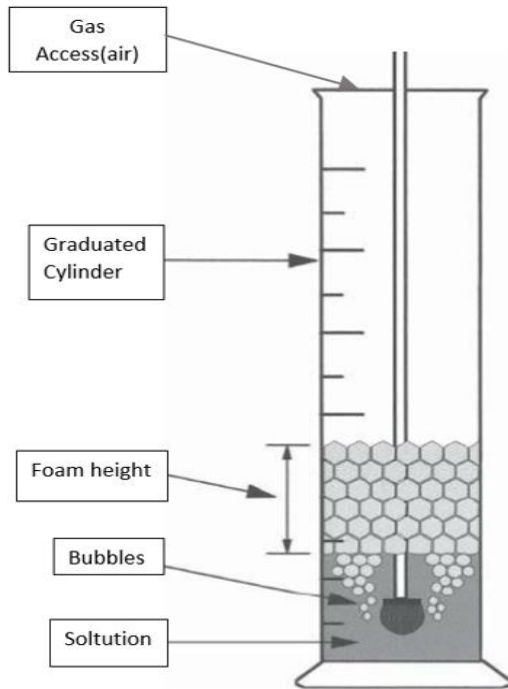


Figure 29: On the left a schematic of foam stability test modified from (Schramm, 2006, and on the right example of foam preparation.

#### 4.7 Spinning Drop method

Interfacial tension measurements are performed with computer controlled Spinning Drop Tensiometer SITE100 from KRUSS GmbH as shown in Figure 30. This apparatus can only measure IFT in the range of 0 – 10 mN/m. The Spinning Drop tensiometer is connected to a camera and controlled by the Kruss DSA2 software, which is used for image acquisition and analysis. This method is used by Bernard Vonnegut (Vonnegut, 1942), where this method is a drop of the light phase is placed in a cylinder containing the heavy phase fluid and spun at high rpm`s. the spherical drop deforms into a cylindrical shape due to the centrifugal force, and the deformation is balanced by the interfacial forces at mechanical equilibrium.

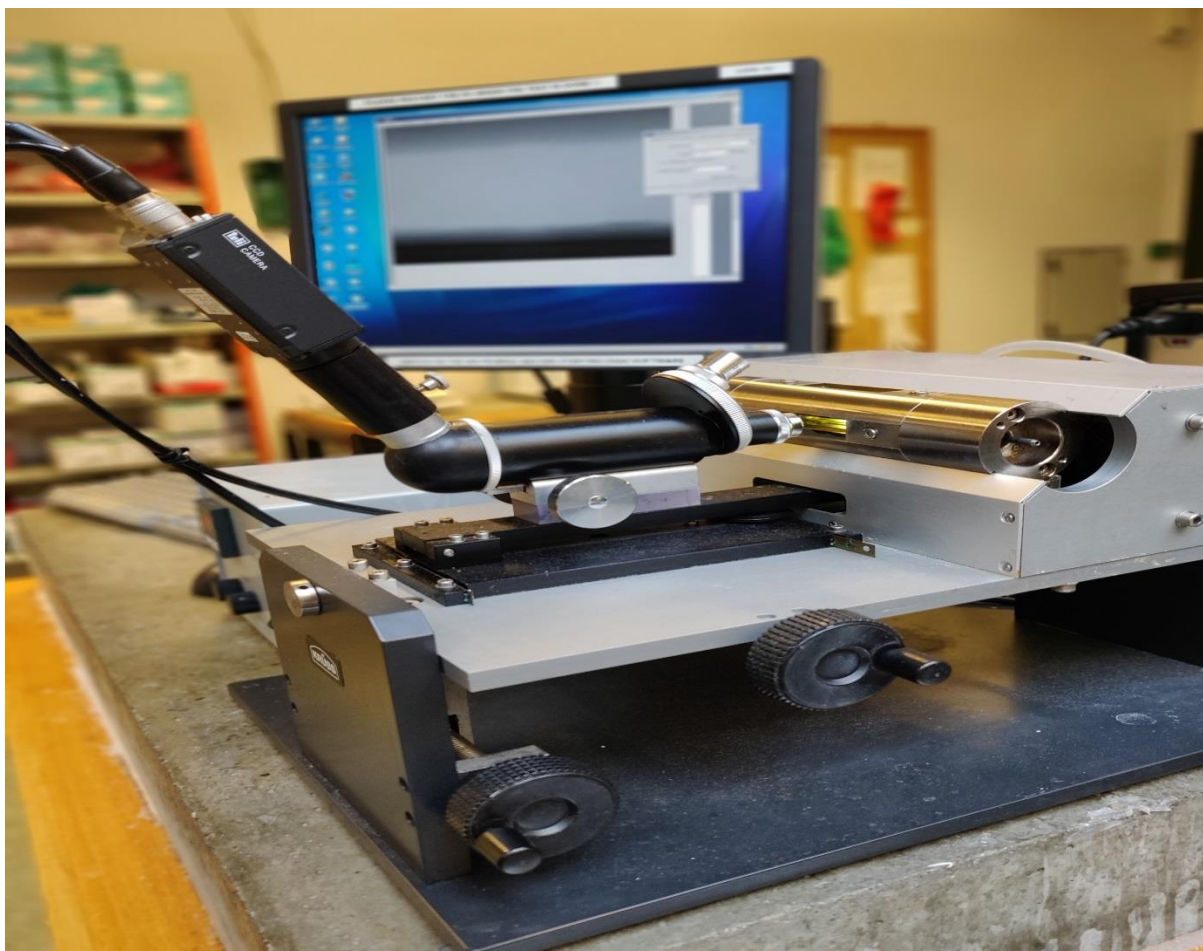


Figure 30: Setup for measurements of IFT with the Spinning Drop Tensiometer SITE100.

Before each measurement, the apparatus is cleaned with toluene, methane, and distilled water, and then filled with the heavy phase (aqueous phase) by 10 ml Plastipak syringe and long capillary needle. The cylinder is then spun at 6000 rpm to remove air bubbles from the system. A drop of the light phase (crude oil) is then injected into the cylinder with a Hamilton syringe and a long capillary needle. The stage is then tilted horizontally so the light phase droplet is placed approximately in the center of the spinning cylinder. Further, the rotational frequency is adjusted so the length of the drop is approximately 4 times the width. The high-speed camera then analyses the picture to obtain the length and width of the light phase droplet using the contrast between the two phases.

Figure 31 illustrates the drop behavior inside the rotating cylinder, as the rotational frequency is increased, where  $R_o$  is the sphere radius,  $R_1$  is and  $R_2$  are the deformed radii.

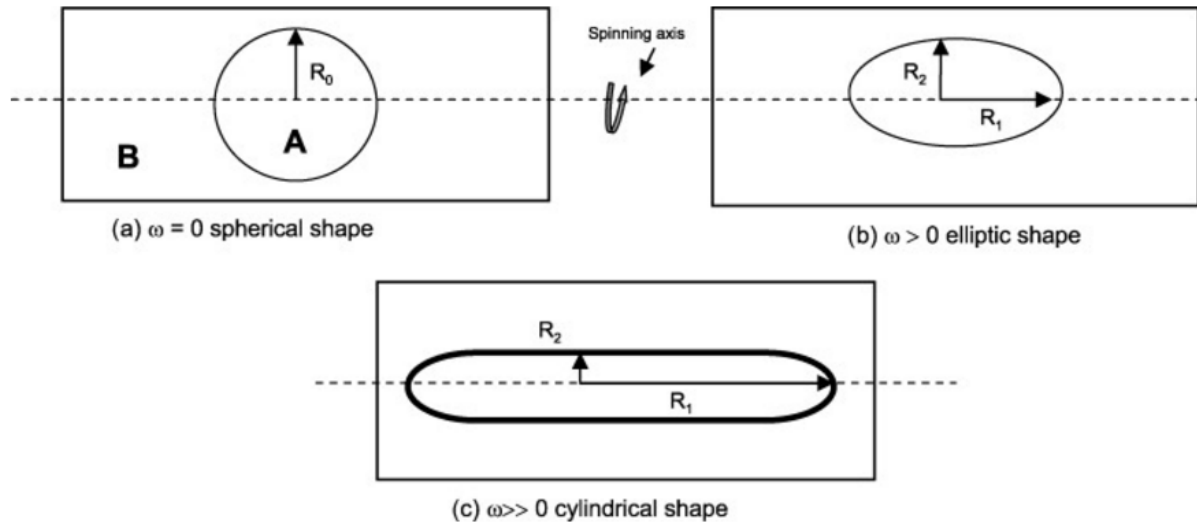


Figure 31: Spinning drop Method, modified from (Viades-Trejo and Gracia-Fadrique, 2007)

The surface or interfacial tensions are calculated automatically using the following equation (Viades-Trejo and Gracia-Fadrique, 2007)

$$\sigma = \frac{\Delta\rho\omega^2}{4} R^3 \quad (14)$$

Where  $\sigma$  is the interfacial tension,  $\Delta\rho$  the density difference between phases,  $\omega$  the angular velocity and  $R$  as the cylinder radius.

## Chapter 3: Results and Discussion

## 5. Results

### 5.1 Solubility tests

Solubility tests are performed to study the limits of the AOS (anionic) and MTAB (cationic) surfactants in different three single salt solutions, NaCl, MgCl<sub>2</sub> and CaCl<sub>2</sub> each at different concentrations, and in three complexes brines. AOS and MTAB concentration are kept constant at 0.5 wt.% active material in all the solubility tests. The temperature is 22 ± 1°C. Based on visual observations, the solubility is qualitatively defined as soluble, cloudy or precipitation. Examples of observations from the solubility tests can be found in Appendix A Figure 51 and 52.

During brine preparation, NaCl salt showed no precipitation across the concentration range used, up to 15 wt.%. As for the surfactant solubility, AOS is soluble in brine up to 7 wt.% NaCl, while MTAB showed no precipitation up to maximum salt concentration used (15 wt.% NaCl). Table 8 below shows the results from the solubility tests with NaCl.

Table 8: Solubility limit of AOS and MTAB in different concentrations of NaCl solutions (22±1°C)

Concentration NaCl (wt. %)	Ionic strength (mol/L)	Solubility of salts (Soluble/Precipitation)	Solubility of surfactant (Soluble/Precipitation)	
			AOS	MTAB
0	0	Soluble	Soluble	Soluble
1	0.17	Soluble	Soluble	Soluble
2	0.34	Soluble	Soluble	Soluble
5	0.86	Soluble	Soluble	Soluble
7	1.20	Soluble	Soluble	Soluble
8	1.37	Soluble	Precipitation	Soluble
10	1.71	Soluble	Precipitation	Soluble
15	2.57	Soluble	Precipitation	Soluble

Like NaCl, MgCl<sub>2</sub> salt is soluble in distilled water for up 40 wt.%. As for the surfactant solubility, AOS is soluble in MgCl<sub>2</sub> solution for up to 30 wt.% MgCl<sub>2</sub>, but it precipitated in 40 wt.% MgCl<sub>2</sub> solution. MTAB, on the other hand, is soluble in 40 wt.% MgCl<sub>2</sub> solution. Table 9 below shows the results from the solubility tests with MgCl<sub>2</sub>.

Table 9: Solubility limit of AOS and MTAB in different concentrations of MgCl<sub>2</sub> solutions (22±1°C)

Concentration MgCl <sub>2</sub> (wt. %)	Ionic strength (mol/L)	Solubility of salts (Soluble/Precipitation)	Solubility of surfactant (Soluble/Precipitation)	
			AOS	MTAB
0	0	Soluble	Soluble	Soluble
1	0.31	Soluble	Soluble	Soluble
2	0.63	Soluble	Soluble	Soluble
3	0.94	Soluble	Soluble	Soluble
5	1.57	Soluble	Soluble	Soluble
10	3.15	Soluble	Soluble	Soluble
30	9.40	Soluble	Soluble	Soluble
40	12.60	Soluble	Precipitation	Soluble

As can be seen in table 10 below, CaCl<sub>2</sub> is also soluble in distilled water for up to 10 wt.%. However, surfactant solubility is significantly different than NaCl and MgCl<sub>2</sub> solutions. AOS is soluble in 0.2 wt.% CaCl<sub>2</sub>, and then it is cloudy in 0.5 wt.%, thereafter AOS precipitated in solutions ranging from 1 – 10 wt.% CaCl<sub>2</sub>. However, MTAB precipitated on in 10 wt.% CaCl<sub>2</sub> solution.

Table 10: Solubility limit of AOS and MTAB in different concentrations of CaCl<sub>2</sub> solutions (22±1°C)

Concentration CaCl <sub>2</sub> (wt. %)	Ionic strength (mol/L)	Solubility of salts (Soluble/Precipitation)	Solubility of surfactant (Soluble/Precipitation)	
			AOS	MTAB
0	0.000	Soluble	Soluble	Soluble
0.2	0.05	Soluble	Soluble	Soluble
0.5	0.14	Soluble	Cloudy	Soluble
1	0.27	Soluble	Precipitation	Soluble
2	0.54	Soluble	Precipitation	Soluble
3	0.81	Soluble	Precipitation	Soluble
5	1.35	Soluble	Precipitation	Soluble
10	2.70	Soluble	Precipitation	Precipitation

Table 11 below shows the solubility of AOS and MTAB in typical complex brines. AOS is soluble in brine 1 and 2 while it precipitates in brine 3. On the contrary, MTAB is soluble in all three brines.

Table 11: Solubility of AOS and MTAB in typical complex brines (22±1°C)

Mixture	Ionic strength (mol/L)	Solubility of salts (Soluble/Precipitation)	Solubility of surfactant (Soluble/Precipitation)	
			AOS	MTAB
-				
Brine 1	0.72	Soluble	Soluble	Soluble
Brine 2	1.07	Soluble	Soluble	Soluble
Brine 3	1.52	Soluble	Precipitation	Soluble

Based on the results shown in the Tables 8-10, solubility limits for the two surfactants can be summarized in Figure 32. In general, the tolerance to NaCl is high for both surfactants; tolerance to  $MgCl_2$  is extreme, while tolerance to  $CaCl_2$  is poor for AOS and high for MTAB. The solubility limits found seem more dependent on salt type than ionic strength. These values are in line with what has been reported in the literature (Barakat et al., 1982, Barakat et al., 1983).

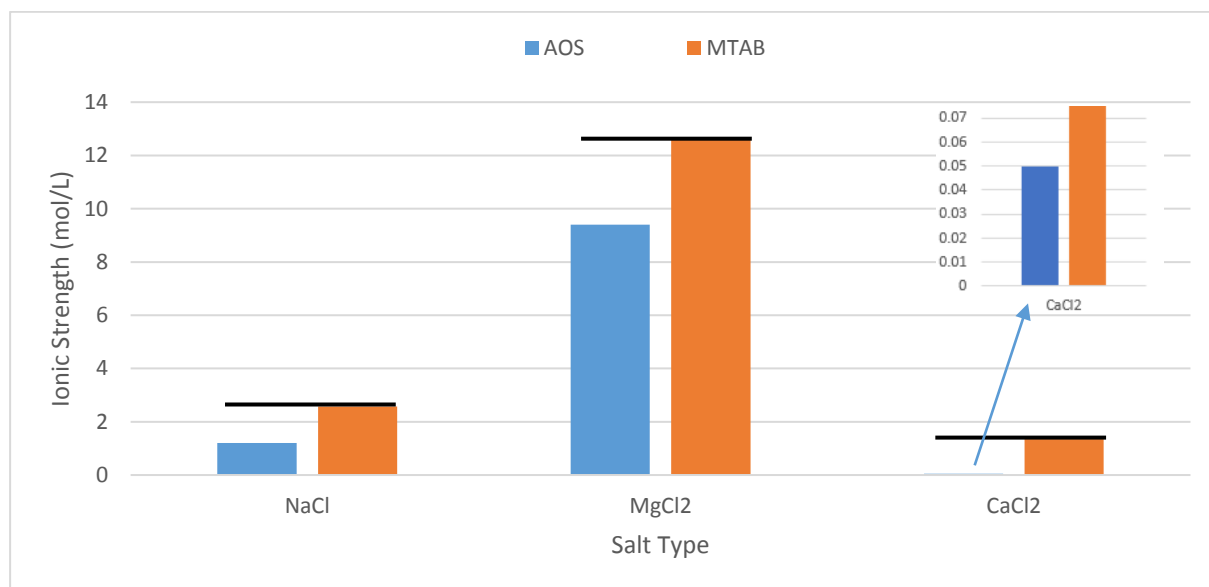


Figure 32: Comparison of AOS and MTAB solubility limits ( $22\pm 1^\circ C$ ), Black lines represent maximum salt ionic strength used

Moreover, these results explain the solubility of AOS and MTAB in the three complexes brines. AOS is insoluble in Brine 3 which has the highest  $Ca^{2+}$  concentration, and AOS tolerance to  $CaCl_2$  solution is poorest (only 0.05 mol/L). On the other hand, MTAB tolerance to  $CaCl_2$  is significantly higher than AOS (1.35 mol/L), and thus it soluble in Brine 3. One can say that salt tolerance depends on surfactant structure, and especially on the hydrophobic branching.

## 5.2 Surface tension and CMC

The CMC is determined for both the anionic and cationic surfactant in different electrolyte solutions from the surface tension measurement. The purpose is to study the effect of salt type, concentration and ionic strength on the CMC. The surface tension measurements are carried out using Du Nöuy ring method at ambient conditions. Table 11 presents the surface tension measurements and table 12 summarizes the corresponding calculated CMC.

Table 12: CMC values for AOS and MTAB surfactants in different electrolyte solutions (22±1°C).

Solution	Ionic strength mol/L	Surface Tension [mN/m] at 0.5 wt.%		CMC (wt.%)	
		AOS	MTAB	AOS	MTAB
Distilled water	0	34.35	34.30	0.0745	0.0810
1 wt. % NaCl	0.2	30.24	33.44	0.0050	0.0270
5 wt. % NaCl	0.9	27.96	33.17	0.0002	0.0026
1 wt. % MgCl <sub>2</sub>	0.3	29.00	34.05	0.0031	0.0110
5 wt. % MgCl <sub>2</sub>	1.6	29.27	33.60	0.0003	0.0025
Brine 1	0.72	29.14	-	0.0005	-
Brine 2	1.07	29.09	-	0.0004	-

The data shows that CMC and surface tension of aqueous solutions decrease in the presence of electrolytes (i.e ionic strength) since the presence of electrolytes decreases the surface activity of surfactants. AOS exhibits lower CMC compared to MTAB indicating stronger AOS surfactant molecules activity and/or affinity to the air-water surface than MTAB molecules. The observed trend is consistent with the reported literature (Wennerstrom et al., 1991). As I mentioned in section 2.3.1 that with an increase in salt concentration, the Debye length,  $K^{-1}$ , decreases, which leads to the reduction in electrostatic repulsion between the head groups. Consequently, more surfactant molecules adsorb at the air-water interface and the surface tension and CMC decreases.

It can be noted that at 5 wt. % salt concentration, the CMC values for the AOS and MTAB are quite similar, respectively, even though the ionic strength is approximately double. A similar trend was found with the same salts and AOS surfactant by (Vikingstad et al., 2005). It should also be noted that the values are extremely low, and accuracy of the instrument and measurements may not be sufficient to conclude on these results.

### 5.3 Effect of surfactant concentration on bulk foamability and stability

In the following tests, AOS and MTAB concentrations are varied from 0.01 to 2.0 wt.% while NaCl concentration is kept constant at 5 wt.%. All surfactant concentrations are well above the surfactants CMC (Table 12). The tests are performed at ambient conditions using 300g of solution. The effect of surfactant concentration on foamability and foam stability can be inferred from the maximum height of the generated foam presented.

#### 5.3.1 Effect of surfactant concentration on bulk foamability

The effect of surfactant concentration on foamability is shown in Figure 33. It is evident from figure 33 that the initial foam volume significantly increased with increasing surfactant concentration. A high



concentration of the surfactant in the bulk solution may increase the rate of the transport of the surfactant molecules towards the interface.

AOS gives more foam than MTAB. This is related to the amount of occupied area of the solution with surfactant. Regards to Table 12, AOS has more activity on the surface which in turn gave us less CMC than MTAB, which means the adsorption is higher and led to high formability.

This is expected because the increase in surfactant concentration leads to high accumulations of surfactant molecules in the bulk solution and gas-liquid interface of the foam which promotes foam generation. could be related to reorganization from spherical to rod-like micelles and further to multilayer laminar or liquid crystalline phases, same suggestion as brought up by (Vikingstad et al., 2005).

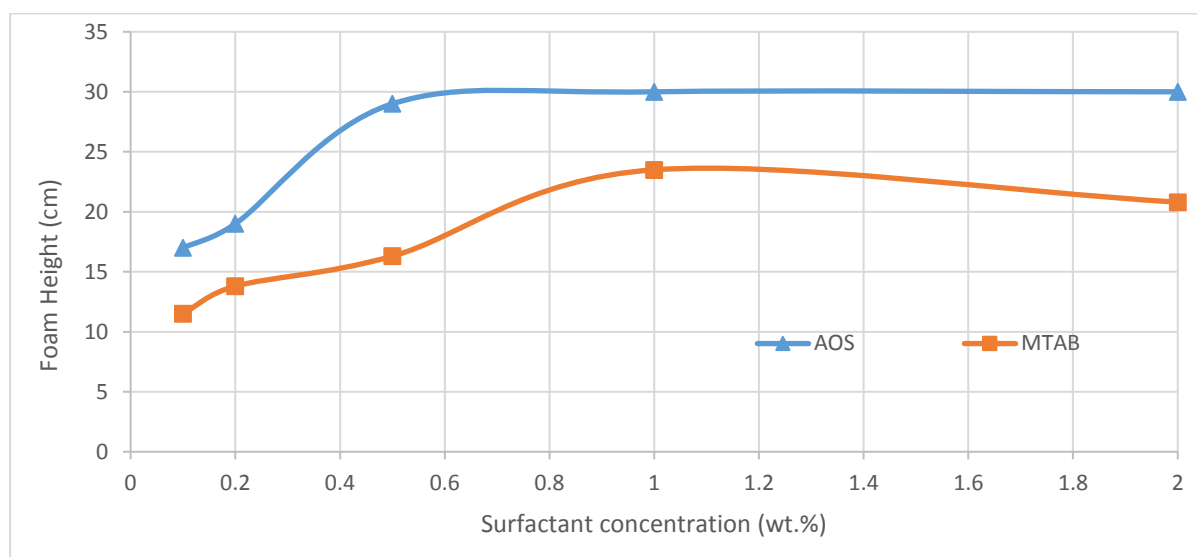


Figure 33: Foamability of AOS and MTAB at different concentrations with a constant concentration of NaCl (5 wt.%) at 0 min after mixing.

### 5.3.2 Effect of surfactant concentration on bulk foam stability

The stability of the foam as a function of surfactant concentration is assessed using half-life criterion which is the time taken to reach half of the foam original height after generation such that the higher the half-time the more stable the foam and vice versa. To examine the influence of surfactants concentration on foam stability, the foam half-life is determined and plotted against the surfactant concentration.

As shown in Figure 34, for AOS surfactant, the foam half-life increases with increasing the surfactant solution concentration. Nevertheless, it can be seen from the figure that foam stability first increases by increasing AOS concentration up to a specific point (0.5 wt.%) beyond which foam stability decreases. This is likely due to the decrease in the Gibbs elasticity of the foam film with increasing

surfactant concentration. Moreover, free water in Figure 34 is the water not occupied by the foam at time  $t = 0$  min after mixing and is not part of the foam column. Free water decreases with increasing surfactant concentration up to a point (0.5 wt.%) beyond which there is no free water.

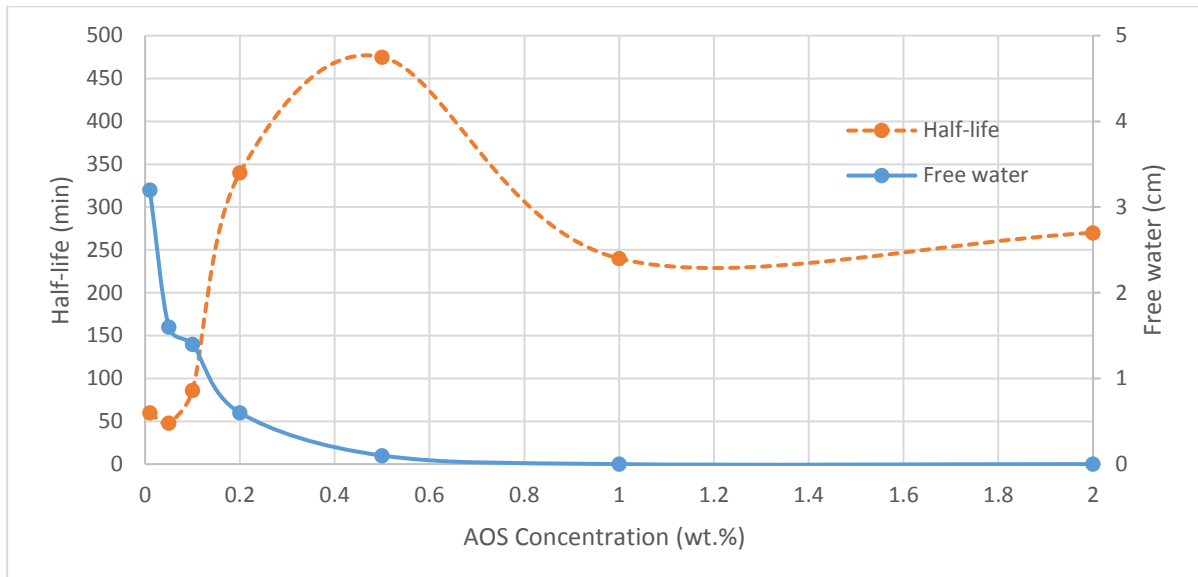


Figure 34: Foam half-life and free water at a function of AOS concentration (5 wt. % NaCl and  $22\pm 1^\circ\text{C}$ )

Similarly, MTAB foam stability increases with increasing the surfactant solution concentration up to 1 wt.%, after that it starts to decrease as shown in Figure 35. Furthermore, free water decreases with increasing surfactant concentration also up to 1 wt.% after which it remains at 0.5 cm.

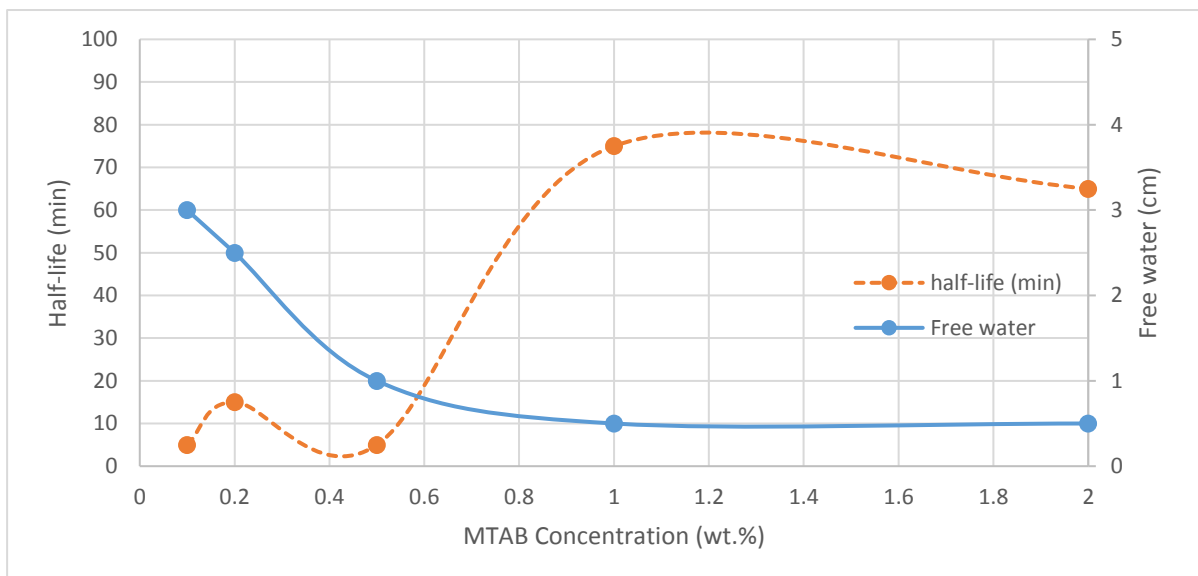


Figure 35: Foam half-life and free water at a function of MTAB concentration (5 wt. % NaCl and  $22\pm 1^\circ\text{C}$ )

Looking at Figures 34 and 35, there is an optimum surfactant concentration at which the half-life is highest, and the free water is lowest. AOS has lower optimum concentration is (0.5 wt.%) than MTAB (1.0 wt.%). Moreover, comparing the two figures, it is evident that AOS foam is much more stable than

MTAB foam since the half-life of AOS foam at optimum concentration is 475 minutes compared to 75 minutes for MTAB. It is also interesting to note that AOS maximum foamability is achieved at 0.5 wt.%, and MTAB at 1.0 wt.%, corresponding the optimum concentrations obtained from half-life and free water measurements. Increasing surfactant concentration beyond the optimum point increases the rate of foam collapse. The increased weight of surfactant increases the influence of gravitational force on foam drainage leading to continuing drainage of the liquid from the space between bubbles and in turn to rupture the liquid films and bubble coalescence (Baz-Rodríguez et al., 2014).

Figure 36 depicts the change in height of generated foam as a function of time for AOS foam. It can be seen from the figure that higher surfactant concentration enhances bulk foam stability and the maximum foam height. At higher concentrations of surfactant, foam stability is predominantly developed by micelles formation. These results are consistent with the reported behavior of foam stability by (Osei-Bonsu et al., 2015). They showed that foam that is generated using a lower concentration of AOS has a significant tendency to be ruptured, which leads to a rapid draining process.

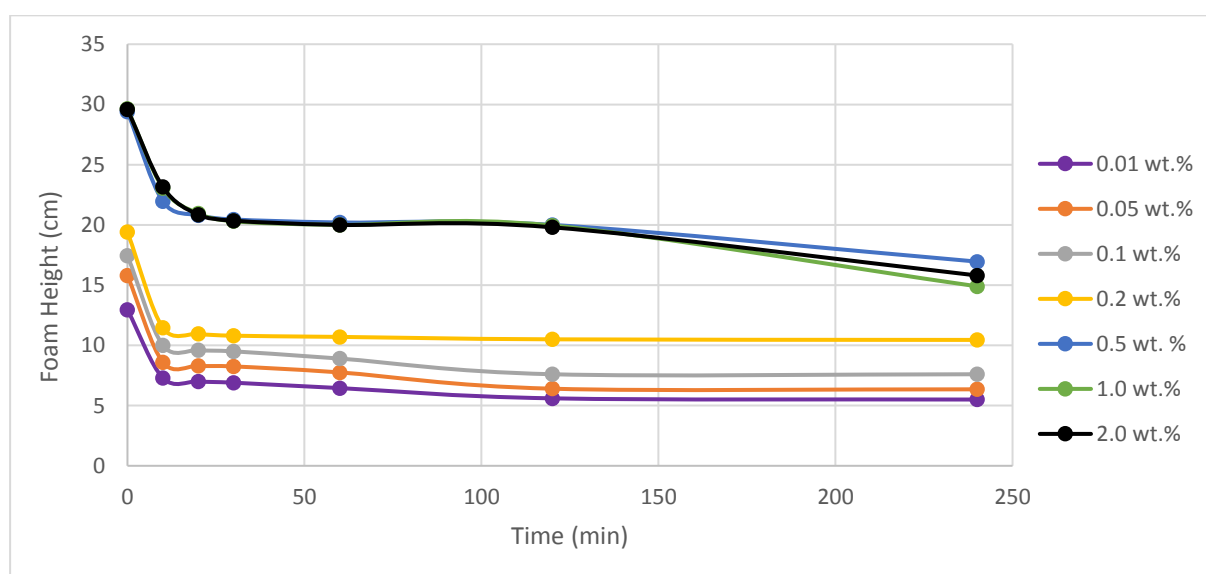


Figure 36: AOS foam height as a function of time

On the other hand, MTAB foam collapse is much faster for high concentrations, where the foam height reaches 0 cm after 4 hours in the case of 2.0 wt.% MTAB (Figure 37). In addition, 1.0 wt.% foam also reaches 0 cm after 4 hours, which is the optimum concentration based on the half-life, free water, and foamability. However, at low MTAB concentrations, the foam is generally stable for a longer period. This indicates that MTAB foam is more complex than AOS and that the optimum surfactant concentration may vary depending on the application for the foam.

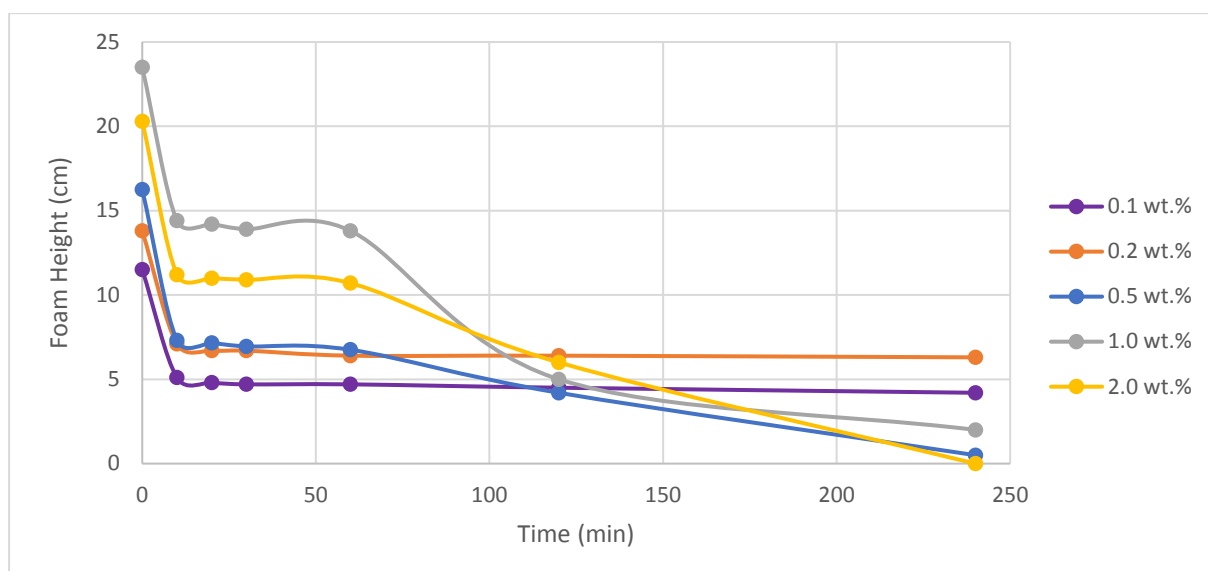


Figure 37: MTAB foam height as a function of time

#### 5.4 Effect of salinity on bulk foamability and stability

In the following tests, different single salt solutions and complex brines at different concentrations are used, while surfactant concentration for AOS or MTAB is kept constant at 0.5 wt.%. The tests are performed at ambient conditions using 300 g of solution.

##### 5.4.1 Effect of salinity on bulk foamability

The effect of the concentration of different single salt solutions and complex brines on the initial height of foams are demonstrated in Figure 38. The presence of NaCl generally increases the AOS foam height, and so does the presence of  $MgCl_2$ . Complex brines 1 and 2 have approximately identical AOS foam height, even though they have ionic strengths of 0.7 and 1.07 mol/L, respectively.

The behavior of MTAB foam with salinity and concentration is not as straight forward as AOS. The presence of 1.0 wt.% NaCl has no influence on MTAB foam height, while 5.0 wt.% NaCl decreases the foam height. The presence of  $MgCl_2$  with concentration of 1.0 wt.% in the solution results in a slight increase in the foam height compared to distilled water, but the further increase of  $MgCl_2$  to 5.0 wt.% decreases the foam height. Complex brines 1 and 2 show identical foam heights.

In general, it can be seen that the effect of NaCl and  $MgCl_2$  on AOS foam height is different from their effect on MTAB foam height, and thus the salinity effect on foam height depends on the type and structure of the used surfactant. Moreover, the height of the foam generated by the anionic AOS surfactant is much higher for all cases than the foam generated by the cationic MTAB surfactant.

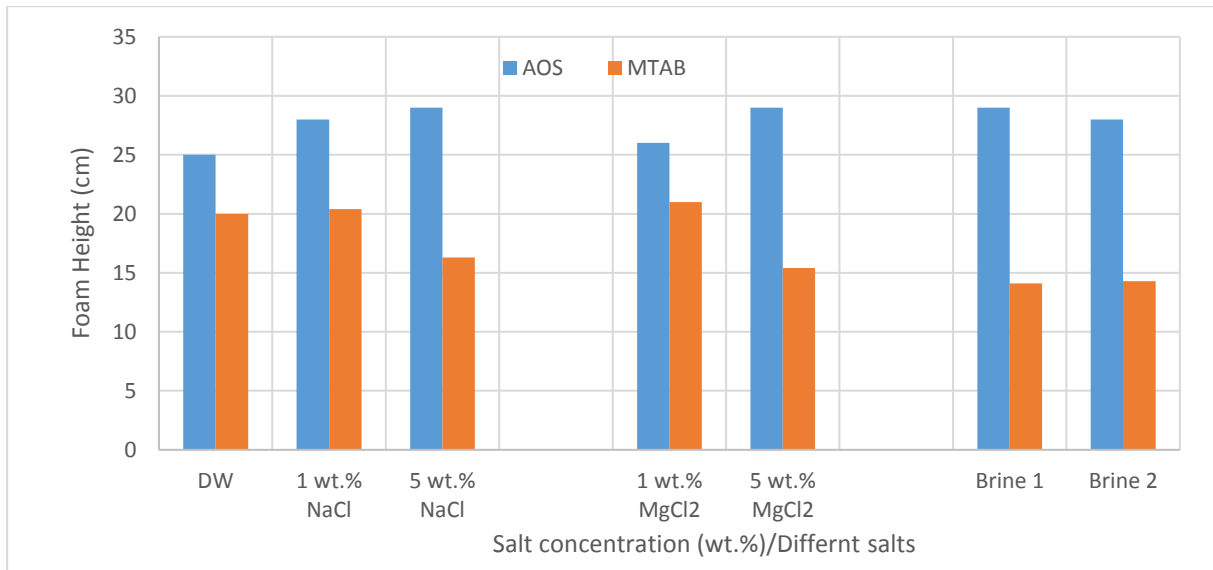


Figure 38: Initial foam height in the presence of salt at different concentration

#### 5.4.2 Effect of salinity on bulk foam stability

The stability of the foam as a function of salt type and concentration for each surfactant is assessed using the aforementioned half-life criterion. Figure 39 shows the foam half-life for AOS with different salt solutions and concentrations, and with complex brines. According to the figure, we can note that AOS foam stability decreases with increasing NaCl concentration, while it increases with increasing MgCl<sub>2</sub> concentration. This suggests an abrupt change in micellar properties (Pandey et al., 2003). In general, for low salt concentration, AOS is more stable in NaCl, while for high salt concentrations AOS foam is more stable in MgCl<sub>2</sub>. The complex brine 2 gives slightly more stable foam than brine 1, which may be due to the higher Mg<sup>2+</sup> concentration.

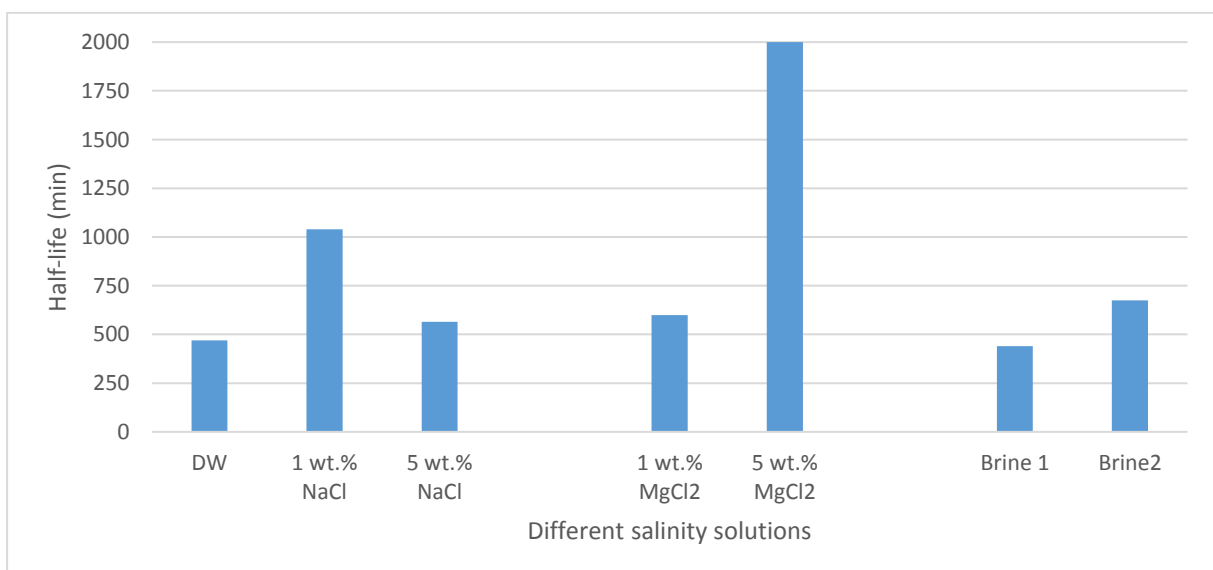


Figure 39: Foam half-life as a function of different salt type and concentration (0.5 wt.% AOS and 22±1°C)

Figure 40 below presents MTAB foam half-life with different salt solutions and concentrations, and with complex brines. It can be seen that MTAB foam stability sharply decreases with increasing NaCl concentration and with increasing MgCl<sub>2</sub> concentration. Moreover, MgCl<sub>2</sub> gives more stable foam than NaCl at low concentrations. Foam generated in brine 1 and 2 are equally stable.

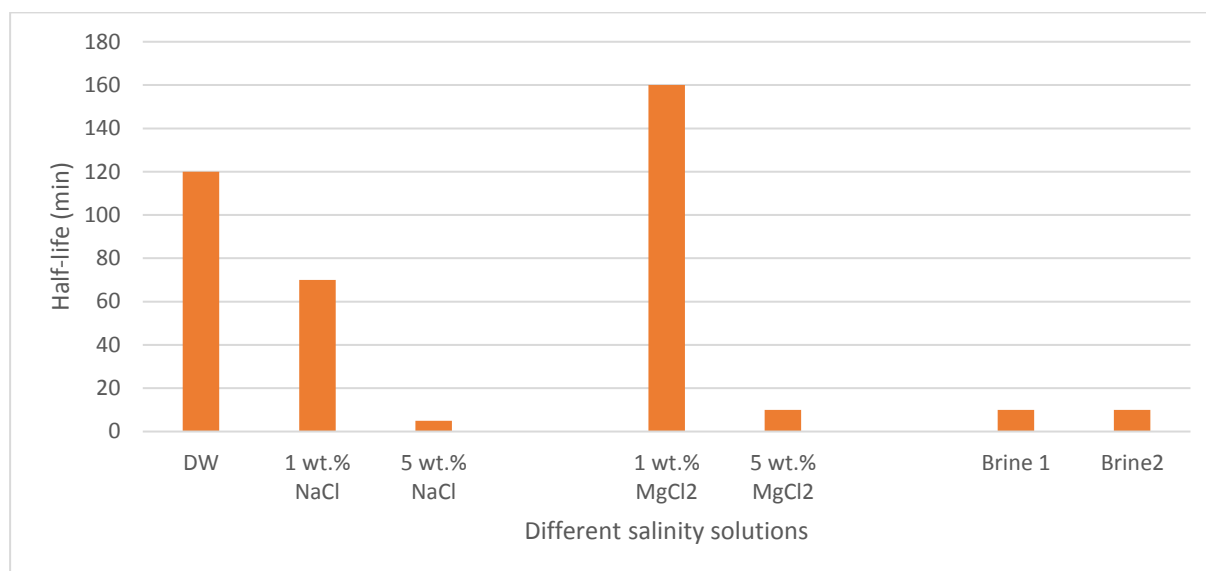


Figure 40: Foam half-life as a function of different salt type and concentration (0.5 wt.% MTAB and 22±1°C)

The role of divalent ions (Mg<sup>+2</sup>) in stabilizing lamella is probably the screening of the repulsion force between the negatively charged head groups of anionic surfactants (AOS), allowing more surfactant monomers to be packed at the interface and thus reducing its surface tension. The lower surface tension may not ensure a result in longer half-life. The opposite effect is expected for the cationic surfactant MTAB.

Figures 38 and 39 show that NaCl effect on AOS foam stability is opposite to its effect on foamability. From figure 38 one can observe that AOS foamability increases with increasing NaCl concentration. However, from figure 39 it is evident that AOS foam stability decreases with increasing NaCl. (Sett et al., 2015) have shown that a rapid destabilization of the surfactant film occurs when a critical concentration of counter-ions is exceeded. On the other hand, MgCl<sub>2</sub> has a similar effect on AOS foamability and stability such that Increasing MgCl<sub>2</sub> concentration enhances both foam properties.

Comparing figures 38 and 40, MTAB foam stability and foamability show similar trends with the concentration of salts. For instance, both foam stability and foamability decrease with increasing NaCl concentration, and with increasing MgCl<sub>2</sub> concentration separately.

As noted previously that there is an optimum concentration of surfactants, one can speculate that there might be an optimum concentration of salt. Therefore, we used a constant surfactant concentration (0.5 wt.%) for AOS and MTAB with more resolution on salt concentration. However, we have become more deeply involved with  $MgCl_2$  due to the lack of reported research with these surfactants, and due to the high solubility of surfactants in  $MgCl_2$ .

Figure 41 shows the height of foam generated by AOS and MTAB at different concentrations of  $MgCl_2$ . For AOS, we found that foam increases by increasing the salt concentration until it levels off and then begins to decline. Unlike AOS, MTAB the tolerance to magnesium salt is high, thus we tested foamability and precipitation up to 40 wt.%. Foam height decreases with increasing salt concentration and then increases up to the salt concentration of 15 wt.% where foam height roughly stabilizes with salt concentration. The rate of collapse of foams is slow in the presence of salt.

In summary, there seems to be an optimum concentration of salt that gives the highest rise of foam and most stable. This concentration depends on the type of surfactants and type of salt. The optimum concentration of magnesium salt is 5 wt.% and 15 wt. % for AOS and MTAB, respectively.

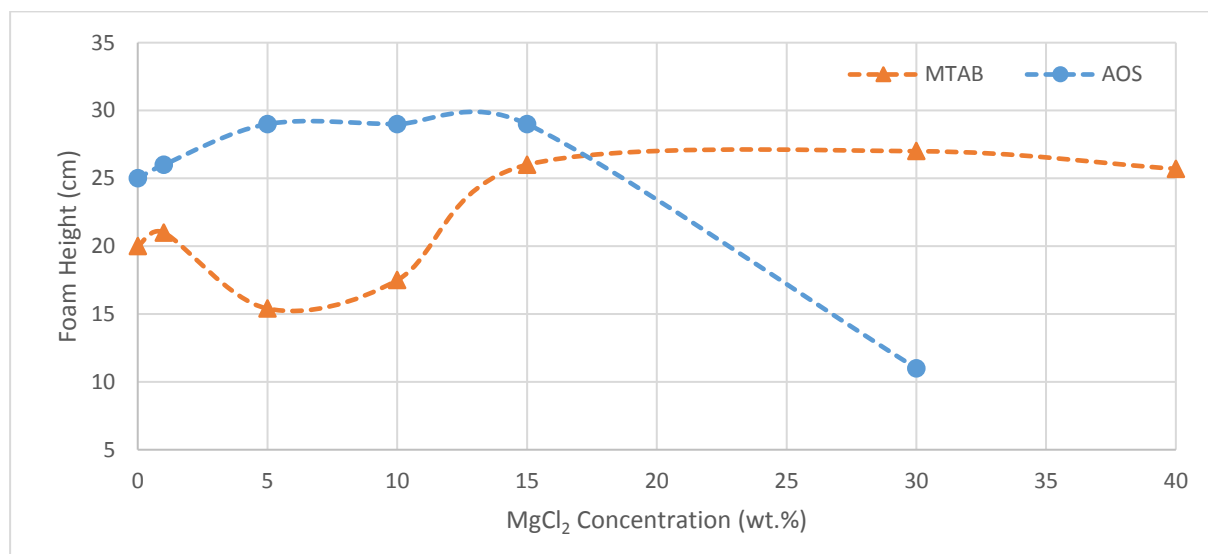


Figure 41: Foam Height vs. Different type of Surfactant at different concentration of  $MgCl_2$  to find the optimum salinity

Ions of different valency have different effects on surfactant foaming and adsorption properties due to their influence on the screening of the electrostatic charge (Behera et al., 2014), 20, which is in line with our results. We used solutions with different salts but identical ionic strengths, and as can be seen from Figure 42, NaCl gives more foam than  $MgCl_2$ . Overall, both give good foamability, and foam height increases with increasing ionic strength.

In general, salinity has a significant effect on surfactant performance. In most of the cases, high salinity has an adverse impact on the efficiency of the foam.

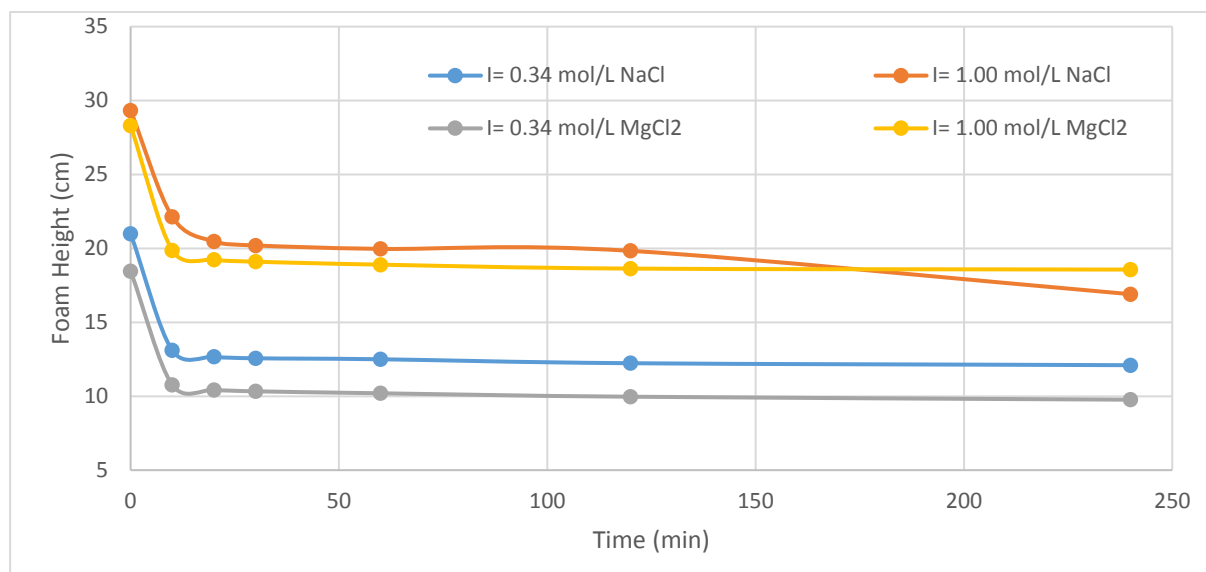


Figure 42: Foam height against time for the same ionic strength of different salts

### 5.5 Effect of surfactant type on Foamability and stability of foam

In order to better understand the effect of surfactant type on foamability, we expanded the previous collection of surfactants, AOS and MTAB, to include two more anionic surfactants, SDS sulfate, and SDS sulfonate. The surfactant concentration is kept at 0.5 wt.% in all solutions, with an arbitrary constant NaCl concentration of 1 wt.%. The properties of the surfactants are shown in Table 11 presented under section 4.1.

Firstly, SDS Sulfonate is insoluble in 1 wt.% NaCl solution at 22.3 °C, which we believe is due to the Krafft temperature. Therefore, the solution is heated to find the Krafft temperature. At approximately 28-29 °C the surfactant dissolves and there is no more precipitation, which is the Krafft temperature of SDS Sulfonate. However, due to its solubility issues, we couldn't include it in the subsequent bulk foam test, which is all conducted at ambient conditions.

The foam heights for the other three surfactants, which had no solubility issues, for the first 4 hours are presented in Figure 43.



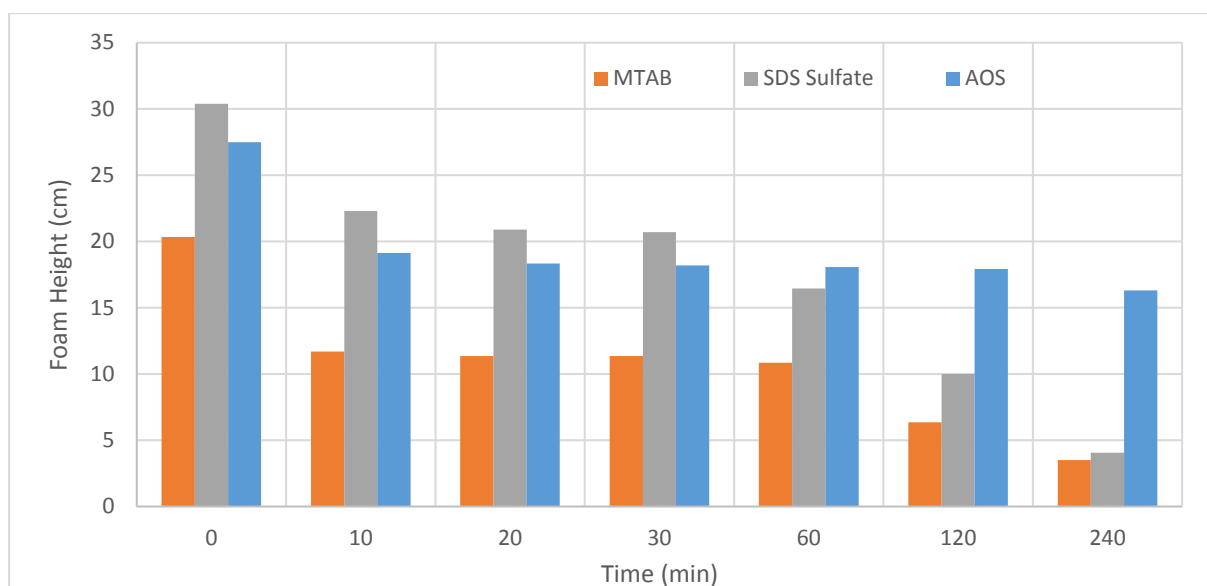


Figure 43: Variation of foam height with time for different surfactants (0.5 wt.% surfactant, 1 wt.% NaCl and  $22 \pm 1^\circ\text{C}$ ).

Overall, anionic surfactants have the best comprehensive foaming ability, followed by the cationic surfactant. Between the two anionic surfactants, SDS generates more foam than the other candidate AOS. This can be attributed to the differences in chemical structure. Generally, sulfate-type surfactants have better foaming ability than sulfonate-type surfactants. In this study, SDS possesses shorter carbon chain but exhibits the best foaming ability which is consistent with the conclusion drawn by Wu and Pan (Wu and Pan, 2010) that surfactants with smaller carbon number tend to have better foaming ability. The cationic surfactant MTAB generates the least foamability and has the shortest half-life time. The reduced foaming ability and stability of the MTAB can be due to the higher carbon number chain and surface tension with MTAB. (Relate this to surface elasticity, surfactant activity and ability to adsorb at the interface).

The results reflect the significant impact of the type of surfactant on foam stability. The surfactant with the smallest carbon chain length (SDS) has the highest foamability initially, followed by AOS and MTAB. However, SDS does not necessarily give the most stable foam. The best foam stability of surfactants does not seem to be directly proportional to the carbon chain length since the activity of foam agents depends not only on surface/interfacial tension but also on the intermolecular interactions.

### 5.6 Foam-oil interactions analyzed by static foam tests

The main purpose of this study is to gain a better understanding of the effect of oil on foam performance. Both oil compositions and surfactant structure are complex, which makes selecting a surfactant for an oil-related application require a lot of screening work. Five crude oils are used in our experiments, denoted oil 1-5, and are obtained from oil fields in the North Sea. The impact of oil

type, surfactant concentration and salinity on the foam performance with the presence of oil are systematically investigated.

### 5.6.1 Effect of oil on AOS foamability and stability

A comprehensive series of experiments are conducted to investigate the surfactants' ability to generate stable foams in the presence of 0.5 wt.% of different oils. Only AOS surfactant is used and the concentration is kept constant at 0.5 wt.% in distilled water. Figure 44 shows the foam height as a function of time and the decay profiles for different oils with AOS. In general, the initial foam volume decreases in the presence of oil, and the foam largely collapsed after a certain time. In comparison to the oil-free case, oils 3 and 2 marginally affected formability, while oils 1, 4 and 5 reduce formability more significantly. On the other hand, all oil samples have an adverse effect on foam stability to a varying extent. Foams generated in the presence of oils 1, 4 and 5 are most unstable, while the effect of oils 2 and 3 on foam stability is not as detrimental. It is noteworthy that for all the oil samples foam collapsed within 24 hours, which is not the case for oil-free foam.

Foamability and stability with oils depend on the type of oil and its physical and chemical properties, where no direct correlation is found. The change in the oil spreading behavior of the foam –oil system is not fully understood and requires further investigation.

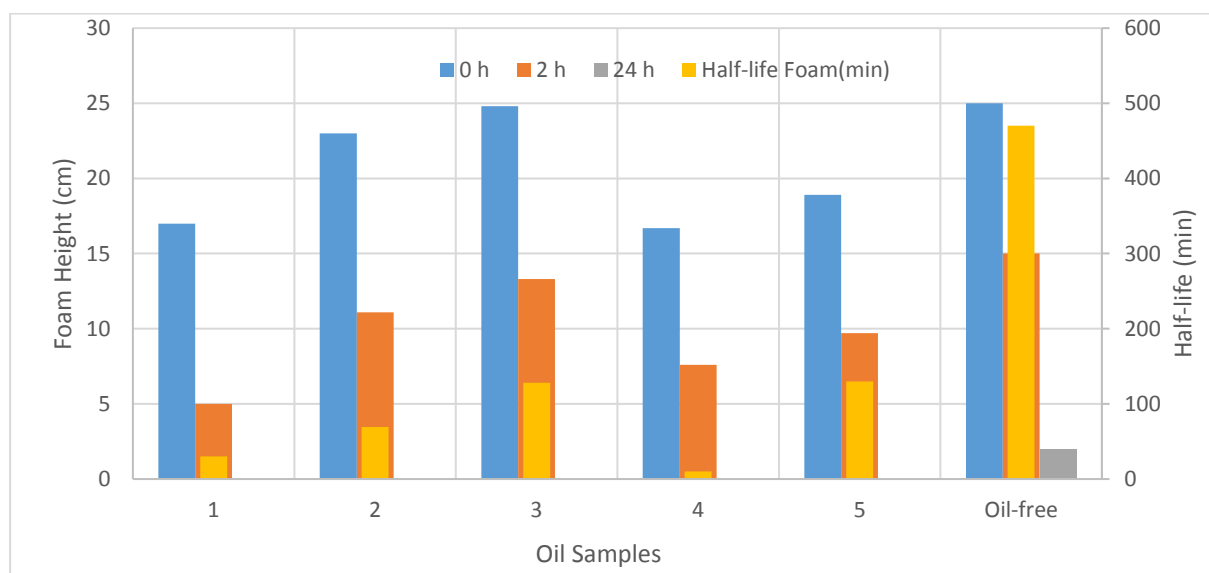


Figure 44: Foam column height as a function of time for the different crude oils and free oils using 0.5 wt.% oil and 0.5wt.% AOS in distilled water

### 5.6.2 Effect of salinity on oil-foam

Salinity effect on oil-foam tests is conducted at ambient conditions with constant AOS concentration of 0.5 wt.% and constant oil content of 0.5 wt.%. According to Figure 45, the NaCl has little to no effect on the foamability in the presence of oil, even at different ionic strengths.

Comparing distilled water and 1 wt.% NaCl solution, the foam height increases with oils 1, 3 and 4 but decreases with NaCl concentration of 5 wt.%. the initial foam height in the presence of oils 2 and 5 appears to be independent of NaCl concentration, as the presence of NaCl salt reduces generated foam height. The process is complicated by the presence of oil to find the correlation of the impact of oil on the foam. These results of crude oil samples 2 and 5 corroborate the findings reported in the literature (Koczo et al., 1992). These results verify that oil-foam systems are more complex and how sensitive they are to the type of crude oil.

The change in salt concentration has a positive effect on foamability in the absence of oil (see Figure 38) but shows a little influence on the foamability when oil is added. Vikingstad et al have observed similar results in their work. Behera et.al also reported that increasing salinity decreases the foam volume at a given oil content (Behera et al., 2014).

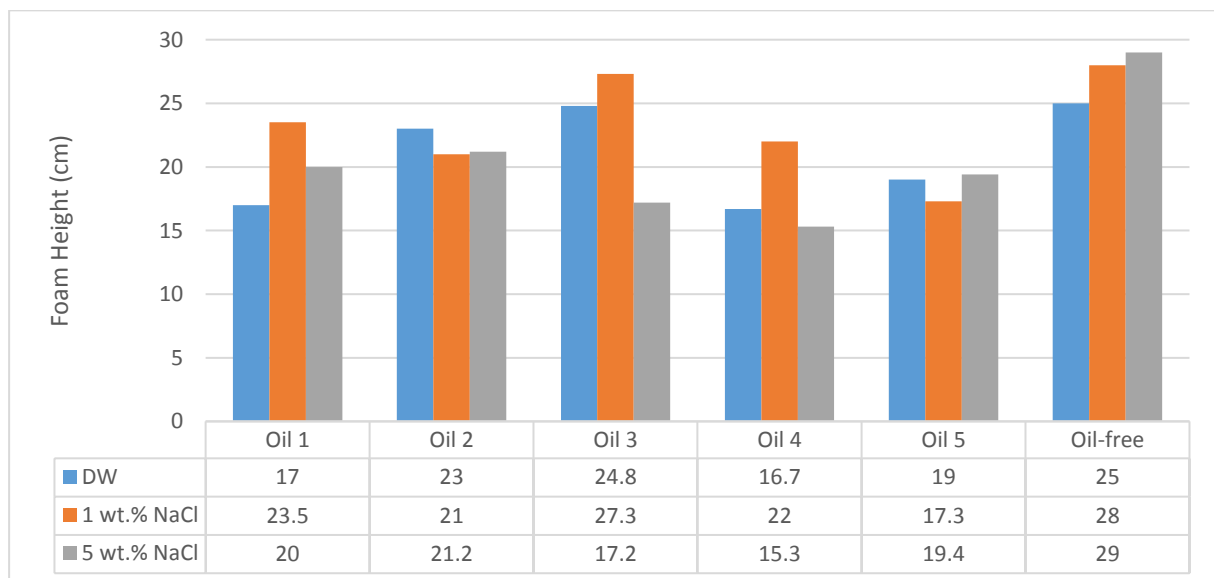


Figure 45: Explanation of the effect of salinity on foamability with different crude oils present.

Contrary to formability, the effect of salinity on foam stability is significant. Oils 1, 2 and 5 are significantly more stable in the presence of oil in 5 wt.% NaCl. When the concentration of NaCl is 1 wt.%, the stability of foam is increased for all crude oil samples except sample 5. The presence of salt may have altered the surface elasticity as well as the surface viscosity of the foam supporting the lamellae stability. The alterations of the surface properties could be caused by depletion of oils at the

gas-liquid interface due to the height viscosity of the surface. For oils 1, 2 and 5, the higher the viscosity and the density (see Table 7), the more stable the oil-foam, which consistent with previous work done by (Osei-Bonsu et al., 2015). They used 1 wt.% NaCl with 2 wt.% SDS with different oils, and they found the opposite trend with oil viscosity. However, crude oil samples 3 and 4, significantly heavier, the oil-foam stability doesn't follow the trend. This could suggest that the trend of oil viscosity-foam stability is valid for light oils.

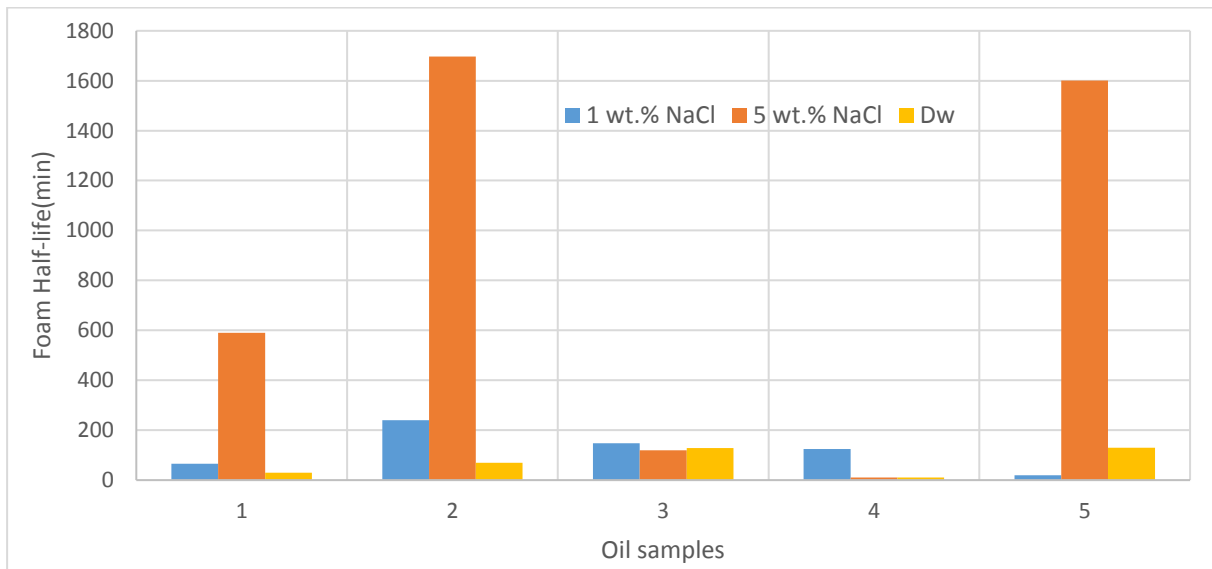


Figure 46: Half-life of foam at different concentration of salts with different oils. The concentration of the oil and AOS are constant 0.5 wt. %

In general, we can summarize that there is little effect of salinity on the foam in presence oil, but this effect could stabilize or destabilize the foam depending on the oil type. Therefore, we can't generalize these results for other crude oil samples. The properties of the oil in a candidate field must be taken into consideration and some other factors before any foam injection process is initiated.

### 5.6.3 Effect of surfactant concentration on foam-oil interaction

The effect of surfactant concentration experiments are conducted with a constant crude oil content of 0.5 wt.% crude oil of sample 3 since this oil sample gives the best foamability and it hardly influences stability. Salt concentration is also kept constant at 5wt.% NaCl. The results are represented in Figure 47. AOS foam height increases significantly when the surfactant concentration is increased from 0.5 wt.% to 1 wt.%, and a further increase of surfactant concentration to 5 wt.% marginally increases foam height. On the other hand, MTAB foam height slightly increases when the surfactant concentration is increased from 0.5 wt.% to 1 wt.%, but foam height increased significantly with 5 wt.% MTAB. It is interesting to note that at 5 wt.% surfactant concentration, MTAB and AOS foam height is almost identical, even though AOS foam height in the absence of oil is higher than MTAB foam height (Figure

33). At high surfactant concentrations, oil seems to have no effect on foamability. Meaning that foamability is the same with and without oil present.

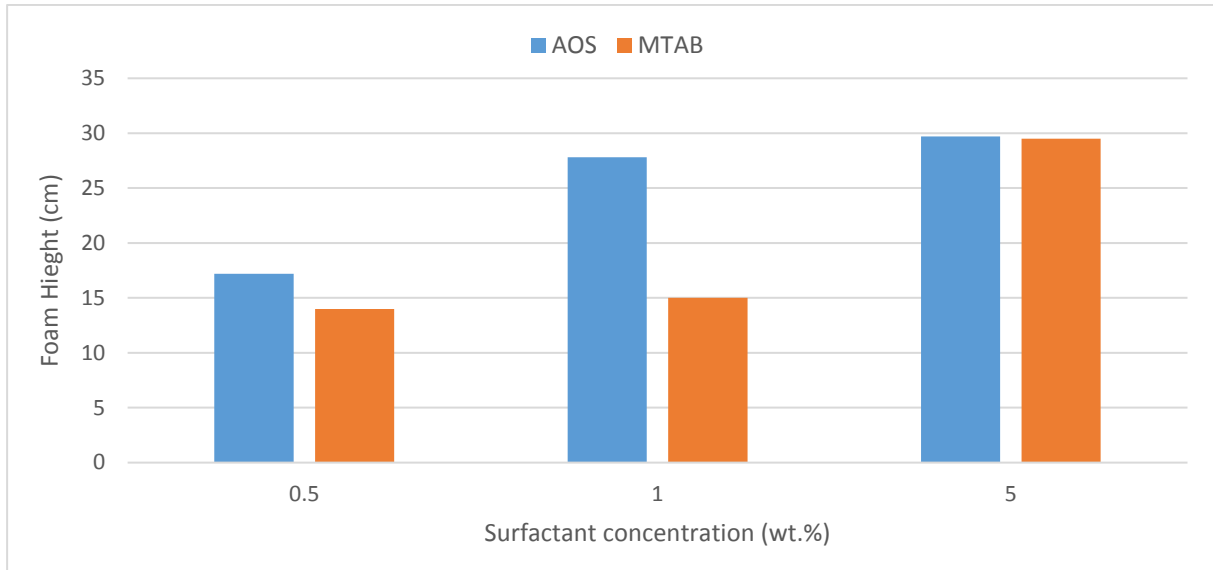


Figure 47: Foamability in the presences of 0.5 wt.% Oil 3 with 5 wt.% NaCl

By increasing the concentration of AOS, the stability of foam increases significantly, as evident in Figure 48. In other words, oil 3 has no apparent effect on AOS foam stability low surfactant concentration, and it has a positive effect on foam stability at high surfactant concentration. This effect can be interpreted by considering the stability of the film.

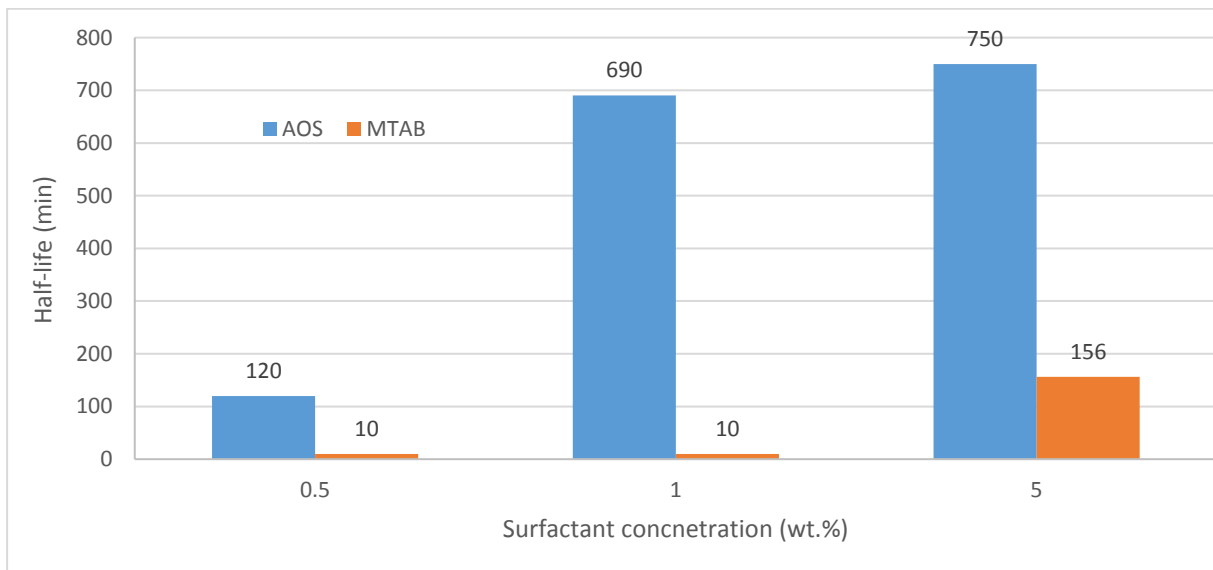


Figure 48: Foam stability in the presence of Oil 3, foam generating from the solution containing 5 wt.% NaCl and different concentration of AOS / MTAB.

The improved foamability and foam stability with increasing surfactant concentration can be interpreted similarly to as without oil present, related to possible reorganization of the micelles from spherical to rod-like micelles and further to multilayer laminar or liquid crystalline phases, same suggestion as brought up by (Vikingstad et al., 2005). With oil present, the transition from spheres to rod-like micelles also causes a moderate increase in the extent of the solubility of non-polar phases (e.g., oils) into the micelles (Christian and Scamehorn, 1995). Therefore, we think that the mechanisms of oil solubilization into the micelles with increasing surfactant concentration could be an explanation for our results.

#### 5.6.4 Spreading, entering and Bridging, and lamella number

The calculated spreading (S), entering (E) and bridging (B) coefficients and lamella numbers (L) for all crude oil samples with different salt concentrations are the main theories which are summarized in Table 13 for AOS surfactant with 1 wt.% NaCl, Table 14 for 5 wt.% NaCl and Table 15 for 5 wt.% MgCl<sub>2</sub>. Oil content is 0.5 wt.% and AOS concentration is 0.5 wt.%. The measured surface/interfacial tensions used in these calculations are also presented in these tables. Air is always used as the gas phase. The equations for calculation of S, E, B and L and the theory behind these parameters are described in Chapter 1 (Eq 19, 20, 21 and 22).

Table 13: Spreading coefficients, entering coefficients, lamella number and bridging coefficients at equilibrium for the AOS with 1 wt.% NaCl

Oils	$\delta_{w/g}$	$\delta_{w/o}$	$\delta_{o/g}$	S	E	B	L
Oil 1	30	1.7	26.3	2.2	5.6	225	2.7
Oil 2	30	2.2	26.2	1.8	6.2	232	2.1
Oil 3	30	2.4	29.4	-1.6	3.2	54	1.9
Oil 4	30	3.3	30.5	-3.5	3.1	-2	1.4
Oil 5	30	4.5	28.9	-3.1	5.9	103	1.0

Table 14: Spreading coefficients, entering coefficients, lamella number and bridging coefficients at equilibrium for the AOS with 5 wt.% NaCl.

Oils	$\delta_{w/g}$	$\delta_{w/o}$	$\delta_{o/g}$	S	E	B	L
Oil 1	28	1.4	26.3	0.3	3.0	93	3.1
Oil 2	28	0.7	26.2	1.1	2.5	97	5.8
Oil 3	28	1.0	29.4	-2.4	-0.5	-82	4.3
Oil 4	28	0.9	30.5	-3.4	-1.6	-143	4.7
Oil 5	28	1.5	28.9	-2.3	0.6	-46	2.9

Table 15: Spreading coefficients, entering coefficients, lamella number and bridging coefficients at equilibrium for the AOS with 5 wt.%  $MgCl_2$

Oils	$\delta_{w/g}$	$\delta_{w/o}$	$\delta_{o/g}$	$S$	$E$	$B$	$L$
Oil 1	29	1.2	26.3	1.5	3.8	150	3.8
Oil 2	29	0.6	26.2	2.2	3.4	153	7.3
Oil 3	29	1.1	29.4	-1.6	0.7	-24	3.9
Oil 4	29	0.9	30.5	-2.3	-0.6	-86	5.1
Oil 5	29	1.3	28.9	-1.2	1.5	10	3.3

Two of the criteria discussed in chapter 1 rely on the spreading and entering coefficients to predict foam stability, while the third criteria relies on bulk-foam properties. Positive spreading coefficient means that oil droplets can enter the foam structure and positive entering coefficient means that oil droplets can move in the lamellas, spread in the liquid films and collapse the foam structure. It is noteworthy that though the values of these coefficients may give insight as to the possibility of oil destroying foam, they do not determine the rate of foam destabilization (Manlowe and Radke, 2017). A comparison of the predictions from the three criteria is provided in Table 16.

According to the three criteria, oils 1 and 2 give unstable foam in almost all cases except Jonas's criterion with 5 wt.% NaCl and this is provided in terms of half-life Figure 46. Oils 3, 4 and 5 with distilled water are unstable based on all three criteria and moderate or stable foam when salt is added.

In relation to the lamella number, all values are between 1 and 7, so all foams are considered as type B foams (negative entering and spreading coefficients). However, for oils 1 and 2 both entering and spreading coefficients are positive, which it is not in agreement with the type B foam concept. Moreover, oil 4 with 5 wt.% NaCl and 5 wt.%  $MgCl_2$  has negative spreading and entering coefficients, which classifies it as type A foam.

These analyses show that the overall foam stability is not dictated solely by these thermodynamic coefficients and it is also related to the interfacial and bulk properties of the surfactant.

Table 16: Comparison of AOS foam stability predictions for different salt concentrations based on different criteria (U: Unstable, M: Moderate, and S: Stable)

Solution	Oil 1			Oil 2			Oil 3			Oil 4			Oil 5		
	Jonas	Simjoo	Lamella	Jonas	Simjoo	Lamella	Jonas	Simjoo	Lamella	Jonas	Simjoo	Lamella	Jonas	Simjoo	Lamella
DW	U	U	U	U	U	U	U	U	U	U	U	U	U	U	U
1 wt.% NaCl	U	U	U	U	U	U	U	U	M	U	M	M	U	U	M
5 wt.% NaCl	M	U	U	S	U	U	M	S	S	M	S	S	S	M	M
5 wt.% MgCl <sub>2</sub>	U	U	U	U	U	U	U	M	M	U	M	M	U	U	M

To compare between AOS and MTAB in terms of the effect of oil on foamability and foam stability, we selected oil 3, since it is expected to give stable foam based on Table 16. The interfacial tension values used to calculate the foam parameters for AOS and MTAB and the calculated foam parameters are shown in Table 17. The spreading and entering coefficients for MTAB are positive while for AOS they are negative. Thus, and according to Simjoo and Lamella criteria, MTAB foam should be unstable while AOS foam should be stable, which is in line with our experimental observations. However, according to Jonas's criterion, both surfactants have good formability, but AOS is more stable than MTAB. This difference is due to the type of Surfactant and the chain number, which in turn to lead difference in surface tensions and therefore the difference in these coefficients.

Table 17: Comparing between AOS and MTAB Oil3 effect in 5 wt.% NaCl on foam

Surfactant Type	$\delta_{w/g}$	$\delta_{w/o}$	$\delta_{o/g}$	<i>S</i>	<i>E</i>	<i>B</i>	<i>L</i>
MTAB	33.6	0.44	29.4	3.8	4.6	265	11.5
AOS	28.0	1.0	29.4	-2.4	-0.5	-81.8	4.3



## 5.7 Visual observations during and after the experiment:

### 5.7.1 Visual observations of foam stability in the absence of Oil

All surfactants with different concentration of salts and with distilled water are able to generate foam in bulk tests. In general, it is observed that the anionic surfactant AOS produced more foam than the cationic MTAB and that the generated foams exhibited different stabilities.

Initially, the bubbles are small and compact in all solutions, but after some time, the bubbles gradually increase at the top of the foam while remaining small in the bottom. These bubbles in the upper part grow larger and then collapse, but the duration of the breakdown varies depending on the concentration and type of salt in the solution. In the presence of salt, these bubbles take longer to collapse compared to in distilled water.

As for the  $MgCl_2$  at for all the concentrations used, after a period of foam formation, a gap develops between the liquid and the foam formed as shown in Figure 49, and there is no correlation between them. This leads to a more stable foam and longer time to completely collapse. It is difficult to distinguish the better stability concerning drainage free water since the difference between the half-life of the height of the fluid for each one is very small. The same is true for complex brine 2, which has high  $Mg^{2+}$  content.

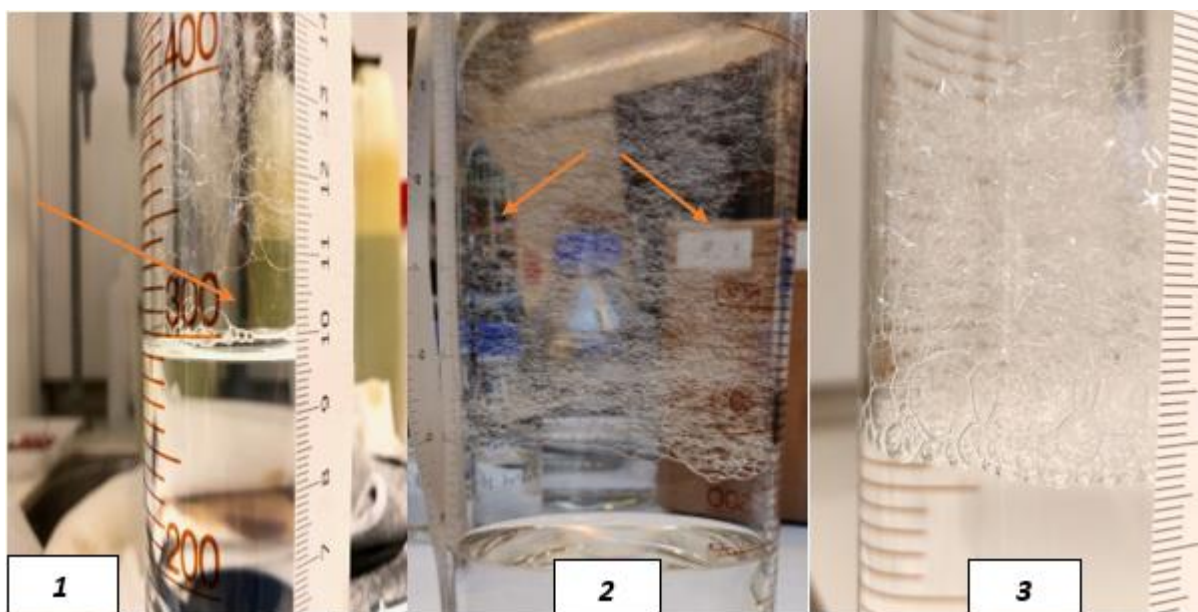


Figure 49: Gap between the foam and the liquid surface for  $MgCl_2$ , 1. AOS with  $MgCl_2$ , 2. MTAB with  $MgCl_2$  and 3. AOS with  $NaCl$

## 5.7.2 Visual observations of foam stability in the presence of oil

Crude oils show different abilities in destabilizing the foam in experiments using 0.5 wt.% of either AOS or MTAB and 0.5 wt.% Crude oil. In distilled water, the foam is unstable with oils, where after 24 h the foam heights are zero with all oils. Furthermore, even with 5 wt.%  $MgCl_2$  in the solution, the foams are unstable. However, with 5 wt.% NaCl the foam height after 24 (h) are about 10 cm. Overall, the presence of crude oil is shown to reduce the surfactant performance compared to that in the absence of oil (i.e., reduced foamability and foam stability). AOS is able to generate foam in the presence of all oils under all of the different experiment conditions applied and MTAB with oil 3. When we increase the surfactant concentration the effect of oil on foamability and the stability of foam is less pronounced, as in Figure 50 where the foam height is 30 cm at 0 min after mixing. This means we reduce the effect of oil on the foam by using a high concentration of surfactant. It may be very expensive too so and thus it is probably an undesirable method.

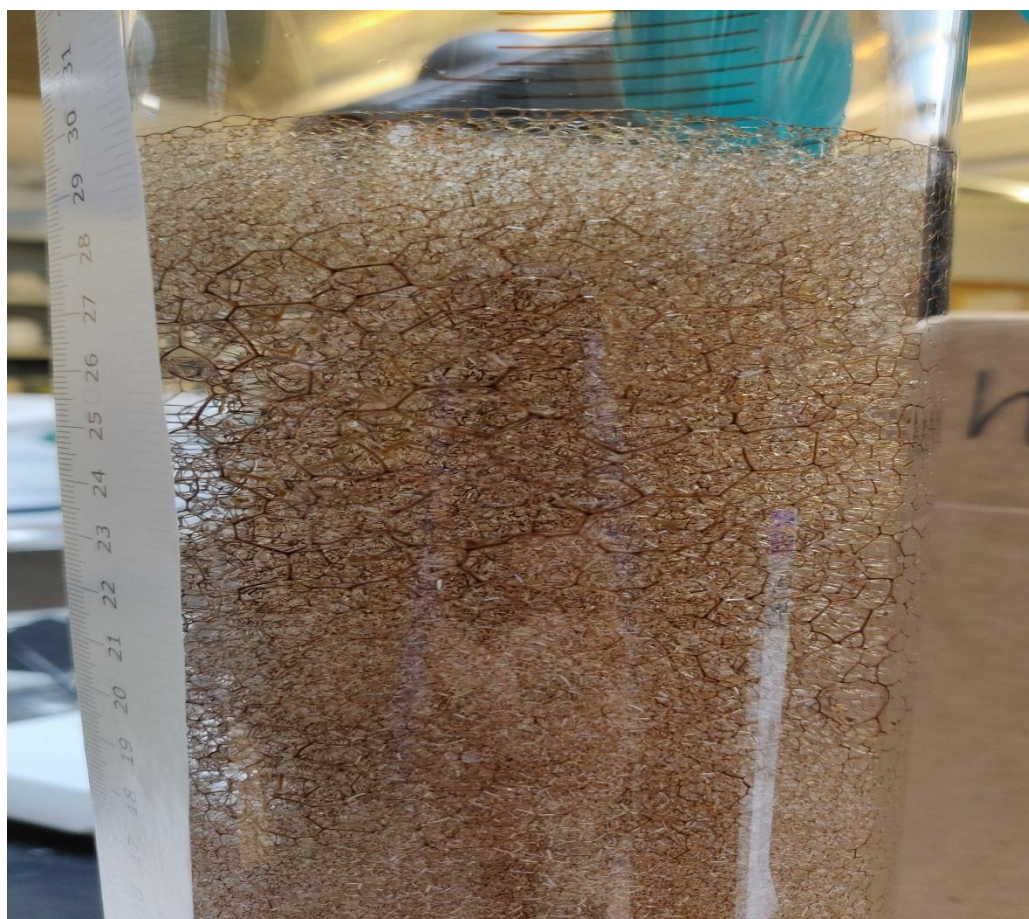


Figure 50 : Foamability of 5 wt.% AOS + 5 wt.% NaCl + 0,5 wt. % Oil 3

## Chapter 4: Summary and Further Work

## 6. Summary

In this thesis, salt effects on bulk foam properties have been evaluated at ambient conditions. Effect of salt type, concentration and ionic strength have been systematically studied and compared with respect to foamability and foam stability properties using anionic and cationic surfactants, respectively. Salt effects on bulk foam properties have also been evaluated in the presence of different crude oils. The following summary can be made from this work:

**Solubility limits** of AOS<sub>C14-C16</sub> (anionic) and MTAB<sub>C17</sub> (cationic) surfactants are identified for single salt solutions of NaCl, MgCl<sub>2</sub> and CaCl<sub>2</sub>, respectively:

- AOS<sub>C14-C16</sub> solubility limits (22°C): 7 wt. % NaCl (1.20 mol/L), 30 wt. % MgCl<sub>2</sub> (9.40 mol/L), and 0.2 wt.% CaCl<sub>2</sub> (0.05 mol/L).
- MTAB<sub>C17</sub> solubility limits (22°C): >15 wt.% NaCl (>2.57 mol/L), >40 wt.% MgCl<sub>2</sub> (>12.60 mol/L), and >5 wt.% CaCl<sub>2</sub> (>1.35 mol/L).

In general, salt effects on surfactant solubility are surfactant depended. The MTAB surfactant shows higher salt tolerance before precipitation compared to the AOS surfactant. Tolerance to NaCl and MgCl<sub>2</sub> is high/extreme with both surfactants, while tolerance to CaCl<sub>2</sub> is poor with the AOS and high for MTAB. Besides the surfactant type, salt effects on surfactant solubility seem more dependent on salt type than ionic strength.

**CMC** of both the anionic and cationic surfactant are found to decrease with ionic strength. Overall, the anionic AOS surfactant displays lower CMC compared to the cationic MTAB surfactant. The observed trend and values of CMC with changes in ionic strength and salt solutions are consistent with that reported in the literature (Wennerstrom et al., 1991). All further experiments in this thesis are conducted with surfactant concentrations above the surfactant's CMC.

- CMC of AOS<sub>C14-C16</sub> (22°C) is found to be in the range of  $7.5 \times 10^{-2}$  to  $4.0 \times 10^{-4}$  wt. % for ionic strengths from 0 to 1.6 mol/L, respectively.
- CMC of MTAB<sub>C17</sub> (22°C) is found to be in the range of  $8.1 \times 10^{-2}$  to  $2.5 \times 10^{-3}$  wt. % for ionic strengths from 0 to 1.6 mol/L, respectively.

**Foamability** refers to the “ability” of the system to form foam and should characterize the foamants (surfactants) different ability to generate foams under given conditions.

**Foamability (without oil)** increases with increasing surfactant concentration with both anionic and cationic surfactant. Both surfactants reach a constant maximum foam height at 0.5-1wt. %, and this might be related to changes in the bulk micelle structure. Foamability is in general better with anionic surfactants (AOS and SDS) compared with cationic MTAB surfactant.

**Foamability (with 0.5 wt% oil)** is in general reduced in the presence of oil compared to without oil. Nevertheless, the results with five different crude oils demonstrated that different amounts of foam can generate in all foam tests. Bulk foamability (using constant oil concentration, 0.5 wt.%) can be increased by increasing the AOS surfactant concentration. At 5 wt.% AOS surfactant concentration the impact of the oil on foamability is very little, in fact, providing the same initial foam height as compared to oil-free system. The same observation is also noticed with the same oil and high concentration (5 wt.%) of MTAB cationic surfactant. The improved bulk foamability with increasing surfactant concentration can be interpreted similar to without oil present, related to possible structural changes to the micelles from spherical to rod-like micelles and further to multilayer lamellar or liquid crystalline phases, same suggestion as brought up by Vikingstad, (2006). With oil present, the transition from spheres to rod-like micelles may also cause a moderate increase in the extent of the solubility of non-polar phases (i.e., oils) into the micelles. Increasing micellar solubilization of oil with increasing surfactant concentration may encapsulate and trap the oil, which may reduce the oil tendency to bridge the surface, or in general reduce spreading and unwanted transport of oil within the lamellae.

**Foamability (salt effects, without oil)** increases with increasing salt concentration and ionic strength of NaCl and MgCl<sub>2</sub>, respectively (using constant AOS surfactant concentration, 0.5 wt.%). Based on tests with NaCl and MgCl<sub>2</sub> salt solutions adjusted to the same ionic strengths, the AOS foamability is found to be more dependent on ionic strength than salt type. Interestingly, an opposite trend is indicated for the MTAB surfactant, in general showing decreasing foamability with increasing salt concentration and ionic strength. The different trends in foamability with salt concentration obtained for anionic and cationic surfactant may be related to different electrostatic interaction depending on the type of head-group. When the surfactant is oppositely charged, the interaction will be attractive. While, when the surfactant is like-charged the interaction will be repulsive. Aggregation is opposed due to the repulsion of the polar head groups as they come closer to each other. For the cationic surfactant, increasing salinity and ionic strength should therefore have provided larger repulsive forces compared to anionic, which overall may reduce the aggregation number, also meaning possible re-

organization of the micelle structure. Changes in the bulk micelle structure may change the foaming ability to surfactants.

**Foamability (salt effects, with 0.5 wt% oil):** Increase in salt concentration and ionic strength has a positive effect on foamability with the AOS surfactant in the absence of oil. However, no clear trend of changes in ionic strength and salt solutions on the foamability is observed when crude oil is added. Besides the surfactant type and concentration, the oil type seems more important on foamability than salt effects.

**Foam stability** is understood as a parameter describing variations of the foam properties (mostly as changes of height or volume) with time, immediately after the foam is generated. Foam stability is governed by a complex interplay of several mechanisms. In this thesis, foam stability is evaluated based on foam decay with time after the foam is generated. We also recorded the total liquid drainage (free water) with time, and correlated foam stability to the “foam half-life” parameter commonly used in the literature.

**Foam stability (without oil):** In general, foam half-life increased with increasing surfactant concentration for both the surfactants. However, there seems to exist an optimum surfactant concentration beyond which foam stability is the same, or slightly decrease with further increase in surfactant concentration. The measured optimum surfactant concentration is 0.5 wt.% with AOS and 1 wt.% with MTAB in 5 wt.% NaCl.

**Foam stability (salt effects, without oil):** In summary, there seems to be an optimum concentration of single salts that provides the highest foamability and most stable foam. At constant surfactant concentration, this salt concentration depends on the type of surfactant and salt used. The optimum concentration of  $MgCl_2$  (using constant surfactant concentration, 0.5 wt.%), is 5 wt.% and 15 wt. % for AOS and MTAB, respectively.

**Foam stability (salt effects, with 0.5 wt% oil):** Three out of five crude oils show improved foam stability with AOS compared to without oil in 5 wt.% NaCl solution. The results indicate that there might be a different influence of salinity and ionic strength on bulk foam stability with and without oil present. Increasing AOS surfactant concentration provides more stable foam in the presence of one oil tested. Increasing MTAB surfactant concentration doesn't improve foam stability in the presence of the same oil. There is still a lack of a general theory explaining the mechanisms of foam generation and stability of all foam systems, especially in the presence of crude oils.

## 7. Further Work

As often happens during a research project, many ramifications from the initial planning appeared. In our studies, we investigated the effect of some parameters such as salt type and concentration, type and concentration of surfactant, type of oil on foamability and foam stability. However, there are some topics may be studied and developed analyze the results obtained from this study. The results can be helpful to develop a better understanding of the interaction between salinity and foam on the one hand, and between oil and foam on the other. In order to improve our results and study, the following may be considered:

- All experiments are performed to measure bulk properties. It would be interesting to perform core-flooding experiments using the determined optimum surfactant concentration to assess the interaction between surfactants, salts and oils in the porous media.
- The quality of the gas used may be important in the formation and stability of the foam. We used to air in our experiments. We could study the effect of other gasses like N<sub>2</sub> or CO<sub>2</sub> on the obtained results. Will the gas affect the stability of the bubble in the bulk test and in porous media?
- Foam forming method may also have a role on the foam. In our experiments, we used the so-called mixing method. It would be useful if another method is used to form the foam for some of the solutions used and compare the results.
- We did not conduct measurements using MTAB in the presence of oil. One can study the effect of different crude oil samples on MTAB foam properties, and how the trends compare to AOS foams.
- Recently, there is an emerging interest in foam stabilized by a mixture of nanoparticle and surfactant; it will be interesting as further work to investigate the stability of foam for mixing the optimum concentration of AOS / MTAB with silicon oxide (SiO<sub>2</sub>) powder.
- Study if there is a correlation between foam stability and surface tension, and the limitations of such a correlation if it exists.

## Reference

- AARRA, M., ORMEHAUG, P. & SKAUGE, A. Foams for GOR control-improved stability by polymer additives. IOR 1997-9th European Symposium on Improved Oil Recovery, 1997.
- AARRA, M., SKAUGE, A. & MARTINSEN, H. FAWAG: A Breakthrough for EOR in the North Sea. SPE annual technical conference and exhibition, 2002. Society of Petroleum Engineers.
- ABBOTT, P. S. Krafft point [Online]. [Accessed].
- ARONSON, A., BERGERON, V., FAGAN, M. E. & RADKE, C. 1994. The influence of disjoining pressure on foam stability and flow in porous media. *Colloids and Surfaces A: Physicochemical and Engineering Aspects*, 83, 109-120.
- BARAKAT, Y., FORTNEY, L., SCHECHTER, R., WADE, W. & YIV, S. Alpha-olefin sulfonates for enhanced oil recovery. Proceedings 2nd European symposium on enhanced oil recovery, Paris, 1982. 11-20.
- BARAKAT, Y., FORTNEY, L. N., LALANNE-CASSOU, C., SCHECHTER, R. S., WADE, W., WEERASOORIYA, U. & YIV, S. 1983. The phase behavior of simple salt-tolerant sulfonates. *Society of Petroleum Engineers Journal*, 23, 913-918.
- BAZ-RODRÍGUEZ, S. A., BOTELLO-ALVAREZ, J. E., ESTRADA-BALTAZAR, A., VILCHIZ-BRAVO, L. E., PADILLA-MEDINA, J. A. & MIRANDA-LÓPEZ, R. 2014. Effect of electrolytes in aqueous solutions on oxygen transfer in gas–liquid bubble columns. *Chemical Engineering Research and Design*, 92, 2352-2360.
- BEHERA, M. R., VARADE, S. R., GHOSH, P., PAUL, P. & NEGI, A. S. 2014. Foaming in micellar solutions: Effects of surfactant, salt, and oil concentrations. *Industrial & Engineering Chemistry Research*, 53, 18497-18507.
- BENT, V. V. D. 2014. Comparative study of foam stability in bulk and porous media.
- BERG, J. C. 2010. *An introduction to interfaces & colloids: the bridge to nanoscience*, World Scientific.
- BEYER, K., LEINE, D. & BLUME, A. 2006. The demicellization of alkyltrimethylammonium bromides in 0.1 M sodium chloride solution studied by isothermal titration calorimetry. *Colloids and Surfaces B: Biointerfaces*, 49, 31-39.
- BROWN, M. A., GOEL, A. & ABBAS, Z. 2016. Effect of electrolyte concentration on the stern layer thickness at a charged interface. *Angewandte Chemie International Edition*, 55, 3790-3794.
- BUREIKO, A., TRYBALA, A., KOVALCHUK, N. & STAROV, V. 2015. Current applications of foams formed from mixed surfactant–polymer solutions. *Advances in colloid and interface science*, 222, 670-677.
- CANTAT, I., COHEN-ADDAD, S., ELIAS, F., GRANER, F., HÖHLER, R., PITOIS, O., ROUYER, F. & SAINT-JALMES, A. 2013. *Foams: structure and dynamics*, OUP Oxford.
- CHU, Z. & FENG, Y. 2011. Empirical correlations between Krafft temperature and tail length for amidosulfobetaine surfactants in the presence of inorganic salt. *Langmuir*, 28, 1175-1181.
- DAVEY, T. W., DUCKER, W. A., HAYMAN, A. R. & SIMPSON, J. 1998. Krafft temperature depression in quaternary ammonium bromide surfactants. *Langmuir*, 14, 3210-3213.
- DENKOV, N. D. 2004. Mechanisms of foam destruction by oil-based antifoams. *Langmuir*, 20, 9463-9505.
- FARAJZADEH, R., ANDRIANOV, A., KRASSTEV, R., HIRASAKI, G. & ROSSEN, W. R. 2012. Foam–oil interaction in porous media: implications for foam assisted enhanced oil recovery. *Advances in colloid and interface science*, 183, 1-13.
- FARAJZADEH, R., KRASSTEV, R. & ZITHA, P. 2008. Foam films stabilized with alpha olefin sulfonate (AOS). *Colloids and Surfaces A: Physicochemical and Engineering Aspects*, 324, 35-40.
- FARAJZADEH, R., MURUGANATHAN, R., ROSSEN, W. & KRASSTEV, R. 2011. Effect of gas type on foam film permeability and its implications for foam flow in porous media. *Advances in colloid and interface science*, 168, 71-78.



- FARZANEH, S. A. & SOHRABI, M. 2015. Experimental investigation of CO<sub>2</sub>-foam stability improvement by alkaline in the presence of crude oil. *Chemical Engineering Research and Design*, 94, 375-389.
- FU, Y., LIU, H. & ZHONG, W. 2010. Wetting characteristics of epoxy resins modified by graphitic nanofibers with different functional groups. *Colloids and Surfaces A: Physicochemical and Engineering Aspects*, 369, 196-202.
- GHORBANI, S., SHARIFI, S., DE BRITO, J., GHORBANI, S., JALAYER, M. A. & TAVAKKOLIZADEH, M. 2019. Using statistical analysis and laboratory testing to evaluate the effect of magnetized water on the stability of foaming agents and foam concrete. *Construction and Building Materials*, 207, 28-40.
- GHOSH, T., GARCÍA, A. E. & GARDE, S. 2001. Molecular dynamics simulations of pressure effects on hydrophobic interactions. *Journal of the American Chemical Society*, 123, 10997-11003.
- GURGEL, A., MOURA, M., DANTAS, T., NETO, E. B. & NETO, A. D. 2008. A review on chemical flooding methods applied in enhanced oil recovery. *Brazilian journal of petroleum and gas*, 2.
- HAUGEN, Å., FERNØ, M. A., GRAUE, A. & BERTIN, H. J. 2012. Experimental study of foam flow in fractured oil-wet limestone for enhanced oil recovery. *SPE Reservoir Evaluation & Engineering*, 15, 218-228.
- HEUSER, J., MOLLER, J., SPENDEL, W. & PACEY, G. 2008. Aqueous foam drainage characterized by terahertz spectroscopy. *Langmuir*, 24, 11414-11421.
- HIRASAKI, G. 1989. A Review of Steam-Foam Process Mechanisms. paper SPE, 19518. Society of Petroleum Engineers (SPE), Richardson, TX.
- HUNTER, R. J. 2013. Zeta potential in colloid science: principles and applications, Academic press.
- JONES, S., VAN DER BENT, V., FARAJZADEH, R., ROSSEN, W. & VINCENT-BONNIEU, S. 2016. Surfactant screening for foam EOR: Correlation between bulk and core-flood experiments. *Colloids and Surfaces A: Physicochemical and Engineering Aspects*, 500, 166-176.
- KOCZO, K., LOBO, L. & WASAN, D. 1992. Effect of oil on foam stability: aqueous foams stabilized by emulsions. *Journal of colloid and interface science*, 150, 492-506.
- KONTOGEOORGIS, G. M. & KIIL, S. 2016. Introduction to applied colloid and surface chemistry, Wiley Online Library.
- KORNEV, K. G., NEIMARK, A. V. & ROZHKOV, A. N. 1999. Foam in porous media: thermodynamic and hydrodynamic peculiarities. *Advances in colloid and interface science*, 82, 127-187.
- KOVSCHEK, A. & RADKE, C. 1994. Foams: Fundamentals and applications in the petroleum industry. ACS Advances in Chemistry Series.
- KRALCHEVSKY, P., DANOV, K., BROZE, G. & MEHRETEAB, A. 1999. Thermodynamics of ionic surfactant adsorption with account for the counterion binding: effect of salts of various valency. *Langmuir*, 15, 2351-2365.
- KUEHNE, D. L., EHMAN, D. I., EMANUEL, A. S. & MAGNANI, C. F. 1990. Design and evaluation of a nitrogen-foam field trial. *Journal of Petroleum Technology*, 42, 504-512.
- KUHLMAN, M. I. 1990. Visualizing the effect of light oil on CO<sub>2</sub> foams. *Journal of Petroleum Technology*, 42, 902-908.
- KUNZ, W. 2010. Specific ion effects, World Scientific.
- LAKE, L. 1984. A technical survey of micellar-polymer flooding. *Enhanced Oil Recovery for the Independent Producer*, 102-141.
- MANDAL, A. 2015. Chemical flood enhanced oil recovery: a review. *International Journal of Oil, Gas and Coal Technology*, 9, 241-264.
- MANLOWE, D. J. & RADKE, C. J. 2017. A pore-level investigation of foam/oil interactions in porous media.
- MANNHARDT, K., NOVOSAD, J. & SCHRAMM, L. Foam/oil interactions at reservoir conditions. SPE/DOE Improved Oil Recovery Symposium, 1998. Society of Petroleum Engineers.
- MANNHARDT, K. & SVORSTØL, I. 2001. Surfactant concentration for foam formation and propagation in Snorre reservoir core. *Journal of Petroleum Science and Engineering*, 30, 105-119.

- MINSSIEUX, L. 1974. Oil displacement by foams in relation to their physical properties in porous media. *Journal of Petroleum Technology*, 26, 100-108.
- MUKERJEE, P. 1967. The nature of the association equilibria and hydrophobic bonding in aqueous solutions of association colloids. *Advances in Colloid and Interface Science*, 1, 242-275.
- NEGIN, C., ALI, S. & XIE, Q. 2017. Most common surfactants employed in chemical enhanced oil recovery. *Petroleum*, 3, 197-211.
- NELSON, R. 1981. Further studies on phase relationships in chemical flooding. *Surface Phenomena in Enhanced Oil Recovery*. Springer.
- NIKOLOV, A. & WASAN, D. 1989. Ordered micelle structuring in thin films formed from anionic surfactant solutions: I. Experimental. *Journal of colloid and interface science*, 133, 1-12.
- NIKOLOV, A., WASAN, D., HUANG, D. & EDWARDS, D. The effect of oil on foam stability: mechanisms and implications for oil displacement by foam in porous media. SPE annual technical conference and exhibition, 1986. Society of Petroleum Engineers.
- OSEI-BONSU, K., SHOKRI, N. & GRASSIA, P. 2015. Foam stability in the presence and absence of hydrocarbons: From bubble-to bulk-scale. *Colloids and Surfaces A: Physicochemical and Engineering Aspects*, 481, 514-526.
- PANDEY, S., BAGWE, R. P. & SHAH, D. O. 2003. Effect of counterions on surface and foaming properties of dodecyl sulfate. *Journal of colloid and interface science*, 267, 160-166.
- PUGH, R. 1996. Foaming, foam films, antifoaming and defoaming. *Advances in Colloid and Interface Science*, 64, 67-142.
- RANSOHOFF, T. & RADKE, C. 1988. Mechanisms of foam generation in glass-bead packs. *SPE reservoir engineering*, 3, 573-585.
- RAO, A., WASAN, D. & MANEV, E. 1982. Foam stability—effect of surfactant composition on the drainage of microscopic aqueous films. *Chemical Engineering Communications*, 15, 63-81.
- RICO-RICO, A., TEMARA, A., BEHRENDT, T. & HERMENS, J. L. 2009. Effect of sediment properties on the sorption of C12-2-LAS in marine and estuarine sediments. *Environmental Pollution*, 157, 377-383.
- ROJAS, Y., KAKADJIAN, S., APONTE, A., MARQUEZ, R. & SANCHEZ, G. Stability and rheological behavior of aqueous foams for underbalanced drilling. SPE International Symposium on Oilfield Chemistry, 2001. Society of Petroleum Engineers.
- ROLAND.CHEM. 2006. Tenside haben hydrophile und hydrophobe Enden [Online]. [Accessed].
- ROMERO-ZERON, L. B. & KANTZAS, A. 2007. The effect of wettability and pore geometry on foamed-gel-blockage performance. *SPE Reservoir Evaluation & Engineering*, 10, 150-163.
- ROSEN, M. J. & TRACY, D. J. 1998. Gemini surfactants. *Journal of Surfactants and Detergents*, 1, 547-554.
- ROSSEN, W. & VAN DUIJN, C. 2004. Gravity segregation in steady-state horizontal flow in homogeneous reservoirs. *Journal of Petroleum Science and Engineering*, 43, 99-111.
- ROSSEN, W. R. 1996. Foams in Enhanced Oil Recovery. *Foams: Theory, Measurement, and Applications*, ed. RK Prud'Homme and S. Khan. New York: Marcel Dekker.
- RUBIO, J., SOUZA, M. & SMITH, R. 2002. Overview of flotation as a wastewater treatment technique. *Minerals engineering*, 15, 139-155.
- SAMMALKORPI, M., KARTTUNEN, M. & HAATAJA, M. 2009. Ionic surfactant aggregates in saline solutions: sodium dodecyl sulfate (SDS) in the presence of excess sodium chloride (NaCl) or calcium chloride (CaCl<sub>2</sub>). *The Journal of Physical Chemistry B*, 113, 5863-5870.
- SCHELERO, N. & VON KLITZING, R. 2015. Ion specific effects in foam films. *Current Opinion in Colloid & Interface Science*, 20, 124-129.
- SCHRAMM, L. L. 1994. Foam sensitivity to crude oil in porous media. *ACS Advances in Chemistry Series*, 242, 165-200.
- SCHRAMM, L. L. 2006. *Emulsions, foams, and suspensions: fundamentals and applications*, John Wiley & Sons.
- SCHRAMM, L. L. & NOVOSAD, J. J. 1990. Micro-visualization of foam interactions with a crude oil. *Colloids and Surfaces*, 46, 21-43.

- SCHRAMM, L. L., TURTA, A. T. & NOVOSAD, J. J. 1993. Microvisual and coreflood studies of foam interactions with a light crude oil. *SPE reservoir engineering*, 8, 201-206.
- SEDEV, R. & EXEROWA, D. 1999. DLVO and non-DLVO surface forces in foam films from amphiphilic block copolymers. *Advances in colloid and interface science*, 83, 111-136.
- SETT, S., KARAKASHEV, S. I., SMOUKOV, S. K. & YARIN, A. L. 2015. Ion-specific effects in foams. *Advances in colloid and interface science*, 225, 98-113.
- SHENG, J. J. 2013. Foams and their applications in enhancing oil recovery. *Enhanced Oil Recovery Field Case Studies*. Elsevier.
- SIGMA Myristyltrimethylammonium bromide.  
<https://www.sigmaaldrich.com/catalog/product/sigma/t4762?lang=en&region=NO>.
- SIMJOO, M., DONG, Y., ANDRIANOV, A., TALANANA, M. & ZITHA, P. L. A CT scan study of immiscible foam flow in porous media for EOR. *SPE EOR Conference at Oil and Gas West Asia, 2012*. Society of Petroleum Engineers.
- SIMJOO, M., DONG, Y., ANDRIANOV, A., TALANANA, M. & ZITHA, P. L. 2013. Novel insight into foam mobility control. *SPE Journal*, 18, 416-427.
- SKARESTAD, M. & SKAUGE, A. 2009. PTEK 213–Reservoarteknikk II. University of Bergen.
- SKAUGE, A., AARRA, M., SURGUCHEV, L., MARTINSEN, H. & RASMUSSEN, L. Foam-assisted WAG: experience from the Snorre field. *SPE/DOE Improved Oil Recovery Symposium, 2002*. Society of Petroleum Engineers.
- SKAUGE, M. S. A. 2012. *Fluid Properties and Recovery Methods*.
- SOLBAKKEN, J. 2015. Experimental studies of N<sub>2</sub>-and CO<sub>2</sub>-foam properties in relation to enhanced oil recovery applications.
- TICHELKAMP, T., VU, Y., NOURANI, M. & ØYE, G. 2014. Interfacial tension between low salinity solutions of sulfonate surfactants and crude and model oils. *Energy & Fuels*, 28, 2408-2414.
- TSUJII, K. & MINO, J. 1978. Krafft point depression of some zwitterionic surfactants by inorganic salts. *The Journal of Physical Chemistry*, 82, 1610-1614.
- UIB. 2016. Eksperimentelle teknikkar i fysikalsk kjemi [Online]. [Accessed].
- VIADES-TREJO, J. & GRACIA-FADRIQUE, J. 2007. Spinning drop method: from Young–Laplace to Vonnegut. *Colloids and Surfaces A: Physicochemical and Engineering Aspects*, 302, 549-552.
- VIKINGSTAD, A. K., SKAUGE, A., HØILAND, H. & AARRA, M. 2005. Foam–oil interactions analyzed by static foam tests. *Colloids and Surfaces A: Physicochemical and Engineering Aspects*, 260, 189-198.
- VONNEGUT, B. 1942. Rotating bubble method for the determination of surface and interfacial tensions. *Review of scientific instruments*, 13, 6-9.
- WANG, H. & CHEN, J. 2013. A study on the permeability and flow behavior of surfactant foam in unconsolidated media. *Environmental earth sciences*, 68, 567-576.
- WEAIRE, D. L. & HUTZLER, S. 2001. *The physics of foams*, Oxford University Press.
- WENNERSTROM, H., KHAN, A. & LINDMAN, B. 1991. Ionic surfactants with divalent counterions. *Advances in Colloid and Interface Science*, 34, 433-449.
- WU, W. & PAN, J. Study on the foamability and its influencing factors of foaming agents in foam-combined flooding. *2010 Asia-Pacific Power and Energy Engineering Conference, 2010*. IEEE, 1-5.
- XU, W., NIKOLOV, A., WASAN, D. T., GONSALVES, A. & BORWANKAR, R. P. 2003. Foam film rheology and thickness stability of foam-based food products. *Colloids and Surfaces A: Physicochemical and Engineering Aspects*, 214, 13-21.
- YAMINSKY, V. V., OHNISHI, S., VOGLER, E. A. & HORN, R. G. 2010. Stability of aqueous films between bubbles. Part 1. The effect of speed on bubble coalescence in purified water and simple electrolyte solutions. *Langmuir*, 26, 8061-8074.
- YAN, H., YUAN, S.-L., XU, G.-Y. & LIU, C.-B. 2010. Effect of Ca<sup>2+</sup> and Mg<sup>2+</sup> ions on surfactant solutions investigated by molecular dynamics simulation. *Langmuir*, 26, 10448-10459.

YU, D., WANG, Y., ZHANG, J., TIAN, M., HAN, Y. & WANG, Y. 2012. Effects of calcium ions on solubility and aggregation behavior of an anionic sulfonate gemini surfactant in aqueous solutions. *Journal of colloid and interface science*, 381, 83-88.

## Appendix

### A. Experimental preparations and observations

Preparing solutions by dilution :

Solutions are often prepared by diluting a more concentrated stock solution. An accurately measured volume of the stock solution is transferred to a new container and brought to a new volume by addition of a known volume of solvent. Since the total amount of solute is unchanged before and after dilution, we know that:

$$C_o \times V_o = C_d \times V_d \quad (14)$$

Where  $C_o$  is the stock solution's concentration,  $V_o$  is the volume of stock solution being diluted,  $C_d$  is the dilute solution's concentration, and  $V_d$  is the volume of the dilute solution.

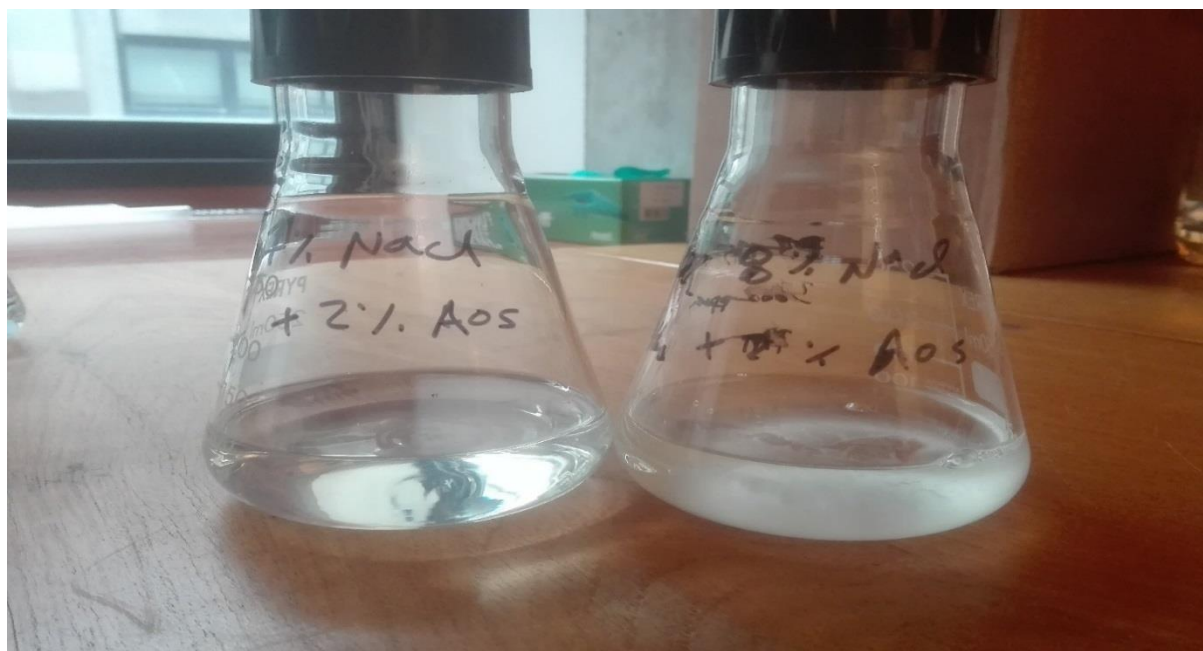


Figure 51: picture shows the solubility limit of AOS fir NaCl solution which is 7 wt. %.



Figure 52: picture shows 2% of the surfactant in different concentrations of CaCl<sub>2</sub>. It notes that AOS completely dissolved at 0.2% CaCl<sub>2</sub>, while precipitated at 0.5 wt. % and 1 wt. % respectively.

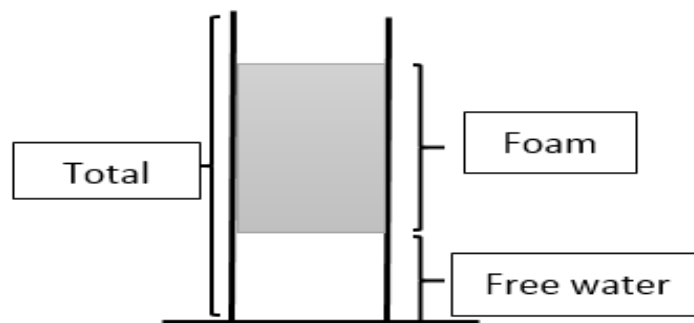


Figure 53: Illustration of the recording of foam height and free water (liquid).

During the measurement of CMC of 0.2 wt.%  $\text{CaCl}_2$  + 2wt.% AOS, we noticed that at the low concentrations of AOS, white clouds began to form and cling to the ring, making it difficult to measure, so we stopped the experiment at that as shown in (Figure 54-1). To make sure of this phenomenon, we have separately experimented. We have added 0,1 wt. % AOS to 0,2 wt.%  $\text{CaCl}_2$  and we got the same result see (Figure 54-2), white clouds, and becomes insoluble, and our knowledge of this phenomenon is useful to many reservoir engineers during the process of right after taking into account this problem and find another way to injection or change the type of surfactant.

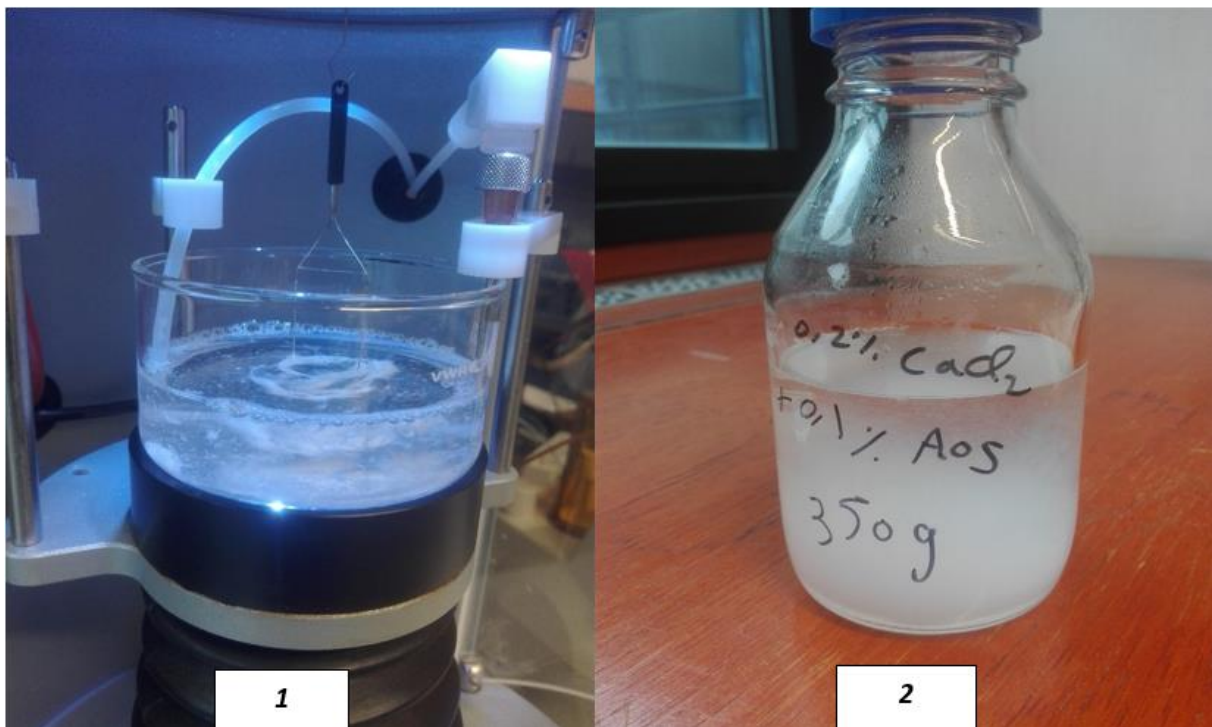


Figure 54: Illustration of cloudy formation in low concentration of AOS+ 0.2%  $\text{CaCl}_2$ .

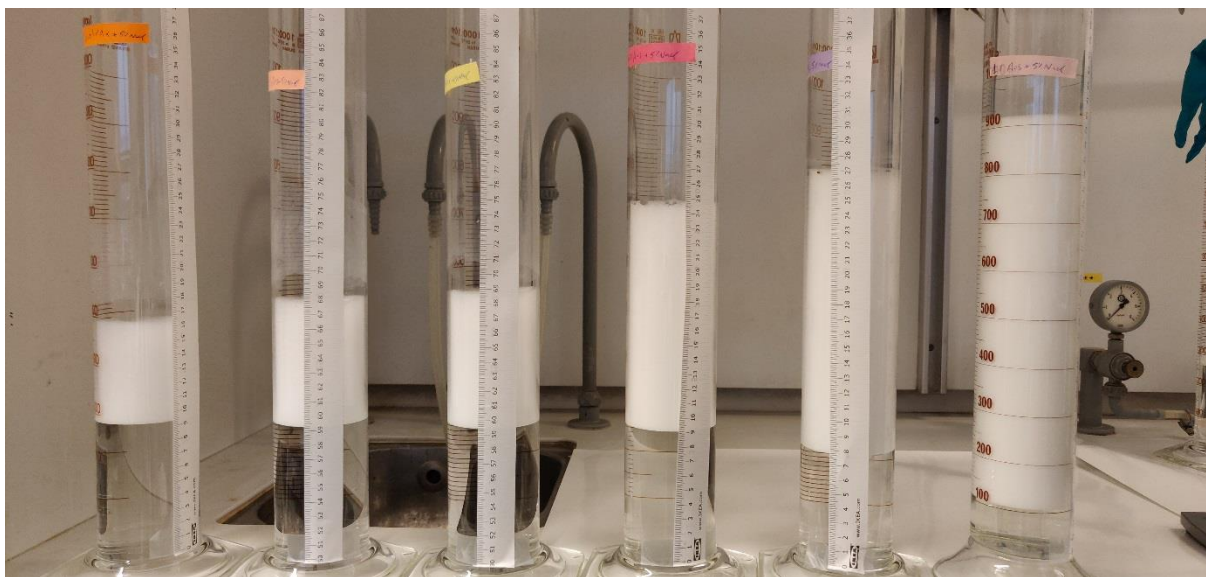


Figure 55: Foam Height for different concentration of AOS with (5.wt. % NaCl).

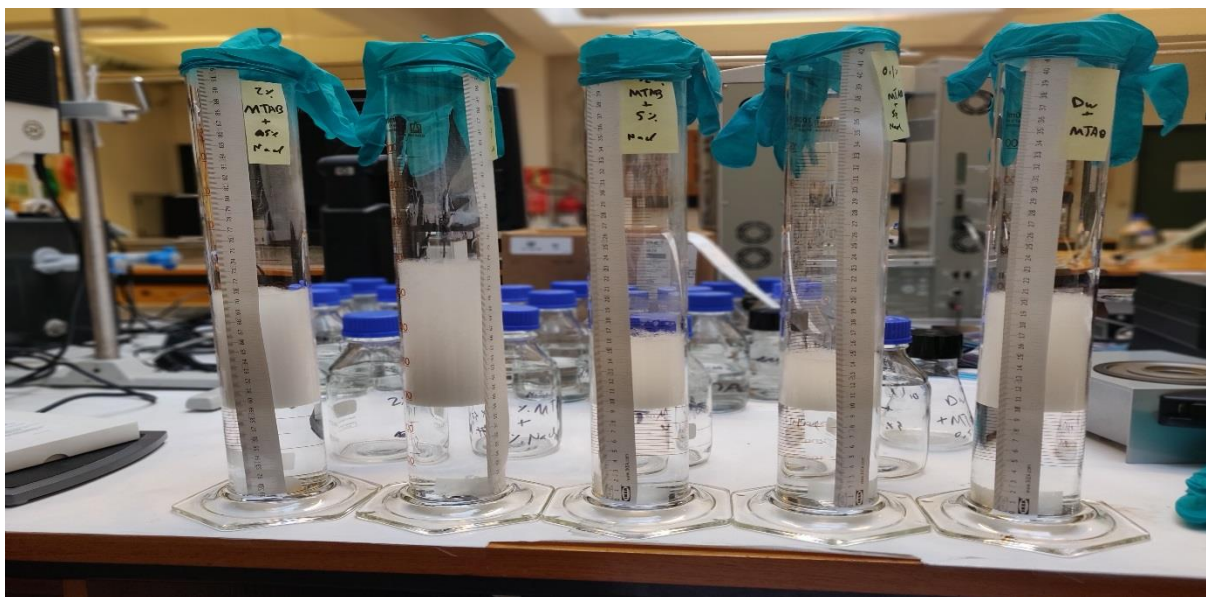


Figure 56: Foam Height for different concentration of MTAB with (5.wt. % NaCl).

The following tables are recipes for Brines used in this thesis

Table 18: composition of Brine 1 for 1 kg solution.

Salt	Mw g/mol	Salt mol/L	Salt g	Ionic strength mol/L
NaCl	58.44	0.4259	24.89	0.43
CaCl <sub>2</sub> ×2H <sub>2</sub> O	111.00	0.0118	1.31	0.04
MgCl <sub>2</sub> ×6H <sub>2</sub> O	95.27	0.0547	5.21	0.16
NaHCO <sub>3</sub>	84.01	0.0023	0.19	0.00
Na <sub>2</sub> SO <sub>4</sub>	142.04	0.0286	4.06	0.09
KCl	74.55	0.0091	0.68	0.01
<b>Total</b>	-	-	-	0.73

Table 19: composition of Brine 2 for 1 kg solution

Salt	Mw g/mol	Salt mol/L	Salt g	Ionic strength mol/L
NaCl	58.44	0.4943	28.89	0.49
CaCl <sub>2</sub> ×2H <sub>2</sub> O	111.00	0.0163	1.81	0.05
MgCl <sub>2</sub> ×6H <sub>2</sub> O	95.27	0.1381	13.16	0.41
NaHCO <sub>3</sub>	84.01	0.0029	0.24	0.00
Na <sub>2</sub> SO <sub>4</sub>	142.04	0.0341	4.85	0.10
KCl	74.55	0.0119	0.89	0.01
<b>Total</b>	-	-	-	1.07

Table 20: composition of Brine 3 for 1 kg solution

Salt	Mw g/mol	[Salt] mol/L	Salt g	Ionic strength mol/L
NaCl	58.44	0.7998	46.74	0.80
CaCl <sub>2</sub> ×2H <sub>2</sub> O	111.00	0.0722	8.01	0.22
MgCl <sub>2</sub> ×6H <sub>2</sub> O	95.27	0.1646	15.68	0.49
KCl	74.55	0.0102	0.76	0.01
<b>Total</b>	-	-	-	1.52



## B. Results

Table 21: Surface tension for different salt solutions and concentrations without surfactant (22°C, atm.)

Solution	Surface Tension mN/m
Distilled water	70.50
1 wt. % NaCl	69.27
5 wt. % NaCl	69.25
1 wt. % MgCl <sub>2</sub>	57.25
5 wt. % MgCl <sub>2</sub>	56.33
10 wt. % MgCl <sub>2</sub>	61.00
0.2 wt. % CaCl <sub>2</sub>	57.87
10 wt. % CaCl <sub>2</sub>	58.14
Brine 1	56.90
Brine 2	67.30

Table 22: Spreading coefficients, entering coefficients, lamella number and bridging coefficients at equilibrium for the AOS with 1 wt.% NaCl

Oils	$\delta_{w/g}$	$\delta_{w/o}$	$\delta_{o/g}$	$S$	$E$	$B$	$L$
Oil 1	30	1.7	26.3	2.2	5.6	225	2.7
Oil 2	30	2.2	26.2	1.8	6.2	232	2.1
Oil 3	30	2.4	29.4	-1.6	3.2	54	1.9
Oil 4	30	3.3	30.5	-3.5	3.1	-2	1.4
Oil 5	30	4.5	28.9	-3.1	5.9	103	1.0

The following Figures 58 – 60 summarize all the different tests in this thesis:

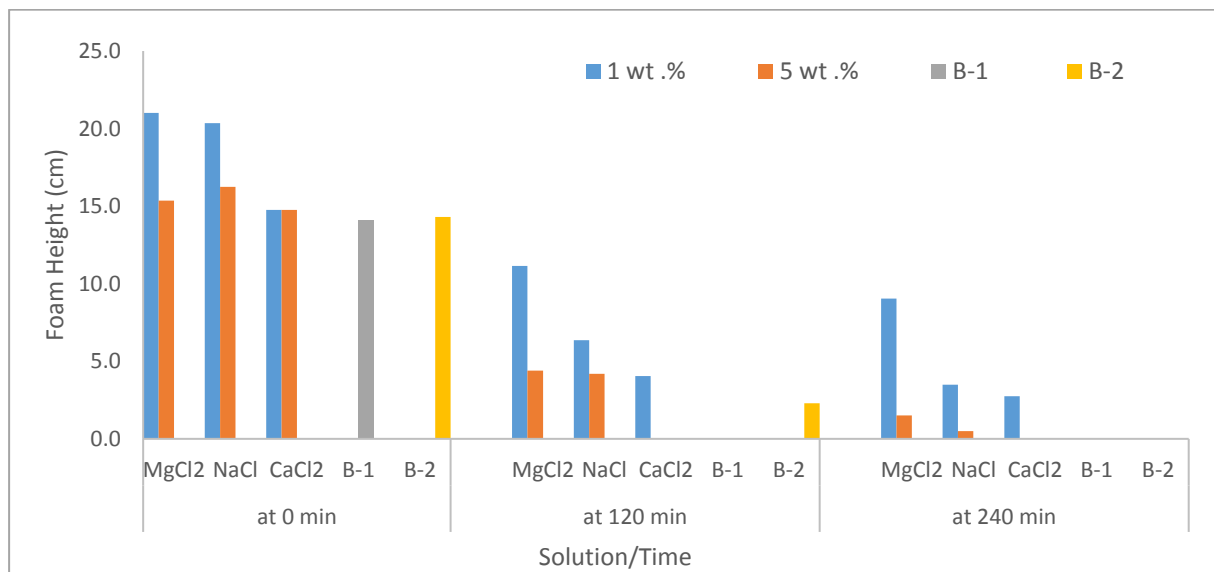


Figure 57: Variation of foam height as a function of time for different solutions with 0.5 wt. % MTAB in the absence of oil.

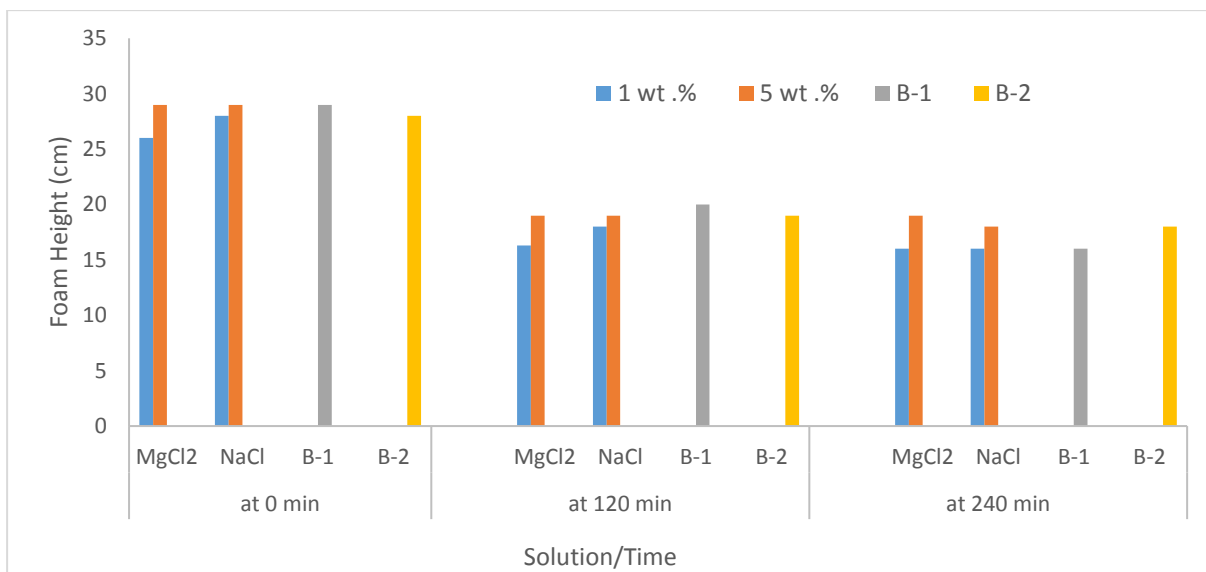


Figure 58: Variation of foam height as a function of time for different solutions with 0, 5 wt. % AOS in the absence of oil.

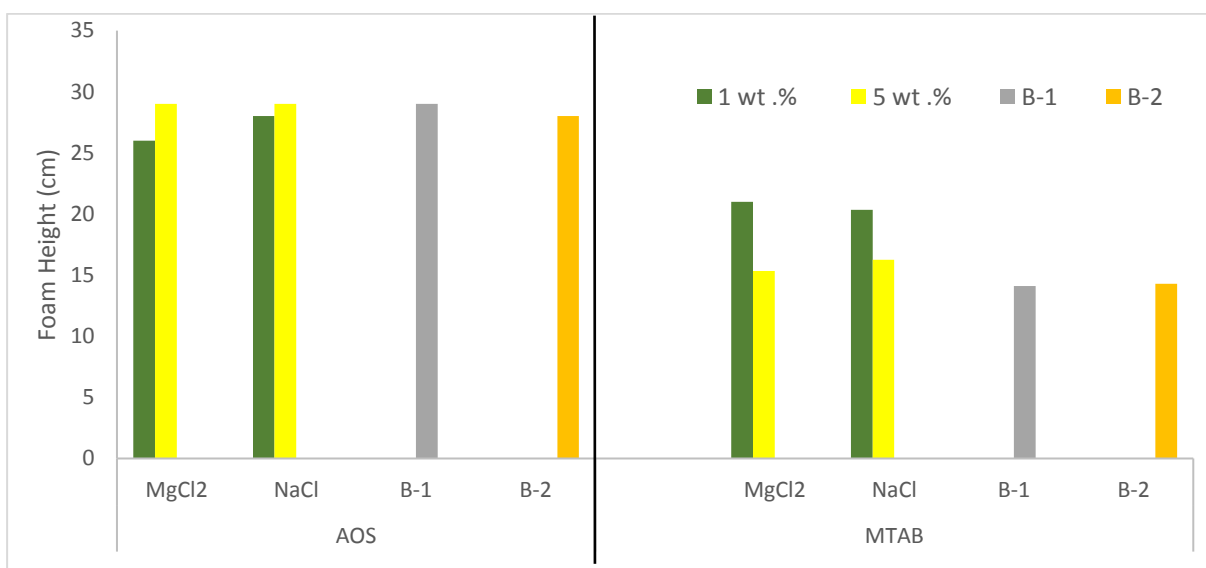


Figure 59: Comparing the foamability between AOS and MTAB at different solutions.

Figures 60 – 63 represent the variation of foam height with time for different oil samples with 0.5 wt.% AOS.

Figures 64- 65 represent the variation of foam height with time for AOS and MTAB in the presence of MgCl<sub>2</sub>.

Figures 66- 67 represent the variation of foam height with time for AOS and MTAB in the presence of NaCl.

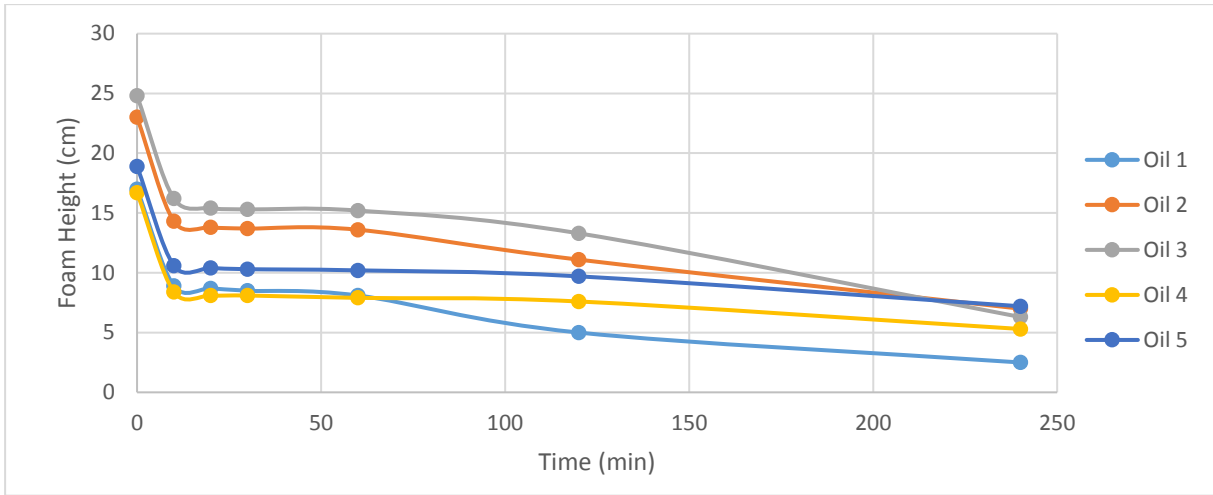


Figure 60: Foam Height Vs, different oils with distilled water in 0.5 w.% AOS.

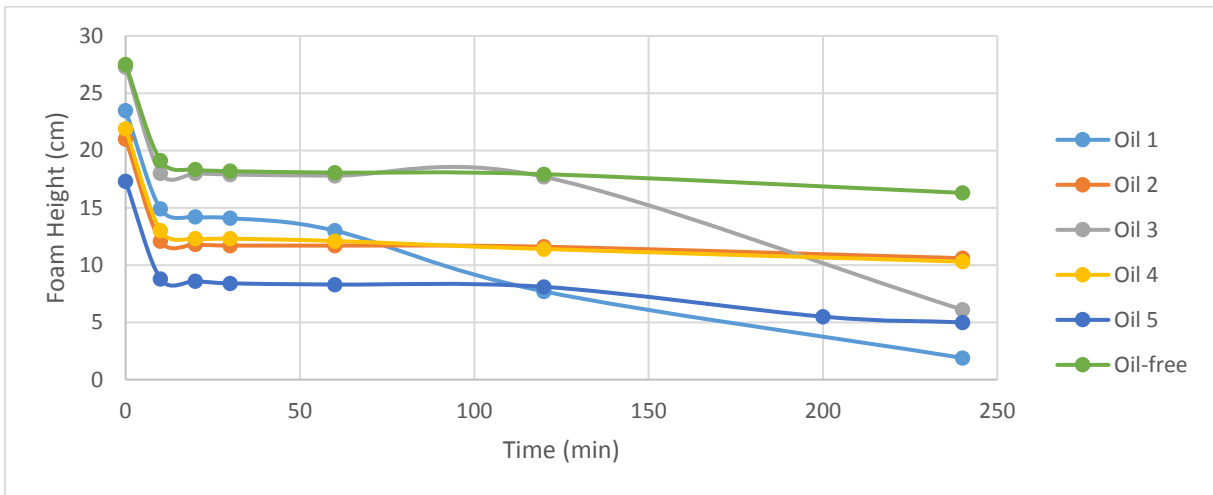


Figure 61: Foam Height Vs, different oils with 1 wt. % NaCl in 0.5 w.% AOS.

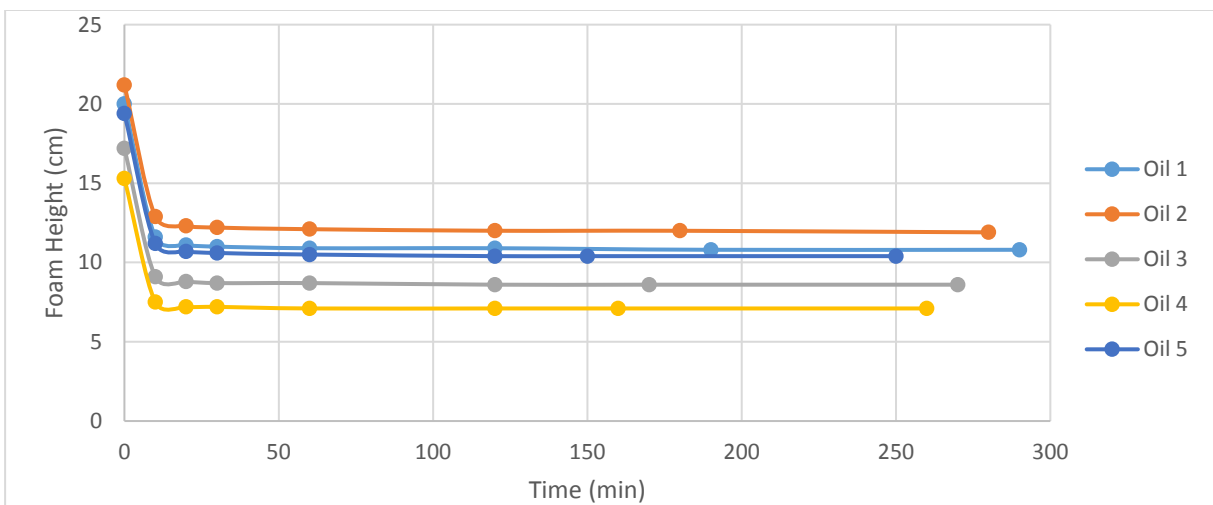


Figure 62: Foam Height Vs, different oils with 5 wt. % NaCl in 0.5 w.% AOS.

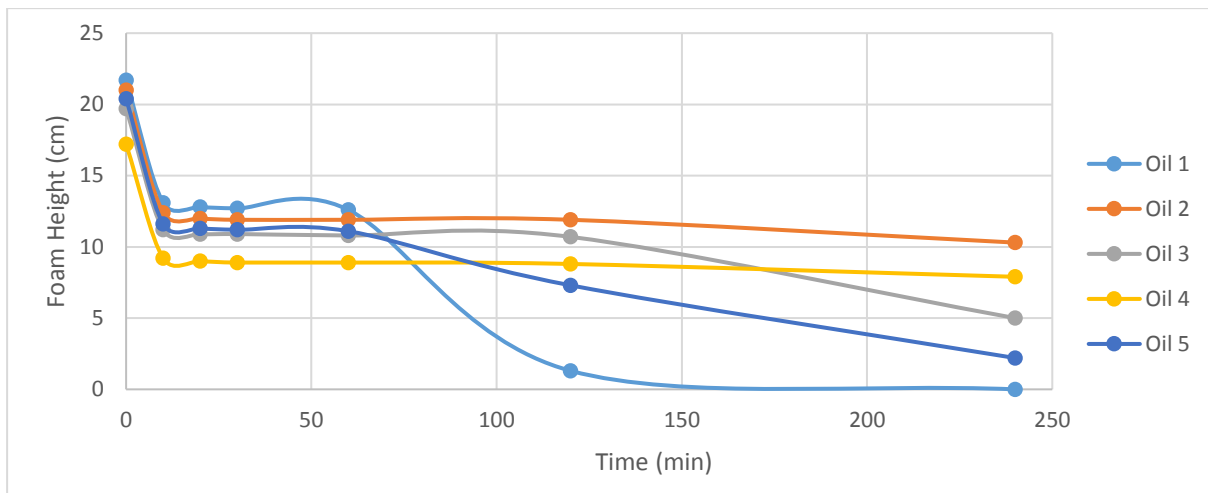


Figure 63: Foam Height Vs, different oils with 5 wt. %  $MgCl_2$  in 0.5 wt.% AOS.

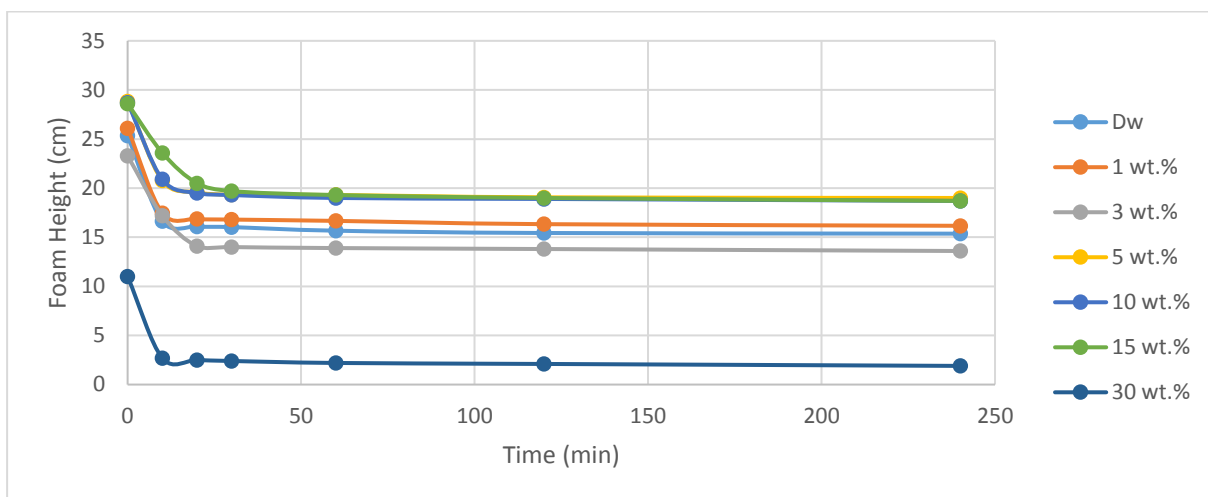


Figure 64: Change in foam height with respect to time for 0.5 wt.% AOS foam in the presence of  $MgCl_2$  at different concentration.

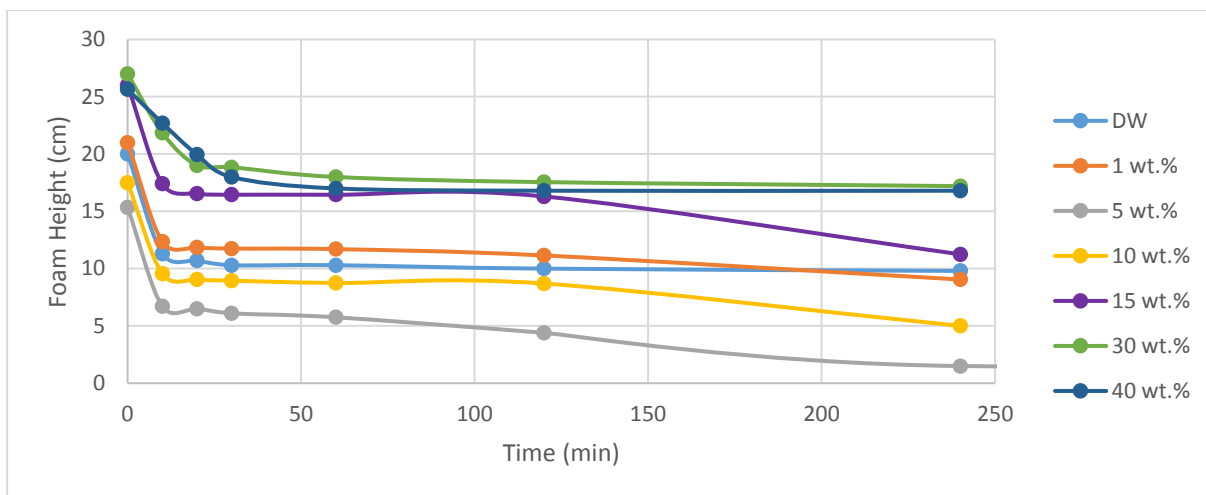


Figure 65: Change in foam height with respect to time for 0.5 wt.% MTAB foam in the presence of  $MgCl_2$  at different concentration.

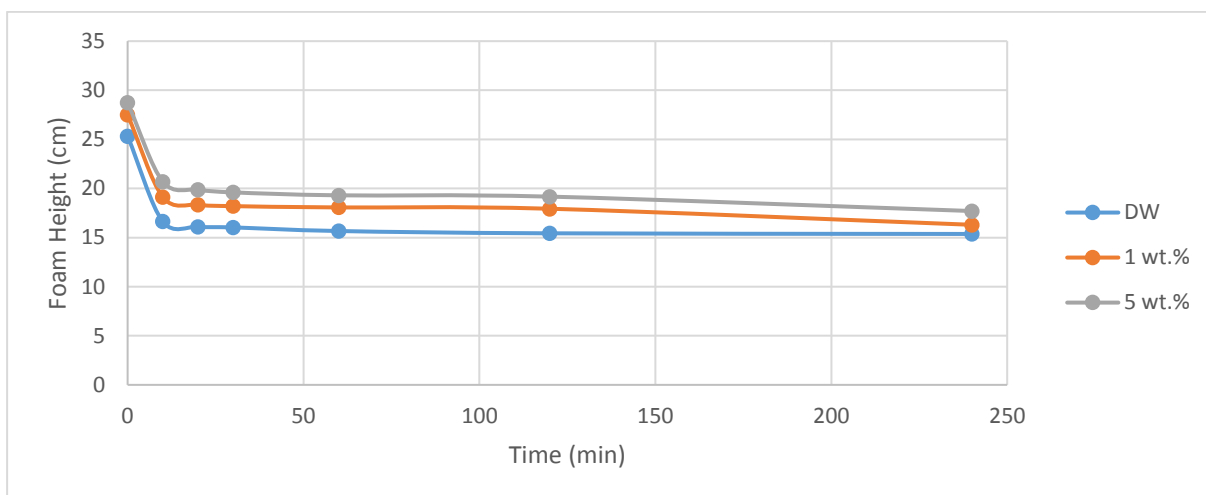


Figure 66: Change in foam height with respect to time for 0.5 wt.% AOS foam in the presence of  $NaCl$  at different concentration.

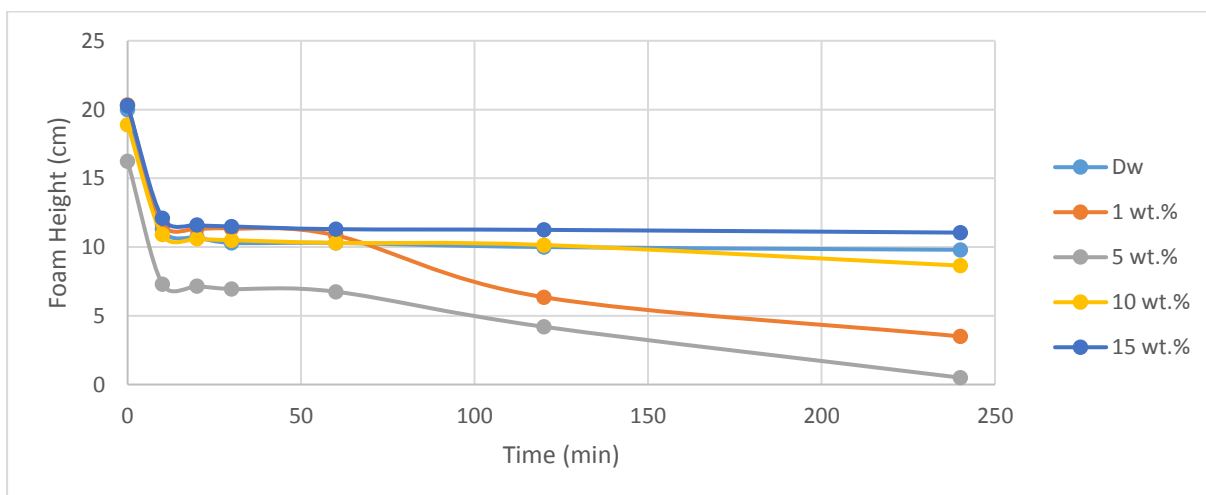


Figure 67: Change in foam height with respect to time for 0.5 wt.% MTAB foam in the presence of  $NaCl$  at different concentration.

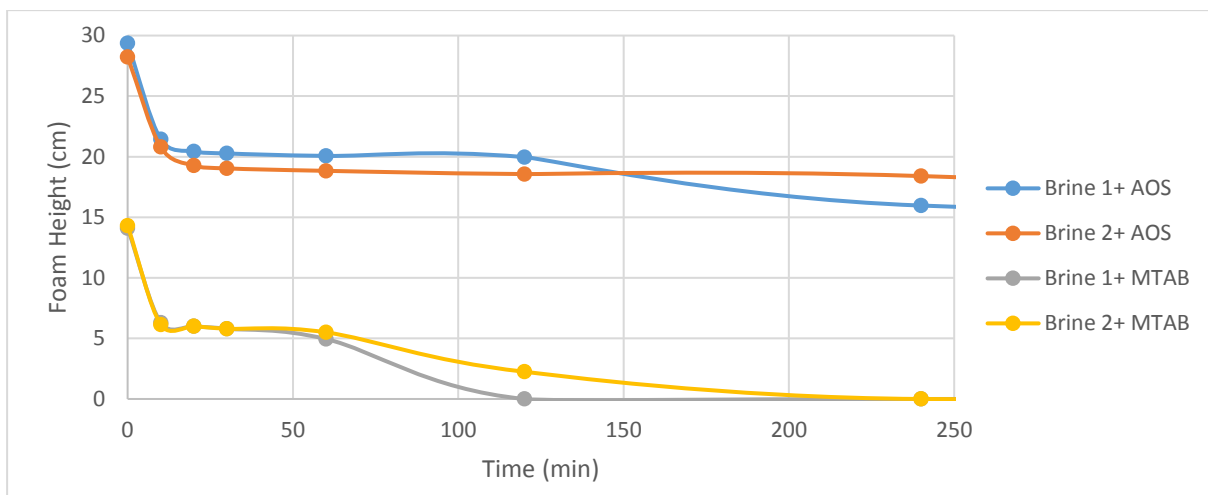


Figure 68: Change in foam height with respect to time for 0.5 wt.% AOS and MTAB foam in the presence of two complex brines.